

# STABILITY AND PERFORMANCE ANALYSIS OF A VARIABLE SPEED CONTROLLED SLIP INDUCTION MOTOR DRIVE

A DISSERTATION

*submitted in partial fulfilment of the  
requirements for the award of the degree*

*of*

MASTER OF ENGINEERING

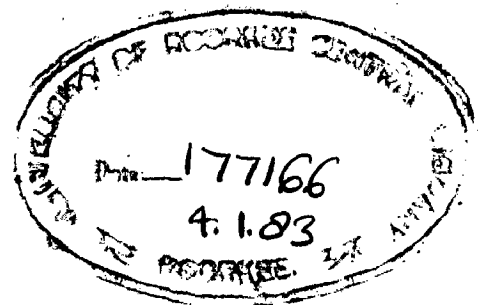
*in*

ELECTRICAL ENGINEERING  
(Power Apparatus and Electric Drives)

CHECKED  
1995

By

MANJU JAIN



DEPARTMENT OF ELECTRICAL ENGINEERING  
UNIVERSITY OF ROORKEE  
ROORKEE-247667 (INDIA)

August, 1982

(i)


C E R T I F I C A T E

Certified that the dissertation entitled " STABILITY AND PERFORMANCE ANALYSIS OF A VARIABLE SPEED CONTROLLED SLIP INDUCTION MOTOR DRIVE", which is being submitted by Miss Manju Jain in partial fulfilment of the requirements for the degree of MASTER OF ENGINEERING in ELECTRICAL ENGINEERING (Power Apparatus And Electric Drives) of the University of Roorkee, Roorkee is a record of student's own work carried out by her under my supervision and guidance. The matter embodied in this dissertation has not been submitted for the award of any other degree or diploma.

This is further certified that she has worked for a period of seven months from January 1982 to July 1982 for preparing this dissertation at this University.

ROORKEE

Dated : August 20, 1982

  
(V. K. VERMA)  
Professor  
Electrical Engineering Deptt.,  
University of Roorkee,  
Roorkee

(ii)

A C K N O W L E D G E M E N T

I wish to express my profound sense of gratitude and indebtedness to Dr. V.K.Verma, Professor of Electrical Engineering, for expert guidance, keen interest and sincere advice given by him during the course of investigations reported herein. The care with which he examined the manuscript is thankfully acknowledged.

I am highly thankful to Dr. D.R. Kohli, Professor and Head, Electrical Engineering Department, University of Roorkee, Roorkee, for providing computer facilities.

Thanks are also due to those who helped me directly or indirectly in preparing this dissertation.

*Manju Jain*  
MANJU JAIN

ABSTRACT

This dissertation concerns an induction-motor drive fed from a rectifier-controlled current inverter source. The use of a speed regulator, p-i current regulator and slip-speed regulator makes this drive a closed-loop system.

The work in the beginning discusses the steady-state performance of the drive. Effect of variation in load torque on the drive power output, induction-motor stator voltages and power factor, and drive efficiency at different p.u. operating frequencies are discussed.

Induction-motor fed from rectifier-controlled-current-inverter source exhibit instability in open-loop mode of operation in unstable zone of torque-speed characteristic. However, this is the only region where the drive can be operated without causing saturation in the induction-motor. As such speed regulator, a p-i current regulator and a slip-speed regulator are used to stabilize the drive. The system characteristic equation is developed by employing the theory of small displacement and the D-partitioning technique is applied for parameter coordination which ensure stable operation of the drive over very wide range of speed variation with a prescribed degree of stability.

A method of predicting the drive performance as affected by stator current harmonics is also presented here. Only the 6th harmonic torque pulsation phenomenon is considered

(iv)

here since only the lowest order harmonic-torque pulsations can affect the steady-state drive performance for practical speed range and system parameters.

The transient response of the drive is determined for all three sets of controller parameters and the optimum set is finally determined.

(v)

LIST OF SYMBOLS

H	inertia constant of induction motor in second
$I_I$	inverter input current
$I_R$	current in d.c. link
$I_R^*$	reference d.c. link current
J	polar moment of inertia in $\text{kg-m}^2$
$K_c$	gain of p-i current controller
$K_{sl}$	proportionality constant of slip regulator
$K_{sp}$	proportionality constant of speed regulator
P	number of poles
$R_F$	filter resistance
T	time constant of p-i current controller
$T_e$	electromagnetic torque in Newton-meter
$T_L$	Load torque in Newton-meter
$V_{as}, V_{bs}$	induction motor phase voltages
$V_{cs}$	
$V_I$	inverter input voltage
$V_R$	output voltage of rectifier
$V_S$	magnitude of line-to-neutral source voltage(r.m.s.)
$X_{CO}$	commutating reactance
$X_F$	inductive reactance of filter circuit
$X_m$	mutual reactance at base frequency
$X_r$	rotor reactance at base frequency
$X_s$	stator reactance of induction motor at base frequency
$f_b$	base frequency
$i_{as}, i_{bs}$	stator phase currents
$i_{cs}$	

$i_{dr}^e$	current in d-axis rotor winding in synchronously rotating reference frame
$i_{ds}^e$	current in d-axis stator winding in synchronously rotating reference frame
$i_{qr}^e$	current in q-axis rotor winding in synchronously rotating reference
$i_{qs}^e$	current in q-axis stator winding in synchronously rotating reference frame
$r_r$	rotor resistance
$r_s$	stator resistance
t	time in second
$v_{ds}^e$	voltage across d-axis stator winding in synchronously rotating reference frame
$v_{qs}^e$	voltage across q-axis stator winding in synchronously rotating reference frame
$\alpha$	firing angle of rectifier
$\theta_e$	angular position of synchronous reference frame
$\theta_r$	angular position of rotor
$\omega_b$	base angular frequency,
$\omega_r$	motor speed of induction motor
$\omega_r^*$	reference rotor speed of induction motor
$\omega_{sl}$	slip speed of induction motor
$\Delta$	represents change in variables
suffix 0	represents variables in steady-state operation
suffix 6	represents variables in 6th harmonic operation
suffix b	represents base quantities

# C O N T E N T S

	PAGES
CERTIFICATE	(i)
ACKNOWLEDGEMENT	(ii)
ABSTRACT	(iii)
LIST OF SYMBOLS	(v)
CHAPTER 1 INTRODUCTION	... 1
1.1 Literature Review	... 1
1.2 Author's Contribution	... 15
CHAPTER 2 THE MATHEMATICAL MODEL OF THE DRIVE	...
Introduction	... 18
2.1 System Studied	... 18
2.2 System Equation (in M.K.S.)	... 19
2.3 Equation in Concordia's p.u. System	... 24
2.4 Equation of Motion	... 27
2.5 Control Strategies	... 29
2.6 System Parameters	... 30
2.7 Conclusion	... 32
CHAPTER 3 THE STEADY-STATE ANALYSIS OF THE DRIVE	...
Introduction	... 33
3.1 Steady-State Equations	... 33
3.2 Results and Discussions	... 37
3.3 Calculation of $K_{s\ell}$	... 41
3.4 Conclusion	... 42
CHAPTER 4 COORDINATION OF DRIVE PARAMETERS FOR SYSTEM STABILITY	...
Introduction	... 44
4.1 System Equations Under Small Displacement Theory	... 44
4.2 Computer Results and Discussion	... 55
4.3 Conclusion	... 58



Contents (contd.)

CHAPTER 5	THE SIXTH HARMONIC ANALYSIS OF THE DRIVE	...	
	Introduction	...	61
5.1	Mathematical Equations for the Sixth Harmonic Effects	...	61
5.2	Results and Discussion	...	76
5.3	Conclusion	...	78
CHAPTER 6	THE TRANSIENT ANALYSIS OF THE DRIVE	...	
	Introduction	...	79
6.1	State Space Equations	...	79
6.2	Computer Result and Discussion	...	83
6.3	Conclusion	...	89
CHAPTER 7	CONCLUSION	...	91
	Scope of Further Work	...	94
	REFERENCES	...	96
APPENDICES			
Appendix - I	The Slip-Regulator-Control Strategy	...	99
Appendix - II	Computer Programme for Steady State Analysis of Drive	...	101
Appendix - III	Computer Programme for Stability Analysis	...	105
Appendix - IV	Computer Programme for 6th-Harmonic Analysis of Drive	...	109
Appendix - V	Computer Programme for Transient Analysis of Drive	...	113

.....

## CHAPTER - I

## INTRODUCTION

## 1.1 LITERATURE REVIEW

An electric drive basically consists of an electric motor associated with control equipment (that may include a frequency converter, rectifier etc.) to convert electrical energy into mechanical energy and thereby to provide a versatile control of speed, torque etc. of the electric motor.

Normally among the statically-controlled electric drives, a d.c. motor, operated under variable speed conditions by a static power controller, is a popular choice. But the main drawbacks of a d.c. motor are

- (i) increase in cost and decrease in power/weight ratio because of elaborate mechanical commutator,
- (ii) accentuated sparking at high currents and speeds,
- (iii) limited armature voltage rating inherent in d.c. machines, and
- (iv) limited armature current due to commutation problem.

Because of the above drawbacks of a d.c. motor, a suggested alternative is to use a squirrel-cage induction motor, a synchronous motor or a reluctance motor, operating at variable frequency and supplied from a static frequency converter. The use of a cage induction motor has the following advantages -

- (i) The cost of the squirrel-cage induction motor is only about one sixth that of a d.c. motor of the same speed and power rating.
- (ii) The power/weight ratio of the squirrel-cage induction motor is about twice that of a d.c. motor.

As a result of availability of SCRs interest in variable speed induction motor drives has shown a tremendous increase and in the recent years many new techniques, suitable for adjustment of the speed of the a.c. motors, have been developed.

One such method is the variable voltage control by thyristors [1,2] used for subsynchronous speed control of the induction motor. In this scheme, normally three pairs of anti-parallel SCRs are installed, one in each line, and firing angles are symmetrically controlled to smoothly regulate the stator voltage of the motor. Thus, the voltage applied to the motor can be varied from zero to full supply voltage. The operating efficiency of this method is poor and derating is necessary at low speeds to avoid overheating due to excessive current and reduced ventilation.

Another method for speed control of induction motors, applicable only in the case of slip-ring type, is variation of the rotor resistance [1,3]. In this method, a portion of the input power fed to the stator is extracted from the rotor

and is dissipated in the external rotor resistance with a consequent reduction in speed. In this method also efficiency is poor because the rotor slip power is dissipated in resistors.

Yet another method for speed control of the slip ring induction motor is the static slip power recovery scheme [1, 4]. In this method slip power is removed from rotor circuit and utilized externally, thereby improving the overall efficiency of the system. In these cascade connections, the slip power is either returned to the supply network or is used to drive an auxiliary motor which is mechanically coupled to the induction motor shaft.

The most versatile method giving efficient wide-range speed control is the variable frequency control [1, 5] of the induction motor. The variable frequency supply alters the synchronous speed of the induction motor.

Polyphase induction motor used in static variable frequency drive systems are versatile torque transducers having operating characteristics and features which meet the requirements of modern variable speed drive systems. Some of these characteristics are the capability for operation at very low and high speeds, at high torque and overloads, in a constant horse power or torque versus speed mode, and in the negative torque range for dynamic braking.

The variable frequency operation of an induction motor is obtained by the use of frequency converter. A frequency

converter is a machine or equipment that can generate or convert the input supply to an a.c. supply of variable frequency and amplitude. The rotating types of frequency converter have been used in past but now-a-days are out-dated and are replaced by the solid-state frequency converters.

The static frequency converters are divided into two categories-

(i) D.C. Link Converters (ii) Cyclo-converters.

A d.c. link converter is a two stage conversion device in which power from the a.c. network is first rectified to d.c. and then inverted to obtain a.c. voltage at variable frequency. This type of inverter can operate over a large frequency range and is suitable for wide-range speed control drives. However, this type of inverter employing thyristors, requires additional commutation circuits and is, therefore, complicated. Also for regeneration capability it requires additional circuits, and hence the cost and complexity are increased.

A cyclo-converter is a device to convert directly the a.c. supply of fixed frequency to that of a lower output frequency and does not require intermediate rectification. The output frequency range is limited to about one-third of the supply frequency and therefore the drives employing cyclo-converters are suitable only for operation at low frequency or speed range. However the basic advantage of a cyclo-converter is its inherent capability of regenerative operation and a close approximation of the output voltage to a sine wave, particularly at low frequencies, since the output wave is fabricated from the segments of the input supply wave form.

In general for wide range speed control and where regenerative braking is not essential a d.c. link converter fed induction motor is the best choice.

For optimum motor performance and effective utilization of core material, the air-gap flux of the induction motor should be maintained constant. It can be maintained approximately constant by keeping a constant voltage/frequency ratio, i.e. varying the supply voltage proportionately as the frequency is varied. However with constant v/f operation, the performance of the motor deteriorates at low frequencies because at low frequencies the influence of stator resistance is increased and consequently the air-gap flux reduces to some extent. Hence, in order to improve the low frequency characteristic, the terminal voltage should be increased more than the proportionate value. The required boost actually depends upon the design and size of the motor. Further, it can be shown that the electromagnetic torque is proportional to square of  $E_1/f_1$  or air gap flux, at a given rotor frequency  $f_2$  [1]. Consequently, if  $E_1/f_1$  or air-gap flux is maintained constant, the torque is solely determined by the absolute rotor frequency,  $f_2$  and is independent of supply frequency,  $f_1$ .

Thus a control scheme in which the rotor slip frequency is directly controlled while maintaining the constant air-gap flux  $E_1/f_1$ , the drive can exhibit a precise control and adjustment of torque at any speed. The air-gap flux of the motor can also

be indirectly determined by the stator current and rotor slip frequency  $f_2$ . In a closed loop system in which  $f_2$  and stator current are held constant the drive develops a constant torque at all motor speed [1]. Thus with a control strategy in which the stator current  $I_1$ , as well as rotor frequency  $f_2$  are controlled in order to maintain the air-gap flux constant high torque can be obtained through out the entire range of speed control. The basic advantage of controlled-current operation is that there is no necessity of large over current capacity of the inverter since there are minimum current surges and thus the inverter design is economical.

The rectifier-inverter system have been more popular in comparison to the cyclo-converter systems in a variety of industrial applications for the purpose of controlling the speed of a.c. motors by adjusting the frequency of the applied voltages. There are many problem associated with this type of variable frequency drive. The problem of drive instability at low frequency operation is one of the major concerns in the design of rectifier-inverter drive systems which are to operate over a wide speed range.

The stability study of a rectifier-inverter induction motor drive has been done by Lipo and Krause [6] by neglecting the harmonic content of the stator voltages and applying Nyquist stability criterion to the small displacement equations obtained by linearization about a steady-state operating point.

This investigation reveals that system instability can occur over a wide speed range with improper selection of drive parameters. The results are verified by comparing the predicted system performance obtained from an analog computer simulation. The regions of instability depend upon various system parameter viz. motor and filter parameters and rectifier commutating reactance. The interchange of energy between the filter components and the magnetic field of the motor causes instability at low operating frequency of this drive.

The stability problem of rectifier-inverter induction motor drive has been studied by F. Fallside employing Routh Hurwitz criterion [ 7 ]. The instability boundaries are found to be double valued. The result of the analysis gives design information which allows motor parameters to be chosen or modified to avoid instability over the working range of operation. This, however may lead to a special design or an inefficient drive. A preferable method which allows standard machine is the use of feed-backs to stabilize the drive.

Most of the solid-state variable frequency power supplies, provide a voltage source rich in harmonics. The associated problem has been discussed in some details by Klingshim and Jordan [ 8 ] for induction motor drives. An important problem is the rotor-speed pulsations. In applications where uniform speed of rotation is mandatory, such as machine tool, antenna positioning, and other applications, it



is important to establish a method for obtaining the magnitude of these speed oscillations.

This problem differs from that of system instability in that the torque pulsation and the resulting speed oscillation is a natural consequence of the inverter voltage wave shape rather than a result of an improper choice of system parameters, the steady-state torque pulsation can not be eliminated completely. In many cases these torque pulsations define the lower limit of the speed range which yields satisfactory system performance.

In previous studies considerable attention has been given to calculating these electromagnetic torque harmonics. Jain [9] by neglecting the stator resistance has established a general equation for the average torque for an arbitrary balanced set of applied voltages. Ward and Kazi [10] have derived an instantaneous expression for the electromagnetic torque by calculating the eigen values of the system characteristic equation. Sabbagn and Shewan [11] also developed an expression for the instantaneous electromagnetic torque by means of the instantaneous symmetrical component transformation. Krause [12] has discussed the effect on harmonic torque considering continuous and discontinuous stator current modes of operation for the case of open-loop rectifier controlled-voltage inverter source fed induction motor drive. In actual system neither the rotor speed nor terminal voltage is constant

The effect of both changes of speed and changes in inverter voltage has been incorporated in this analysis by Krause. However the influence of the 12th and higher harmonics are not considered. It has been shown by means of a hybrid computer solution that these higher harmonics do not contribute appreciably in the speed oscillation. In this paper only the influence of a change in the parameter  $X_{CF}$  (filter circuit capacitance) was investigated in detail. It is clear that other parameters also significantly influence the magnitude of the 6th harmonic torque pulsation. For example the connected load provides damping and additional inertia to the system, and tends to reduce speed deviation, thus decreasing the torque pulsations. If the average value of rectifier voltage is increased, the forcing function of 6th harmonic voltage is increased, thus increasing the 6th harmonic torque pulsation. Hence when the system is operated so as to maintain a constant breakdown torque, the harmonic torque component increase as well as average torque component. It was shown that the 6th-harmonic fluctuations in inverter voltage and rotor speed have a significant effect on the magnitude of the steady-state 6th harmonic torque. For practical systems this pulsation at low frequencies typically becomes two or three times greater than that predicted by a classical constant speed, constant voltage analysis.

Hence such a system is specially suited to operations requiring frequent acceleration and deceleration. [15].

State-variable steady-state analysis of induction motor supplied from ideal current inverter source, is done by Lipo [16]. The exact equations defining steady-state operation of a controlled current induction-motor drive system are derived by solving the system state equations in the stationary reference frame. Saturation has an important effect on motor performance. The slope ratio method was incorporated to account for this effect and the torque-speed characteristic determined. Torque remains very small until the motor approaches synchronous speed, then rises rapidly. Similar characteristic is obtained by Cornell [17] experimentally and by M.L.Macdonald [18] using DQ model. Sharp rise in flux linkage occurs as slip approaches zero. This results in saturation and high losses in a practical machine. Thus operation at full current at low slip is to be avoided [18].

Investigation of feasible operating points indicates that if the motor is to remain unsaturated it must be operated in the open-loop unstable region of its torque-slip characteristic, thus, feedback control is required in order to achieve stable operation [16].

Subsequently, the controlled-current inverter fed induction motor drive system was simulated on an analog computer and simultaneously a 100 HP system was built and

Current source converter for a.c. motor drives has been discussed by Phillips [ 13 ]. An inverter operating from a high impedance d.c. current source is quite different from an inverter which operates from a low impedance d.c. voltage source. Voltage source converters merely change line voltage and frequency to a settable adjustable voltage and frequency which is applied to the motor. The motor is then free to respond within its speed torque parameters as the application dictates. Unusual load variations can and often do, push the motor to its break down point or cause regeneration to occur in the converter by overhauling the motor. In either case, and ultimately shut down or damage to the motor or converter results. Voltage source type inverters use auxiliary impulse commutation. However recent advances in SCR blocking voltage capability makes the complementary impulse commutated current source inverter useful. [ 14 ]

Current source inverter possess certain advantages over the voltage source inverter. The advantages are

- (i) non-inverter grade thyristor can be used
- (ii) commutation capability is load current dependent
- (iii) inverter can recover from a direct short circuit across any two of its output terminals.
- (iv) the inverter converter arrangement is naturally capable of power regeneration.

tested in the laboratory [14]. The control system uses two feed back loops to control motor slip frequency and torque. The slip-control loop measures rotor speed adds in slip frequency, and provides the inverter with the correct synchronous frequency to maintain constant slip. Slip control allows the rotor to be operated at instant power factor over whatever load range is desired. The torque control loop monitors current in the d.c. link, compares it to a reference input, and controls the rectifier bridge triggers to maintain constant current. Since motor torque is proportional to current squared, this loop effectively regulates motor torque. Thus the overall characteristics of this drive are similar to those of a series d.c. motor. Motor torque is determined by the reference input which makes operating speed dependent upon shaft load.

The excellent agreement between computer and laboratory data demonstrates computer simulation as an effective method for designing current source inverter induction motor drives.

The steady-state performance of an inverter fed induction motor drive by means of time-domain complex variables is carried out by D.W.Novotny [20]. The analysis method and result presented in this paper provide a simple means of obtaining waveform information for inverter driven induction motor.

The steady-state solution for a current forced inverter fed three phase induction motor is discussed using Boundary Value Approach by K.R.Rao [ 21 ]. The linearity of the different equations at constant slip was utilized for using the superposition ideas and for obtaining a quick guess in respect of the initial vectors.

The modelling and design of controlled-current induction motor drive system is done by Cornell et al [17 ]. Transfer function approach to the transient response investigation is formulated by means of d-q variables in the synchronously rotating reference frame. The steady-state characteristics have been shown to correlate within a few percent of the theoretical predictions using the state-variable technique by Lipo [16]. Transfer function for various input and output is found out from equations which describe the behaviour of machine during small excursion about a steady-state operating point. For stability studies locations of poles and zeros are examined. If an open-loop operation is attempted the system will either slow down to zero speed or speed up and operate in a highly saturated condition. A closed-loop control is imperative for stable operation. Independent current magnitude and slip frequency control will result in stable operation for full motoring and regenerative operation. Additional system damping is achieved by constraining slip frequency to respond to change in d.c. link current. By doing so rated air gap flux is maintained in induction motor.

The frequency response measurements made on a hybrid computer simulation and actual laboratory hardware establish the validity of this approach.

M.L.MacDonald in his paper [18] presents a systematic study of the various control loops in a current source inverter induction motor drive and their effects on the dynamic response and stability of the system. A d-q model is developed which incorporates the induction motor and the inverter power supply with current feedback. The model is first used to determine steady-state curves to determine operating points. A linearized small signal model is developed to study stability and provide suitable transfer functions for various control strategies. A slip speed control stabilizes the system. Two implementations of flux control were used earlier by Lipo [17] and Macdonald [18] are shown to have little difference. In general flux control has been shown to further improve dynamic performance and to enable simplification of the drive model i.e. several pole-zero cancellations are possible.

The transient response of controlled-current inverter fed induction motor with independent current and slip frequency controls, is investigated by B.deFornell and B. Noyes [22] and compared with open-loop system. Its transient behaviour is stable for all operating points, and the control of the rotor current frequency and the shape and amplitude of the

stator currents results in a great reduction in the maximum amplitudes of torque oscillations during starting. Thus, the constraints imposed upon the converter are less than in the case of a voltage-fed system. This permits a very fast response drive without an exaggerated overrating of the static converters.

A simplified analytical model for steady-state analysis of a rectifier current source inverter (CSI) induction motor drive is developed by s. semir [ 23 ] and verified by comparing computer results with those obtained for the same system represented in details. The simplified model, which represents system behaviour in the synchronous reference frame, neglects converter harmonics but include an approximation of the voltage spikes produced during inverter commutation. The/ <sup>computer</sup> simulation result demonstrates the usefulness of the simplified model for the study of control dynamics.

## 1.2 AUTHOR'S CONTRIBUTION

The author considers a closed-loop induction motor drive operated from a rectifier-controlled-current inverter source. It is well known that such a drive, in the open-loop mode of operation, exhibits instability in almost entire operating range. The author has attempted to stabilise the drive over very wide range of operating speeds through proper coordination of the parameters of the controllers. The controllers used are -



- (i) proportional speed controller
- (ii) p-i controller working on d.c.link current
- (iii) slip regulator.

The author first develops a mathematical model of drive in per unit system.

Next, in chapter 3, she discusses the steady-state drive performance, such as power output, voltage, power factor, efficiency etc. as affected by change in load torque at different p.u. operational frequencies.

In Chapter 4 the stability analysis of the drive is carried out. The author uses the D-partitioning technique to coordinate drive parameters. The controller parameters are determined to ensure a certain minimum degree of relative stability of the system and give similar performance at all p.u. operating frequencies.

The subject matter of the chapter 5 is the problem of torque and speed pulsations caused due to nonsinusoidal current waveform of the inverter output. A detailed study has been made to determine the magnitude of the sixth harmonic torque, current, voltage and rotor speed pulsations of the motor when operating under different speed and load conditions.

In chapter 6 the transient performance of the drive is discussed using a nonlinear 5th-order state-space model of the

system under various operating conditions of the drive like starting, sudden speed changes in both up and down direction and reversal in the direction of rotation of the motor.

The concluding chapter sums up the various studies made in this dissertation and gives a recommendation concerning the best set of regulator parameters to achieve high-performance characteristics of the drive. The dissertation concludes with further scope of future work.

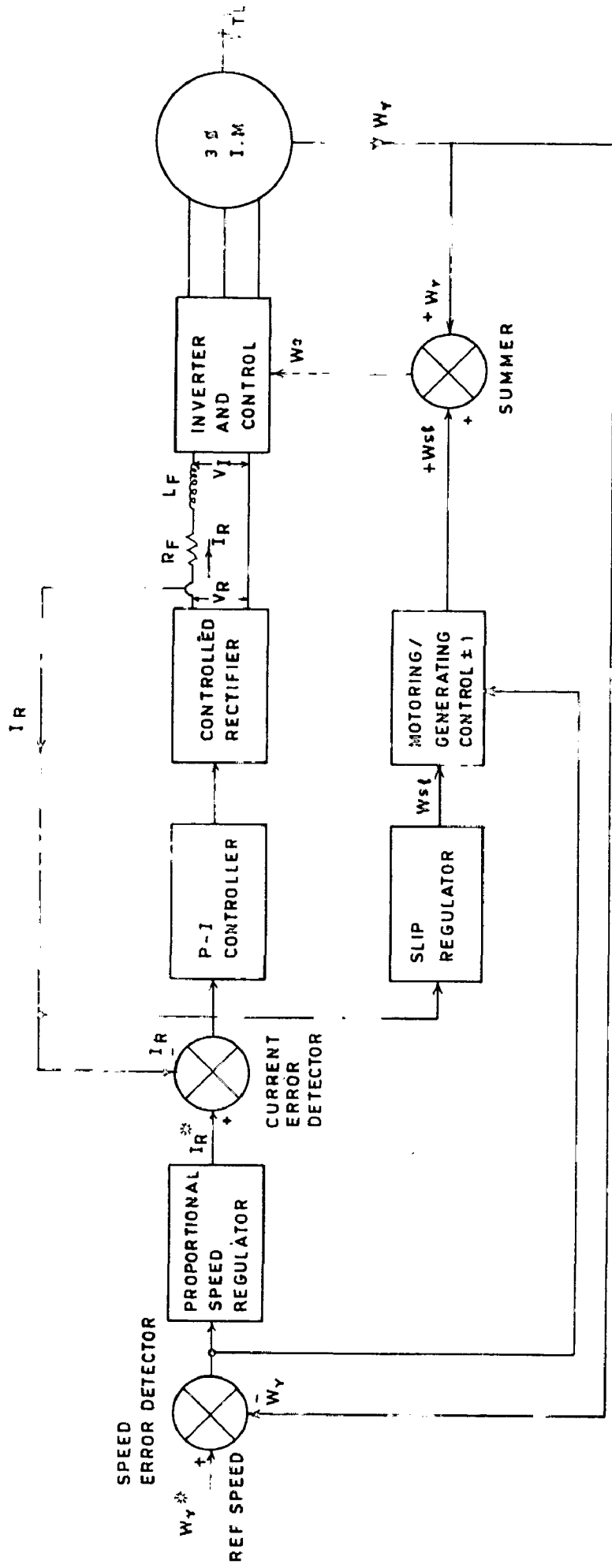


Fig 21 VARIABLE SPEED CONTROLLED SLIP INDUCTION MOTOR DRIVE

## CHAPTER - 2

## THE MATHEMATICAL MODEL OF THE DRIVE

An a.c. drive, employing the current source converter consists of a controlled rectifier, a d.c. link filter choke (without a capacitor bank) and a current mode inverter. The controlled rectifier and filter choke combine to form a d.c. current regulator which supplies a regulated d.c. current to the current mode inverter. A closed loop rectifier controlled-current inverter source fed induction motor drive is considered here. A drive structure containing a proportional speed regulator, a p-i current controller for stabilization of the drive and a slip regulator to maintain the rated air gap flux in the induction motor, has been selected. The induction motor has been mathematically modelled in its synchronously rotating reference frame. Complete mathematical equations of the drive suitable for both motoring and braking operations, have been systematically developed in Concordia's per-unit system.

## 2.1 SYSTEM STUDIED

A diagram of the drive system studied is shown in Fig. 2.1. This system comprises of a three-phase power source, controlled rectifier bridge, a d.c. link smoothing reactor, a current-controlled inverter (CCI) and three-phase squirrel-cage induction motor. The magnitude and polarity of speed error are used to determine the d.c. link current reference value. Rectifier output voltage is controlled by a p-i

controller working on the d.c. link current error. The d.c. link current is used to set the value of slip speed through the slip regulator. This maintains the air-gap flux in machine at a constant value. The slip speed is added to, or subtracted from, the rotor speed in order to determine the synchronous speed, which then decides the inverter operating frequency.

## 2.2 SYSTEM EQUATIONS (In M.K.S.)

When supplied from a current-controlled inverter the motor phase currents are not sinusoidal but are rectangular in nature and flow for only 120 degrees of each half cycle (neglecting commutation effects). Ideally only two phases conduct at any instant of time resulting in six distinct modes of operation of the inverter. Fig. 2.2 shows resulting line currents under the assumption of quasi-steady-state conditions.

With  $I_R$  as the magnitude of the current in the d.c. link and  $\omega_e$  the inverter frequency, these stepped currents exciting the three stator phases can be represented by the Fourier Series expansions given by equation (2.1),

$$i_{as} = \frac{2\sqrt{3}}{\pi} I_R \left[ \cos \omega_e t - \frac{1}{5} \cos 5 \omega_e t + \frac{1}{7} \cos 7 \omega_e t - \frac{1}{11} \cos 11 \omega_e t \dots \dots \right]$$

$$i_{bs} = \frac{2\sqrt{3}}{\pi} I_R \left[ \cos \left( \omega_e t - \frac{2\pi}{3} \right) - \frac{1}{5} \cos \left( 5 \omega_e t + \frac{2\pi}{3} \right) + \frac{1}{7} \cos \left( 7 \omega_e t - \frac{2\pi}{3} \right) \dots \dots \right]$$

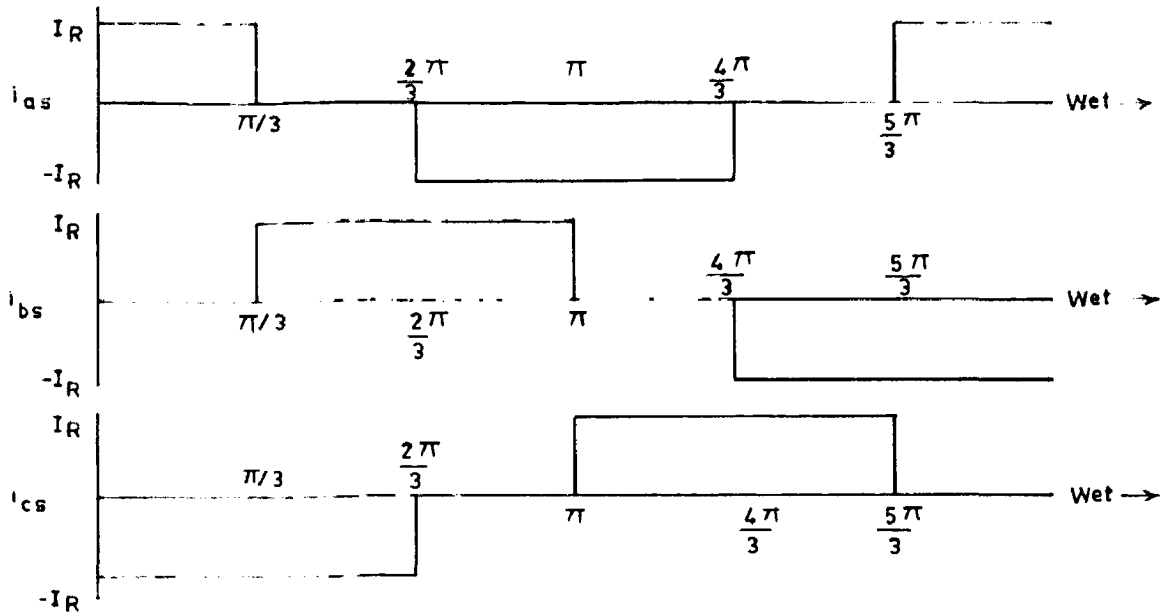


Fig.22 IDEALIZED MOTOR LINE CURRENTS

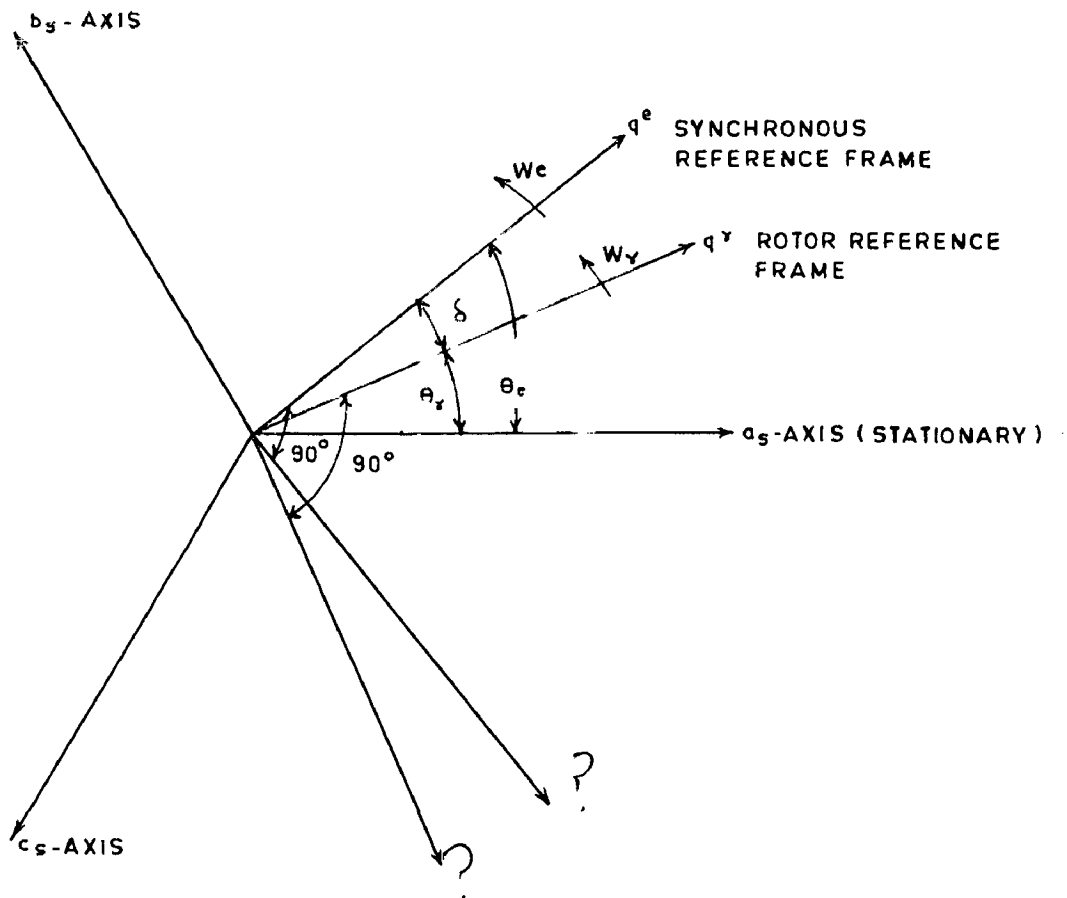


Fig.23 REFERENCH FRAMES

$$i_{cs} = \frac{2\sqrt{3}}{\pi} I_R \left[ \cos(\omega_e t + \frac{2\pi}{3}) - \frac{1}{5} \cos(5\omega_e t - \frac{2\pi}{3}) + \frac{1}{7} \cos(7\omega_e t + \frac{2\pi}{3}) \dots \right] \quad \dots (2.1)$$

The phase current expressions can be transformed to a  $q^e - d^e$  reference frame running at the synchronous electrical angular velocity of the fundamental component of the current applied to the machine stator (i.e.  $\omega_e$ ). The  $q^e$  axis of the reference frame is assumed to coincide with the stator a - phase axis ( $a_s$ ) at  $t = 0$ . Fig. 2.3 shows the various reference axes. The following equations of transformation will be used to transform  $i_{as}$ ,  $i_{bs}$  and  $i_{cs}$  to the  $q^e - d^e$  reference frame,

$$\left. \begin{aligned} i_{qs}^e &= \frac{2}{3} \left[ i_{as} \cos \theta_e + i_{bs} \cos(\theta_e - \frac{2\pi}{3}) + i_{cs} \cos(\theta_e + \frac{2\pi}{3}) \right] \\ i_{ds}^e &= \frac{2}{3} \left[ i_{as} \sin \theta_e + i_{bs} \sin(\theta_e - \frac{2\pi}{3}) + i_{cs} \sin(\theta_e + \frac{2\pi}{3}) \right] \\ i_{os}^e &= \frac{1}{3} [i_{as} + i_{bs} + i_{cs}] \end{aligned} \right\} \quad \dots (2.2)$$

Substitution of  $i_{as}$ ,  $i_{bs}$  and  $i_{cs}$  from equations (2.1) in equations (2.2) yields

$$\begin{aligned}
 i_{os}^e &= 0 \\
 i_{qs}^e &= \frac{2\sqrt{3}}{\pi} I_R \left[ 1 - \frac{2}{35} \cos 6 \omega_e t - \frac{2}{143} \cos 12 \omega_e t \right. \\
 &\quad \left. \dots \dots \dots \right] \\
 i_{ds}^e &= \frac{2\sqrt{3}}{\pi} I_R \left[ -\frac{12}{35} \sin 6 \omega_e t - \frac{24}{143} \sin 12 \omega_e t \right. \\
 &\quad \left. \dots \dots \dots \right]
 \end{aligned}
 \quad \dots(2.3)$$

Equations (2.3) may also be written as

$$\begin{aligned}
 i_{qs}^e &= \frac{2\sqrt{3}}{\pi} I_R g_{qs}^e \\
 i_{ds}^e &= \frac{2\sqrt{3}}{\pi} I_R g_{ds}^e
 \end{aligned}
 \quad \dots(2.4)$$

where

$$\begin{aligned}
 g_{qs}^e &= \left[ 1 - \frac{2}{35} \cos 6 \omega_e t - \frac{2}{143} \cos 12 \omega_e t \dots \right] \\
 g_{ds}^e &= \left[ -\frac{12}{35} \sin 6 \omega_e t - \frac{24}{143} \sin 12 \omega_e t \dots \right]
 \end{aligned}
 \quad \dots(2.5)$$

If it is assumed that no power is lost in the inverter then

$$\begin{aligned}
 V_R I_R &= (V_{as} i_{as} + V_{bs} i_{bs} + V_{cs} i_{cs}) \\
 &= \frac{3}{2} [v_{qs}^e i_{qs}^e + v_{ds}^e i_{ds}^e]
 \end{aligned}
 \quad \dots(2.6)$$

Substituting the value of  $i_{qs}^e$ ,  $i_{ds}^e$  from equations (2.4) in equation (2.6), the inverter voltage can be expressed as

$$V_I = \frac{3\sqrt{3}}{\pi} [v_{qs}^e g_{qs}^e + v_{ds}^e g_{ds}^e] \quad \dots (2.7)$$

The differential equation for the d.c.link is given by

$$V_{RX} = V_I + \left( R_F + \frac{p}{\omega_b} X_F \right) I_R \quad \dots (2.8)$$



where  $V_{RX}$  is rectifier output voltage and is given by

$$V_{RX} = \frac{3\sqrt{3}}{\pi} V_s \cos \alpha - \frac{3}{\pi} X_{CO} I_R \quad \dots (2.9)$$

where

$V_s$  = supply line voltage (rms)

$X_{CO}$  = commutating reactance (ohms)

$\alpha$  = firing angle

Defining

$$\frac{3\sqrt{3}}{\pi} V_s \cos \alpha = V_R$$

Thus

$$V_{RX} = V_R - \frac{3}{\pi} X_{CO} I_R \quad \dots (2.10)$$

Substituting the expression of  $V_{RX}$  from equation (2.10) in equation (2.9) results in

$$V_R = V_I + \left( R_F + \frac{3}{\pi} X_{CO} + \frac{p}{\omega_b} X_F \right) I_R \quad \dots (2.11)$$

The induction motor can be adequately modelled using a two-axis representation developed from the generalized machine theory. Several assumptions are required in order to use this relatively elegant representation. These are as follows :

- (i) The 3-phase stator windings of the motor are balanced and sinusoidally distributed in space.
- (ii) Rectifier output voltage is pure d.c.
- (iii) No saturation occurs and thus superposition theorem is applicable.

- (iv) The switching transients in the inverter are ignored i.e. the commutation period is negligible.
- (v) There are no core losses in the induction machine and all solid-state devices are assumed to be loss-free.

The motor can then be described by the following fourth-order matrix equation

$$\begin{bmatrix} v_{qs}^e \\ v_{ds}^e \\ 0 \\ 0 \end{bmatrix} = \begin{bmatrix} r_s + \frac{p}{\omega_b} X_s & \frac{\omega_e}{\omega_b} X_s & \frac{p}{\omega_b} X_m & \frac{\omega_e}{\omega_b} X_m \\ -\frac{\omega_e}{\omega_b} X_s & r_s + \frac{p}{\omega_b} X_s & -\frac{\omega_e}{\omega_b} X_m & \frac{p}{\omega_b} X_m \\ \frac{p}{\omega_b} X_m & \frac{\omega_{sl}}{\omega_b} X_m & r_s + \frac{p}{\omega_b} X_r & \frac{\omega_{sl}}{\omega_b} X_r \\ -\frac{\omega_{sl}}{\omega_b} X_m & \frac{p}{\omega_b} X_m & -\frac{\omega_{sl}}{\omega_b} X_r & r_s + \frac{p}{\omega_b} X_r \end{bmatrix} \begin{bmatrix} i_{qs}^e \\ i_{ds}^e \\ i_{qr}^e \\ i_{dr}^e \end{bmatrix} \quad \dots(2.12)$$

Here  $\omega_e$  denotes the angular velocity of the synchronously rotating reference frame, while  $\omega_r$  the equivalent electrical angular velocity of the rotor.  $\omega_b$  represents the base or reference angular velocity used to establish a per-unit system ( $\omega_b = 2\pi f_b$ ). Further,

$$\omega_{sl} = \omega_e - \omega_r \quad \text{ER/sec} \quad \dots (2.13)$$

The electromagnetic torque equation of the motor is

$$T_e = \frac{3}{2} \cdot \frac{P}{2} \frac{1}{\omega_b} X_m [i_{qs}^e i_{dr}^e - i_{ds}^e i_{qr}^e] \quad \dots (2.14)$$

where  $P =$  number of poles.

### 2.3 EQUATIONS IN THE CONCORDIA'S p.u. SYSTEM

From equations (2.1),

$$i_{as} = \frac{2\sqrt{3}}{\pi} I_R \left[ \cos \omega_e t - \frac{1}{5} \cos 5 \omega_e t + \frac{1}{7} \cos 7 \omega_e t - \frac{1}{11} \cos 11 \omega_e t \dots \right]$$

Let the r.m.s. value of base current on machine side be  $I_b$  amps. per phase (subscript b stands for base). Maximum value of this base current is  $\sqrt{2} I_b$  amps. Defining 1 p.u. d.c. link current ( $I_{Ib}$ ) as that current which gives 1 p.u. machine phase currents. Thus, from above equation

$$\sqrt{2} I_b = \frac{2\sqrt{3}}{\pi} I_{Ib}$$

$$\text{Hence } I_{Ib} = \frac{\sqrt{2} \pi}{2\sqrt{3}} I_b \quad \dots (2.15)$$

$$\text{Unit power on inverter side} = V_{Ib} I_{Ib}$$

Unit power on machine side ( $G$ ) =  $3 V_b I_b$  (under unit power factor conditions) where  $V_{Ib}$  is inverter base voltage.

and  $V_b$  is machine base voltage.

Equating power on inverter side to power on machine side for finding out inverter base voltage, assuming lossless inverter

$$V_{Ib} I_{Ib} = 3 V_b I_b$$

$$\text{Hence } V_{Ib} = \frac{3 V_b I_b}{I_{Ib}} \quad \dots (2.16)$$

Substituting the expression for  $I_{Ib}$  from equation (2.15) in equation (2.16)

$$\begin{aligned} V_{Ib} &= \frac{3 V_b I_b}{\sqrt{2} \pi I_b} 2\sqrt{3} \\ &= \frac{3\sqrt{6}}{\pi} V_b \end{aligned} \quad \dots (2.17)$$

$$\begin{aligned} \text{Base Impedance on machine side} &= \frac{V_b}{I_b} \\ &= z_b \text{ ohms/phase} \end{aligned} \quad \dots (2.18)$$

$$\begin{aligned} \text{Base Impedance on inverter side} &= \frac{V_{Ib}}{I_{Ib}} \\ &= \frac{\frac{3\sqrt{6}}{\pi} V_b}{\frac{\sqrt{2} \pi}{2\sqrt{3}} I_b} \\ &= \frac{18}{\pi^2} z_b \text{ ohms} \end{aligned} \quad \dots (2.19)$$

$$\begin{aligned} \text{Base torque (Nm)} &= T_{\text{base}} \\ &= \frac{G}{2\pi f_b / P/2} \end{aligned} \quad \dots (2.20)$$

where  $f_b$  is base frequency in Hz.

Dividing both sides of equation (2.11) by  $V_{Ib}$

$$\frac{V_R}{V_{Ib}} = \frac{V_I}{V_{Ib}} + (R_F + \frac{3}{\pi} X_{CO} + \frac{p}{\omega_b} X_F) \frac{I_R}{I_{Ib}} \cdot \frac{I_{Ib}}{V_{Ib}}$$

$$\text{or } V_R' = V_I' + (R_F' + X_{CO}' + p X_F') I_R' \quad \dots (2.21)$$

Dash shows various quantities in p.u.

In Concordia's p.u. system  $p = \frac{d}{d\tau}$  with  $\omega_b = 1$  and  $\tau = 2\pi f_b t$  p.u. time.

Considering equation (2.1)

$$i_{as} = \frac{2\sqrt{3}}{\pi} I_R \left[ \cos \omega_e t - \frac{1}{5} \cos 5 \omega_e t + \frac{1}{7} \cos 7 \omega_e t - \frac{1}{11} \cos 11 \omega_e t \dots \right]$$

Dividing both sides by  $\sqrt{2} I_b$

$$\frac{i_{as}}{\sqrt{2} I_b} = \frac{2\sqrt{3}}{\pi} \cdot \frac{I_R}{\sqrt{2} I_b} \left[ \cos \omega_e t - \frac{1}{5} \cos 5 \omega_e t + \frac{1}{7} \cos 7 \omega_e t - \frac{1}{11} \cos 11 \omega_e t \dots \right]$$

or

$$i_{as}' = I_R' \left[ \cos \omega_e t - \frac{1}{5} \cos 5 \omega_e t + \frac{1}{7} \cos 7 \omega_e t - \frac{1}{11} \cos 11 \omega_e t \dots \right] \quad \dots (2.22)$$

Similarly other equations can be written in p.u. and are given below

$$v_{I'} = v_{qs}^{e'} g_{qs}^e + v_{ds}^{e'} g_{ds}^e \quad \dots (2.23)$$

$$i_{qs}^{e'} = I_R' g_{qs}^e \quad \dots (2.24)$$

$$i_{ds}^{e'} = I_R' g_{ds}^e \quad \dots (2.25)$$

equations (2.12) also can be written in p.u. as follows -

$$\begin{bmatrix} v_{qs}^{e'} \\ v_{ds}^{e'} \\ 0 \\ 0 \end{bmatrix} = \begin{bmatrix} r_s' + pX_s' & \omega_e' X_s' & pX_m' & \omega_e' X_m' \\ -\omega_e' X_s' & r_s' + pX_s' & -\omega_e' X_m' & pX_m' \\ pX_m' & \omega_{sl}' X_m' & r_r' + pX_r' & \omega_{sl}' X_r' \\ -\omega_{sl}' X_m' & pX_m' & -\omega_{sl}' X_r' & r_r' + pX_r' \end{bmatrix} \begin{bmatrix} i_{qs}^{e'} \\ i_{ds}^{e'} \\ i_{qr}^{e'} \\ i_{dr}^{e'} \end{bmatrix} \quad \dots(2.26)$$

Now considering equation (2.14)

$$T_e = \frac{3}{2} \frac{p}{2} \frac{1}{\omega_b} X_m [i_{qs}^{e'} i_{dr}^{e'} - i_{ds}^{e'} i_{qr}^{e'}] \quad \dots(2.27)$$

Dividing both sides by  $T_{base}$  i.e.  $\frac{3 V_b I_b}{2\pi f_b/p/2}$

$$T_e' = X_m' [i_{qs}^{e'} i_{dr}^{e'} - i_{ds}^{e'} i_{qr}^{e'}] \quad \dots(2.28)$$

In the above equations dash variables are used to differentiate between p.u. system and M.K.S. system quantities. In the succeeding chapters the dashes will be dropped out for the sake of notational convenience and it will be remembered that all equations are in the Concordia's p.u. system with motoring convention.

#### 2.4 EQUATION OF MOTION

Equation of motion is given by the following expression (in M.K.S. unit).

$$\frac{2J}{p} \frac{d\omega_r}{dt} = T_e - T_L \quad \dots (2.29)$$

where

$J$  = Polar moment of inertia,  $\text{kg-m}^2$

$p$  = Number of poles

$\omega_r$  = Speed, electrical radians per second

$t$  = Time, seconds

$T_e$  = Electromagnetic torque, Newton meter

$T_L$  = Load torque, Newton meter

Dividing both side of equation (2.29) by  $T_{\text{base}}$  (equation 2.20)

$$\frac{J}{p^2/4} \cdot \frac{2\pi f_b}{G} \frac{d\omega_r}{dt} = T_e - T_L \quad \dots (2.30)$$

where

$T_e$  and  $T_L$  are in p.u.

The inertia constant of the machine  $H$  in seconds is given by

$$H = \frac{\frac{1}{2} J \left( \frac{\omega_b}{p/2} \right)^2}{G}$$

where  $\omega_b$  is base angular speed in electrical radians/sec. i.e.

$$\omega_b = 2\pi f_b.$$

Rewriting equation (2.30)

$$\frac{2 \frac{1}{2} J \left( \frac{\omega_b}{p/2} \right)^2}{G} \frac{d}{dt} \left( \frac{\omega_r}{\omega_b} \right) = T_e - T_L$$

$$\text{or } 4\pi f_b H \frac{d}{dt} \left( \frac{\omega_r}{\omega_b} \right) = T_e - T_L$$

$$\text{or } 4\pi f_b H \frac{d}{dt} (\omega_r') = T_e - T_L \quad \dots (2.31)$$

where  $\tau = 2\pi f_b t$  and  $\omega_r' = \frac{\omega_r}{f_b}$

As before, for notational convenience  $\omega_r'$  is written simply as  $\omega_r$  and hence,

$$4\pi f_b H p \omega_r = T_e - T_L \quad \dots (2.32)$$

where  $p = \frac{d}{d\tau}$

## 2.5 CONTROL STRATEGIES

The difference between the set value of speed and actual speed (i.e. speed error) decides the d.c. link reference current.

$$I_R^* = K_{sp} (\omega_r^* - \omega_r) \quad \dots (2.33)$$

where  $\omega_r^*$  and  $\omega_r$  are in p.u.

$K_{sp}$  is the proportionality constant.  $I_R^*$  should not be more than a set maximum value  $I_{max}$  as shown in Fig.(2.4).

The controlled rectifier output voltage is dependent upon the d.c. link current error (i.e. difference between the set value of d.c. link current and actual d.c. link current), thus

$$V_R = \frac{K_C(1 + T \omega_b p)}{\omega_b p} (I_R^* - I_R) \quad \dots (2.34)$$

The air-gap flux of the induction motor must be controlled to give improved performance of the drive. There are several methods for flux control, viz. direct flux sensing, voltage sensing and current-slip frequency control. The last method is most



suitable for the present case because the motor current can be easily controlled by the current-source inverter. For constant V/f ratio slip speed (p.u.) is merely proportional to d.c. link current and is given by

$$\omega_{s\ell} = K_{s\ell} I_R \quad \dots(2.35)$$

Where  $K_{s\ell}$  is the proportionality constant.  $\omega_{s\ell}$  is really not proportional to  $I_R$  for smaller values of  $I_R$  due to the magnetising current component (Fig. 2.5). With an approximation  $\omega_{s\ell}$  will be considered to be proportional to  $I_R$  for the entire range in  $I_R$  [ 18 ]. The relationship between  $I_R$  and  $\omega_{s\ell}$  depends upon machine parameters and does not depend upon p.u. operating frequency. Its proof is given in Appendix ( I ). The synchronous speed is given by

$$\omega_e = \omega_r \pm \omega_{s\ell} \quad \dots(2.36)$$

Where positive sign for  $\omega_{s\ell}$  is taken if  $(\omega_r^* - \omega_r)$  is positive i.e. for motoring operation and negative if  $(\omega_r^* - \omega_r)$  is negative i.e. for generating (braking) operation.

## 2.6 SYSTEM PARAMETERS

The specification of the induction motor selected for illustration is as below [ 16 ]

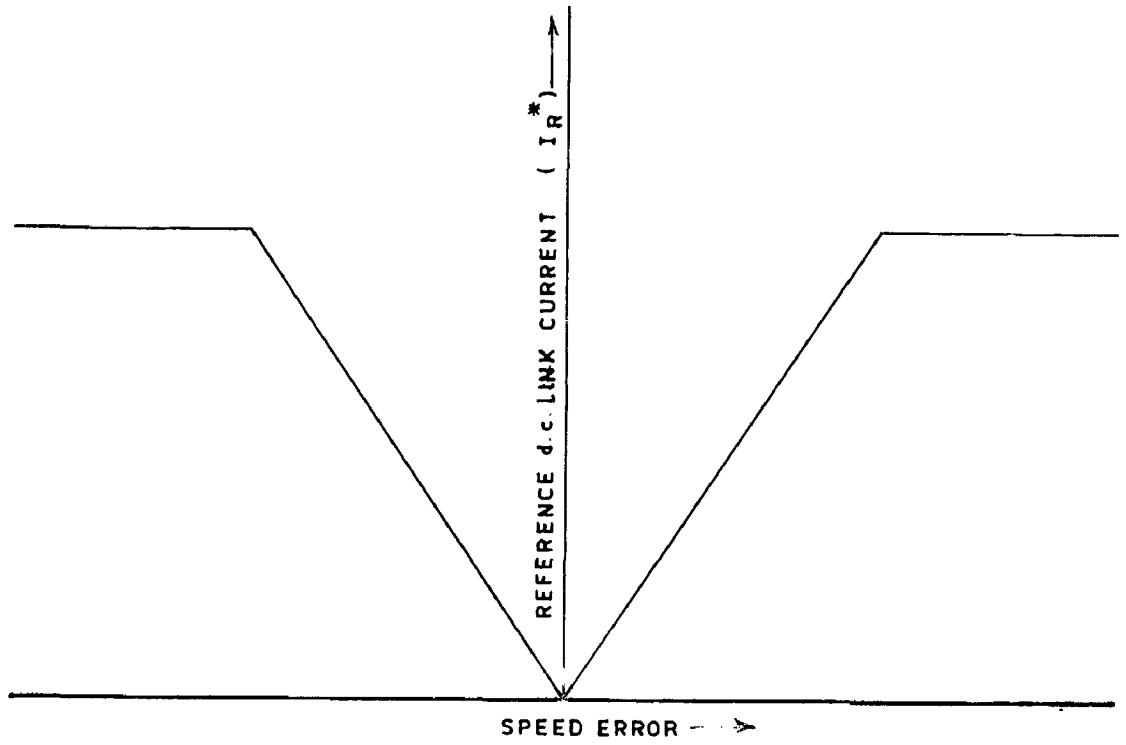


Fig 2-4 PROPORTIONAL SPEED REGULATOR CHARACTERISTIC

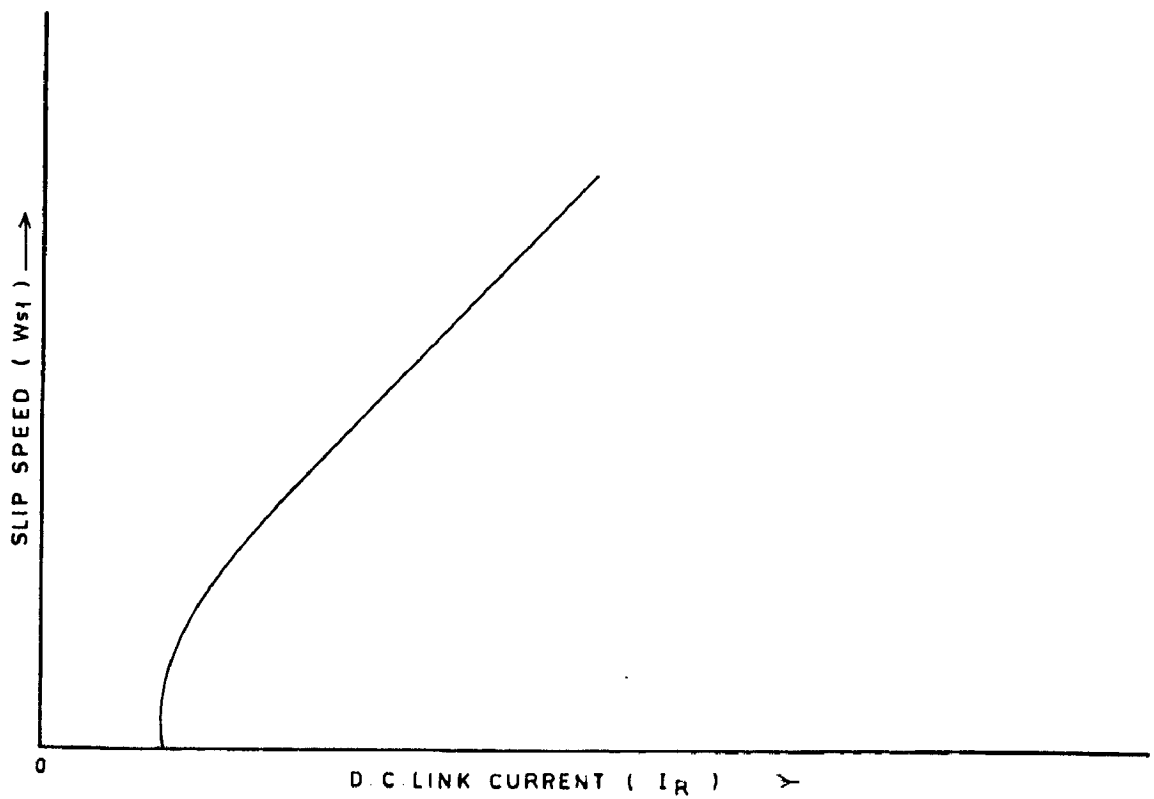


Fig.25 SLIP REGULATOR CHARACTERISTIC

Motor name plate data

18.6 KW

4 pole

3-phase Y-connected

 $\omega_b = 314$  rad/sec $J_{\text{Total}} = 0.31$  kg-m<sup>2</sup> $V_{\text{rated}} = 230$  V (r.m.s.) $I_{\text{rated}} = 64$  A (r.m.s.) $T_{\text{rated}} = 118.411$  N-mMotor and filter parameters

	M.K.S. (ohm)	p.u.
$r_s$	0.079	0.038
$r_r$	0.041	0.020
$x_s$	4.793	2.310
$x_r$	5.002	2.41
$x_m$	4.542	2.189
$x_F$	5.500	1.453
$R_F$	0.09	0.0240
$x_{CO}$	0.063	0.016

Base Quantities

$$V_{\text{base}} = 132.8 \text{ volts}$$

$$I_{\text{base}} = 64 \text{ Amps}$$

$$T_{\text{base}} = 164.4 \text{ N-m}$$

$$Z_b = 2.075 \text{ ohm}$$

$$Z_{Ib} = 3.78 \text{ ohm}$$

$$H = 0.15 \text{ sec.}$$

## 2.7 CONCLUSION

The mathematical model of the current-source inverter fed variable speed induction motor has been developed in the Concordia's p.u. system in this chapter. The induction motor equations are written in a synchronously rotating reference frame under quasi-steady-state conditions in its stator circuit. The air-gap flux in the induction motor is proposed to be held at rated value under below-rated speed conditions of the drive by a slip regulator. A proportional speed regulator, working on the speed error, will set the d.c. link current references while a p-i controller is proposed to maintain the actual d.c. link current equal to the reference value.

Using this mathematical model various aspects of the drive performance, such as steady-state performance, stability analysis, harmonic torque pulsation, transient performance are investigated in the following chapters.

## CHAPTER - 3

## THE STEADY-STATE ANALYSIS OF THE DRIVE

The introduction of controlled-current inverter employing thyristors has made the use of variable speed induction motor drive technically attractive. In this chapter the steady-state drive equations are first developed using the mathematical model developed in the previous chapter. The steady-state performance of the drive is determined and the results are discussed.

## 3.1 STEADY-STATE EQUATIONS

Following additional assumption, in addition to those in the mathematical modelling, is made to derive the steady-state equations of the drive.

The effect of harmonics is neglected. Thus only fundamental component of a.c. is considered (i.e.  $g_{ds}^e = 0$  and  $g_{qs}^e = 1$  in equations (2.24) and (2.25)).

Under steady-state conditions the machine variables in  $q^e - d^e$  reference frame and d.c. link variables are constants. Hence, in this case substituting differential terms as zero and also substituting  $g_{ds}^e = 0$  and  $g_{qs}^e = 1$  equation (2.21) to (2.28) can be expressed in the following form -

$$V_{RO} = V_{IO} + (R_F + X_{CO}) I_{RO} \quad \dots (3.1)$$

$$V_{IO} = v_{qso}^e \quad \dots (3.2)$$

$$i_{qso}^e = I_{RO} \quad \dots (3.3)$$

$$i_{dso}^e = 0.0 \quad \dots (3.4)$$

$$\begin{bmatrix} v_{qso}^e \\ v_{dso}^e \\ 0 \\ 0 \end{bmatrix} = \begin{bmatrix} r_s & \omega_e X_s & 0 & \omega_e X_m \\ -\omega_e X_s & r_s & -\omega_e X_m & 0 \\ 0 & \omega_{sl} X_m & r_r & \omega_{sl} X_r \\ -\omega_{sl} X_m & 0 & -\omega_{sl} X_r & r_r \end{bmatrix} \begin{bmatrix} i_{qso}^e \\ i_{dso}^e \\ i_{qro}^e \\ i_{dro}^e \end{bmatrix} \quad \dots(3.5)$$

$$\left. \begin{aligned} T_e &= X_m [i_{qso}^e \ i_{dro}^e] \\ &= T_L \end{aligned} \right\} \quad \dots(3.6)$$

$\omega_e$  is ratio of the applied electrical frequency to the base frequency. It can be interpreted as the per-unit operating frequency.

From equations (3.4) and (3.5)

$$v_{qso}^e = r_s i_{qso}^e + \omega_e X_m i_{dro}^e \quad \dots(3.7)$$

$$0 = r_r i_{qro}^e + \omega_{sl} X_r i_{dro}^e \quad \dots(3.8)$$

$$0 = -\omega_{sl} X_m i_{qso}^e - \omega_{sl} X_r i_{qro}^e + r_r i_{dro}^e \quad \dots(3.9)$$

From equation (3.8)

$$i_{qro}^e = -\frac{\omega_{sl} X_r}{r_r} i_{dro}^e \quad \dots(3.10)$$

Substituting value of  $i_{qro}^e$  from equation (3.10) in equation (3.9) and solving for  $i_{dro}^e$

$$i_{dro}^e = \frac{\omega_{sl} X_m r_r}{(\omega_{sl} X_r)^2 + (r_r)^2} i_{qso}^e \quad \dots(3.11)$$

Substitution of the expression for  $i_{dro}^e$  from equation (3.11) in equations (3.7), (3.6) and (3.10) respectively, gives the following -

$$v_{qso}^e = \left[ \gamma_s + \frac{\omega_e \omega_{sl} (x_m)^2 \gamma_r}{(\omega_{sl} x_r)^2 + (\gamma_r)^2} \right] i_{qso}^e \quad \dots(3.12)$$

$$T_e = \frac{\omega_{sl} x_m^2 \gamma_r}{(\omega_{sl} x_r)^2 + (\gamma_r)^2} (i_{qso}^e)^2 \quad \dots(3.13)$$

$$i_{qro}^e = - \frac{(\omega_{sl})^2 x_r x_m}{(\omega_{sl} x_r)^2 + (\gamma_r)^2} i_{qso}^e \quad \dots(3.14)$$

Rewriting equation for  $v_{dso}^e$  from equation (3.5)

$$v_{dso}^e = -\omega_e x_s i_{qso}^e - \omega_e x_m i_{qro}^e \quad \dots(3.15)$$

Substitution of the expression for  $i_{qro}^e$  from equation (3.14) in equation (3.15) results in

$$v_{dso}^e = \left[ -\omega_e x_s + \frac{\omega_e (\omega_{sl})^2 x_r x_m^2}{(\omega_{sl} x_r)^2 + (\gamma_r)^2} \right] i_{qso}^e \quad \dots(3.16)$$

With reference to Fig. 2.3, since the  $q^e$  axis, is assumed to coincide with  $a_s$  phase axis at  $t = 0$ .

$$\text{Hence, } \theta_e = \omega_e t$$

$$i_{as} = i_{qs}^e \cos \theta_e$$

$$v_{as} = v_{qs}^e \cos \theta_e + v_{ds}^e \sin \theta_e$$

$$= v_{as} \cos (\theta_e + \phi_e)$$

$$v_{as} = \sqrt{(v_{qso}^e)^2 + (v_{dso}^e)^2} \quad \dots(3.17)$$

$$\text{Power factor (lag)} = \cos \left[ \tan^{-1} \left( - \frac{v_{dso}^e}{v_{qso}^e} \right) \right] \quad \dots(3.18)$$

Rewriting equation (3.1)

$$V_{RO} = V_{IO} + (R_F + X_{CO}) I_{RO} \quad \dots(3.19)$$

Substitution of the expressions for  $V_{IO}$  and  $I_{RO}$  from equations (3.2) and (3.3) in equation (3.19) yields

$$V_{RO} = v_{qso}^e + (R_F + X_{CO}) i_{qso}^e \quad \dots(3.20)$$

#### Copper Losses of the Drive

$$\text{Copper losses in induction motor stator} = r_s (i_{qso}^e)^2 \quad \dots(3.21)$$

$$\text{Copper losses in induction motor rotor} = r_r \left[ (i_{dro}^e)^2 + (i_{qro}^e)^2 \right] \quad \dots(3.22)$$

Substituting expression for  $i_{qro}^e$  from equation (3.14) and expression for  $i_{dro}^e$  from (3.11) in equation (3.22)

$$\text{Copper losses in rotor} = \frac{r_r \omega_{sl}^2 x_m^2}{(\omega_{sl} x_r)^2 + (r_r)^2} (i_{qso}^e)^2 \quad \dots(3.23)$$

$$\text{Losses in d.c. link} = R_F I_{RO}^2$$

Substituting the expression of  $I_R$  from equation (3.3) in above equation gives

$$\text{Losses in d.c. link} = R_F (i_{qso}^e)^2 \quad \dots(3.24)$$

Ignoring the iron friction and windage losses total losses are determined as follows -



Total losses in Drive = losses in induction motor stator +  
 losses in induction motor rotor +  
 losses in filter

$$= \left[ r_s + R_F + \frac{r_r (\omega_{sl})^2 X_m^2}{(\omega_{sl} X_r)^2 + (r_r)^2} \right] (i_{qso}^e)^2 \quad \dots(3.25)$$

$$\begin{aligned} \text{Efficiency of the drive} &= \frac{T_e \omega_r}{T_e \omega_r + \text{Total losses in drive}} \\ &= \frac{T_e (\omega_e - \omega_{sl})}{T_e (\omega_e - \omega_{sl}) + \text{total losses in drive}} \end{aligned} \quad \dots(3.26)$$

$$\begin{aligned} \text{Power Output} &= T_e \omega_r \\ &= T_e (\omega_e - \omega_{sl}) \end{aligned} \quad \dots(3.27)$$

### 3.2 RESULT AND DISCUSSION

In this section theoretical results concerning the steady-state performance of induction motor drive are discussed. The computer programme is given in Appendix - II.

For determining the drive performance the values of induction motor stator voltages, power factor, torque, power output and efficiency can be calculated for different p.u. operating frequency and slip at any particular fixed value of the d.c. link (stator) current.

All the performance characteristics are plotted with respect to torque i.e. stator voltage vs torque, power output vs torque, efficiency vs torque, power factor vs torque, total losses vs torque, and slip vs torque.

### 3.2.1 Induction-Motor Stator Voltage vs Torque

The characteristic curves are plotted in Fig.3.2. Corresponding to each value of torque there are two values of stator voltage one in positive - slope (unstable) region and another in negative - slope (stable) region of torque - slip characteristic. In the stable zone of torque slip characteristic of induction motor, the range of operating slip is very small but the stator voltages are very high. Thus machine operation in stable zone is not permissible due to high saturation. Stator voltages in unstable zone of torque slip characteristic of induction motor are not high. However, open-loop operation in unstable zone is not possible. With the help of feed back, operation in unstable zone is possible.

As p.u. operating frequency is decreased stator voltages in both zones decrease. In the graph stator voltage-torque curves are plotted for four different p.u. operating frequencies. As p.u. operating frequency decreases the difference in voltages in both zones also decreases. Thus the machine is highly saturated in stable zone under high p.u. frequency of operation.

### 3.2.2 Power Output vs Torque

The power output vs torque characteristic of the drive for different p.u. frequency of operation, are shown in Fig.3.1. As expected, the power output is more for a given electrical torque at higher p.u. frequency of operation. For any p.u. frequency of operation, however, the output power is less for operation in unstable zone in comparison to operation in stable

zone of torque-slip characteristic due to increased rotor losses (core losses are ignored).

### 3.2.3 Drive Efficiency vs Torque

The relevant curves are plotted in Fig. 3.3, For each value of torque there are two corresponding efficiencies one for operation in stable zone of torque slip characteristic and another for operation in unstable zone of torque slip characteristic. In stable zone efficiency is high while in unstable zone efficiency is comparatively low. In stable zone machine operates under highly saturated condition which will lead to high iron losses. The iron losses, however, have been ignored in the calculation. Thus Fig. 3.3 shows higher efficiencies under stable zone compared to reality.

As p.u. operating frequency decreases the efficiencies in both zones decreases and the difference between efficiencies in the two zone starts increasing at a given p.u. frequency of operation.

### 3.2.4 Power Factor vs Torque

The relationship between power factor vs torque is shown in Fig. 3.4. Just as in the preceding case for each value of torque there are two values of power factor, one for operation in stable zone of torque-slip characteristic and another for operation in unstable zone of torque slip characteristic. Power factor is poorer in stable zone and good in unstable zone. For any p.u. operational frequency

( $\omega_e$ ) trend of curve is similar to induction motor, at a certain critical slip power-factor is highest and on either side of this slip power-factor reduces.

As p.u. operating frequency decreases power factor improves in both zones. For a particular value of slip an increase in operational frequency means higher stator and rotor reactances, thereby poorer power factor.

### 3.2.5 Total losses In Drive vs Torque

Fig. 3.5 illustrates the relationships between total losses and torque. For one value of torque there are two values of total losses, one corresponding to stable zone of torque-slip characteristic another to unstable zone of torque-slip characteristic. Losses in unstable zone are more compared to in stable zone. This is because in analysis iron losses are neglected. In stable zone, due to saturation, there are more iron losses while in unstable zone due to higher slip of operation, there are more rotor copper losses.

It is observed that on varying p.u. operating frequency there is no variation in total losses i.e. total copper losses do not depend upon p.u. operating frequency.

### 3.2.6. Slip vs Torque

The characteristic curves are plotted in Fig.3.6. For each value of torque there are two values of slip, one in stable (negative-sloped) region and another in unstable

(positive sloped) region of operation. In unstable zone of operation slip is large whereas in stable zone of operation slip is small when p.u. operating frequency decreases the slip increases. The magnitude of pull out torque remains constant but corresponding slip increases as p.u. operating frequency decreases.

### 3.3 CALCULATION OF $K_{s\phi}$

Stator voltage-slip curves for different d.c. link current under rated speed setting ( $\omega_e = 1$  p.u.) have been determined and plotted in Fig. 3.7. For each current setting, the slip for rated stator voltage has been identified. The dotted line in Fig. 3.8 shows the exact variation of d.c. link current as function of slip speed in order to maintain rated stator voltage under rated speed setting (i.e. for maintaining rated flux in the induction motor at every p.u. operating frequency).

It is noted that, except for beginning part,  $I_R$  vs  $\omega_{s\phi}$  curve is very nearly linear, though not passing through the origin. Initial non-linearity is due to higher percentage of magnetising current. The exact relationship between  $I_R$  vs  $\omega_{s\phi}$  is replaced by an approximate relationship as indicated by the straight line passing through the origin and its slope ( $\omega_{s\phi}/I_R$ ) is defined as  $K_{s\phi}$ . Such an approximate representation is necessary to develop a linearised mathematical model for stability and harmonic performance

study. The gain  $K_{s\phi}$  determined here, is a characteristic constant of the induction motor. This value of  $K_{s\phi}$  decide the gain setting of the slip regulator to maintain rated flux in the air-gap of the induction motor.

### 3.4 CONCLUSION

An analytical method for determining the steady-state performance of the drive with the induction motor supplied from current-source inverter has been set forth in this chapter.

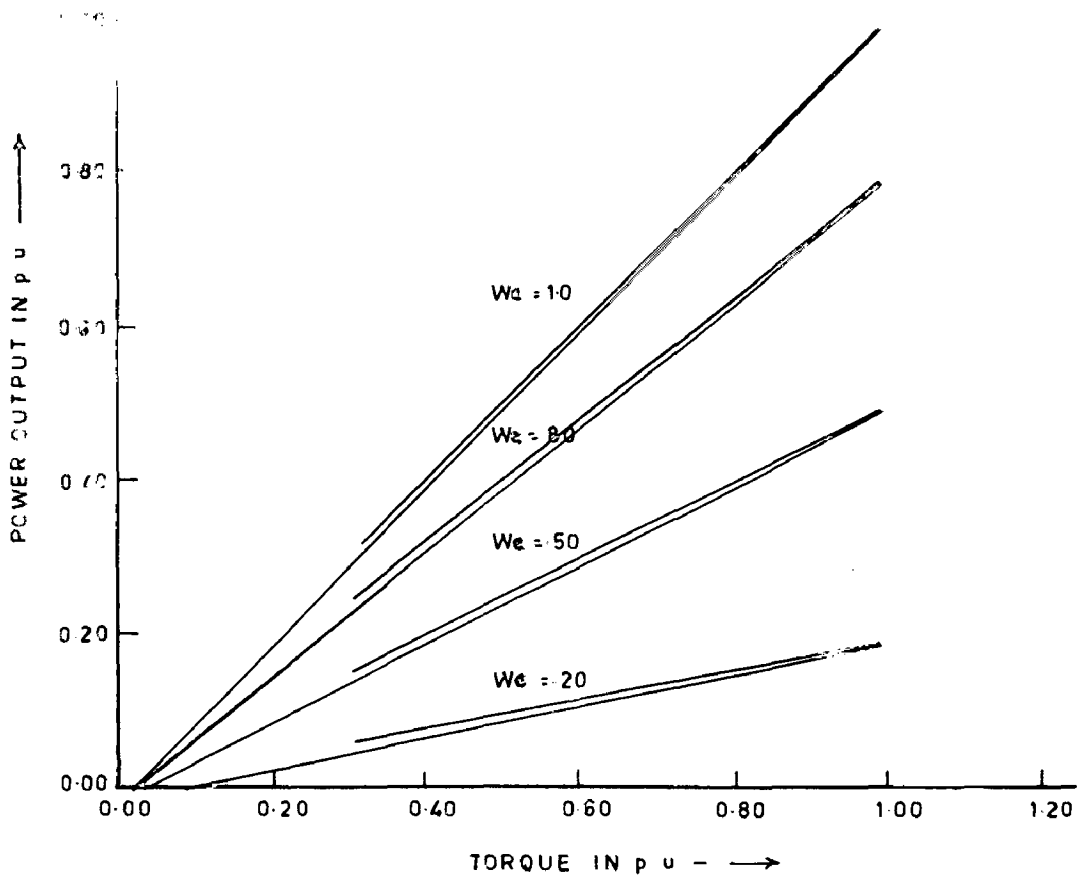
The torque-slip characteristic indicates two regions of operation, one with a positive slope and the other with a negative-slope. The positive-sloped portions of the torque-slip characteristics are well known to be inherently unstable, so open-loop operation of drive is not possible in this zone. With the help of feed back the drive can operate in this zone. The negative-sloped region of the torque-slip characteristic is inherently stable and drive can operate in this region without any feedbacks. Since the breakdown torque occurs at the very small slip, the negative-sloped region of the torque-slip characteristic is small.

The voltage-torque characteristic shows that in the stable zone of the torque-slip characteristic the induction motor stator voltages are very high. So drive operation is practically not possible due to excessive saturation iron losses and magnetising current.

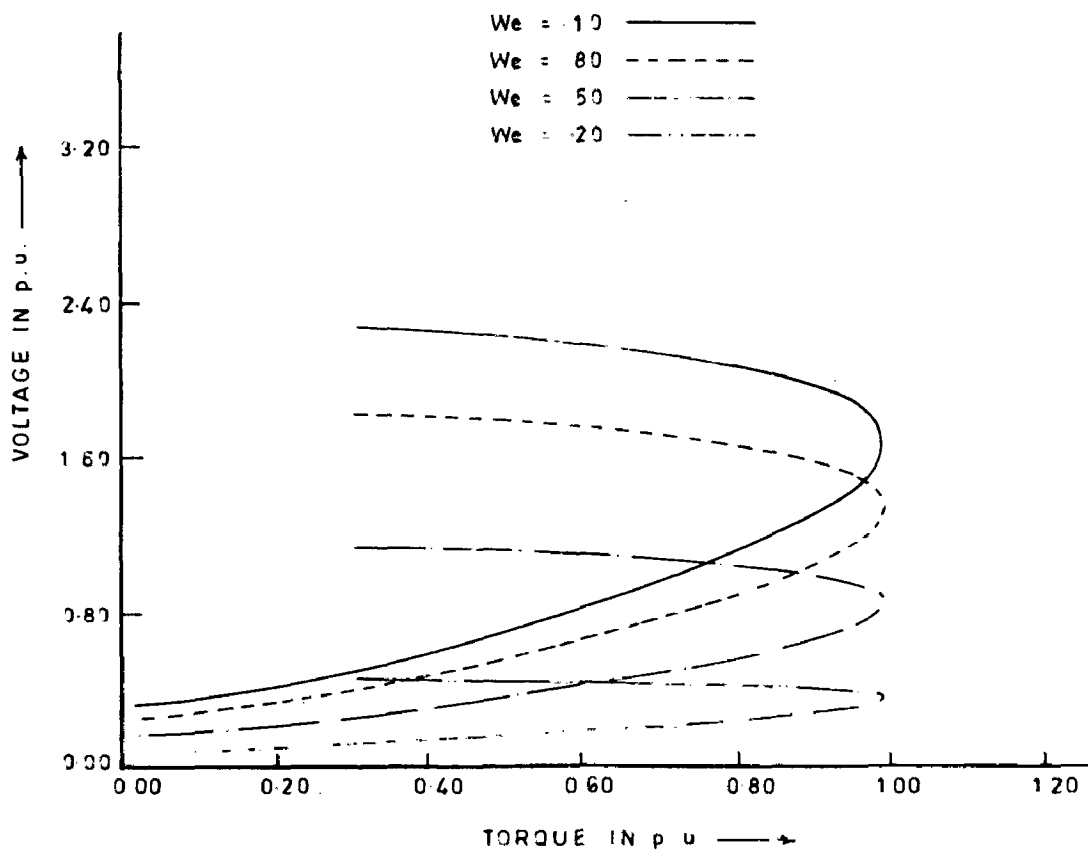
In the unstable zone of the torque slip characteristics stator voltages are small and induction motor power factor is good in comparison to that in stable zone of the torque slip characteristic. Drive efficiency is good in stable zone in comparison to unstable zone because in the analysis iron losses have been neglected. Drive will operate at higher slip in unstable zone in comparison to stable zone and the power output is more in stable zone in comparison to unstable zone. Total copper losses in the drive are more in unstable zone in comparison to stable zone.

A p.u. operating frequency is decreased induction motor stator voltages reduces, power factor improves, drive efficiency and power output reduces, the total copper losses in the drive remains same.

Since it is advisable to work under rated flux conditions closed loop drive is proposed to equipped with a slip regulator which will vary the slip speed proportion to d.c. link current for all p.u. frequencies of operation. The proportionality factor ( $K_{s\phi}$ ) is an absolute constant and depends purely on the machine parameters. It's value has been calculated for subsequent use in the close loop operation of the drive.



g. 3.1 VARIATION OF POWER OUTPUT WITH LOAD TORQUE AT DIFFERENT OPERATIONAL FREQUENCIES



g. 3.2 VARIATION OF I M STATOR VOLTAGE WITH LOAD TORQUE AT DIFFERENT OPERATIONAL FREQUENCIES



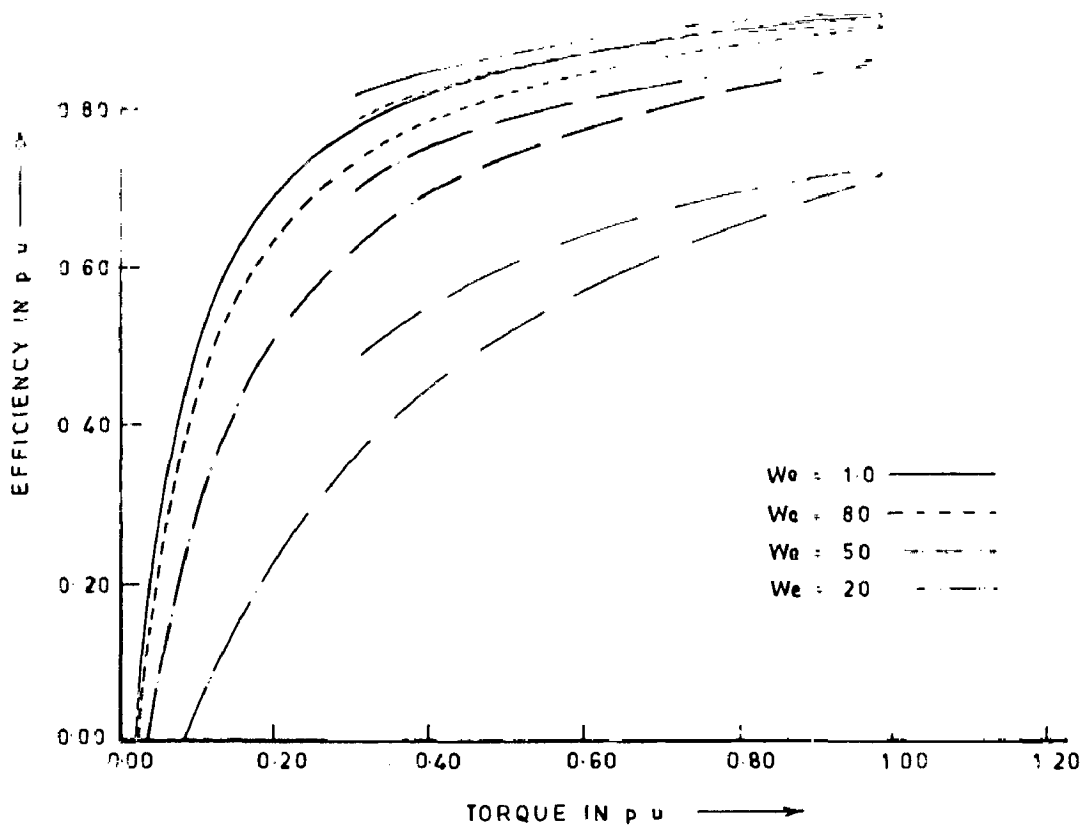


Fig.33 VARIATION OF EFFICIENCY WITH LOAD TORQUE AT DIFFERENT OPERATIONAL FREQUENCIES

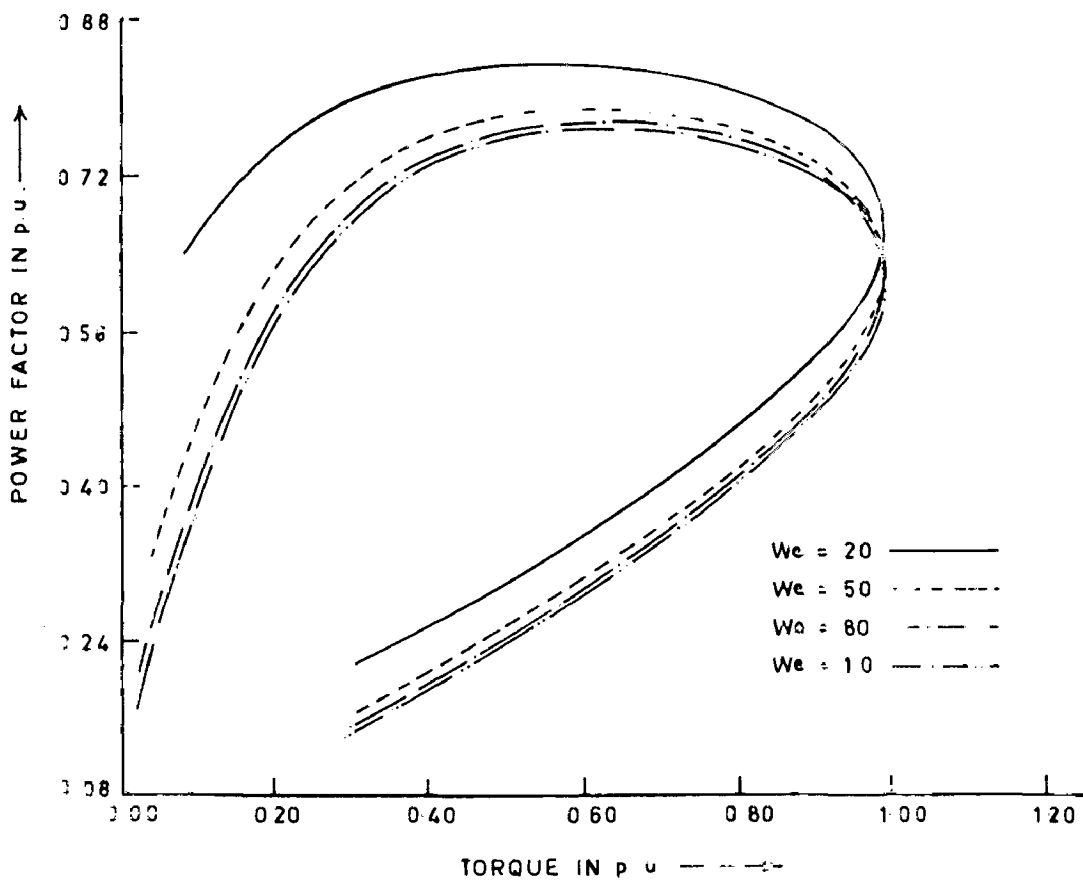


Fig 34 VARIATION OF I M POWER FACTOR WITH LOAD TORQUE AT DIFFERENT OPERATIONAL FREQUENCIES

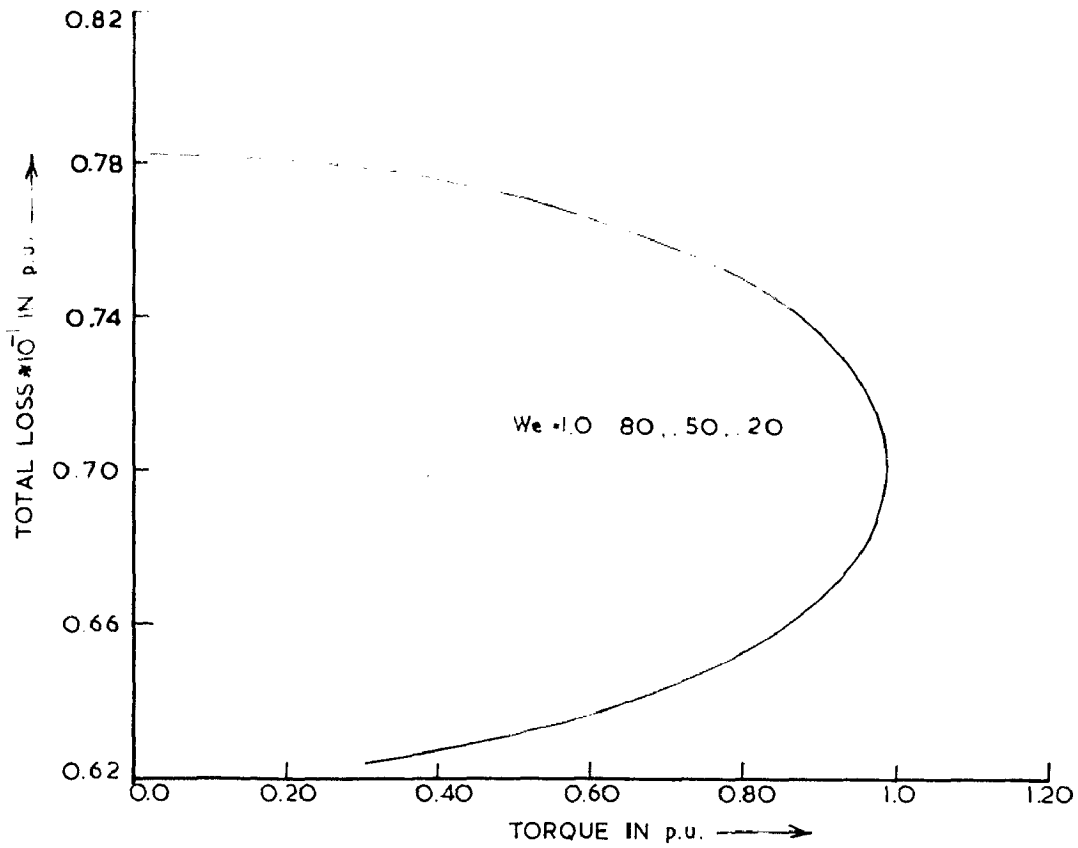


FIG. 3.5. VARIATION OF TOTAL LOSS WITH LOAD TORQUE AT DIFFERENT OPERATIONAL FREQUENCIES.

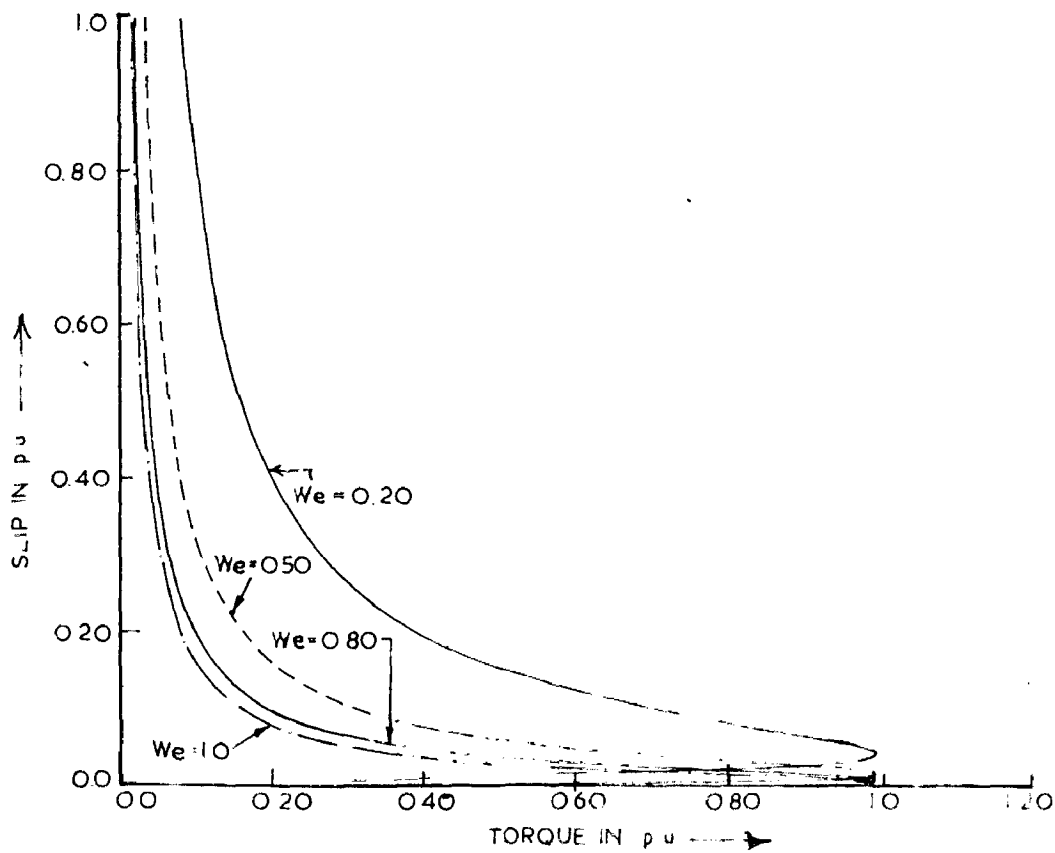


FIG. 3.6. VARIATION OF I.M. SLIP WITH LOAD TORQUE AT DIFFERENT OPERATIONAL FREQUENCIES

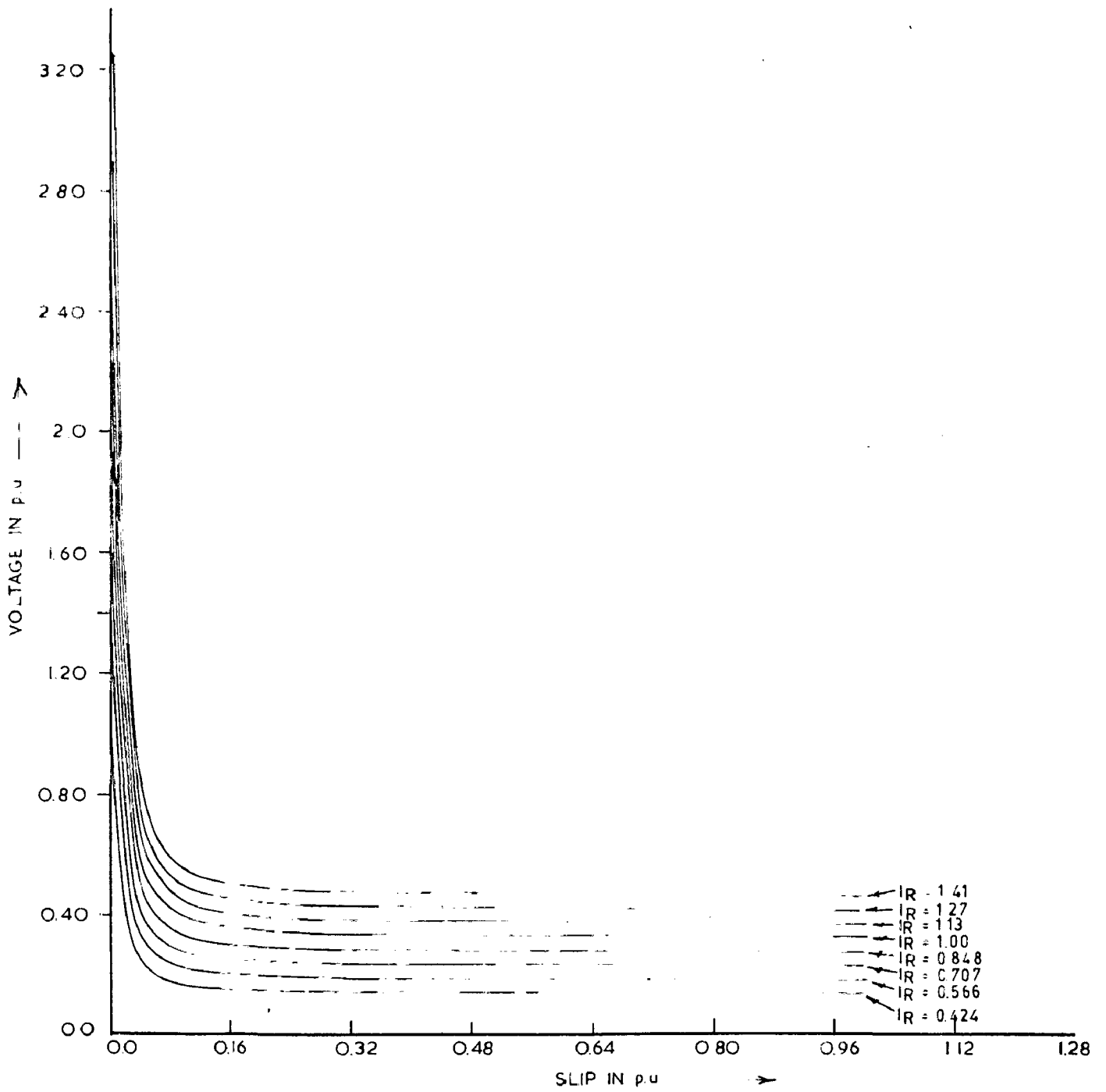


FIG. 3.7. VARIATION OF I.M. STATOR VOLTAGE WITH SLIP AT DIFFERENT D.C. LINK CURRENTS

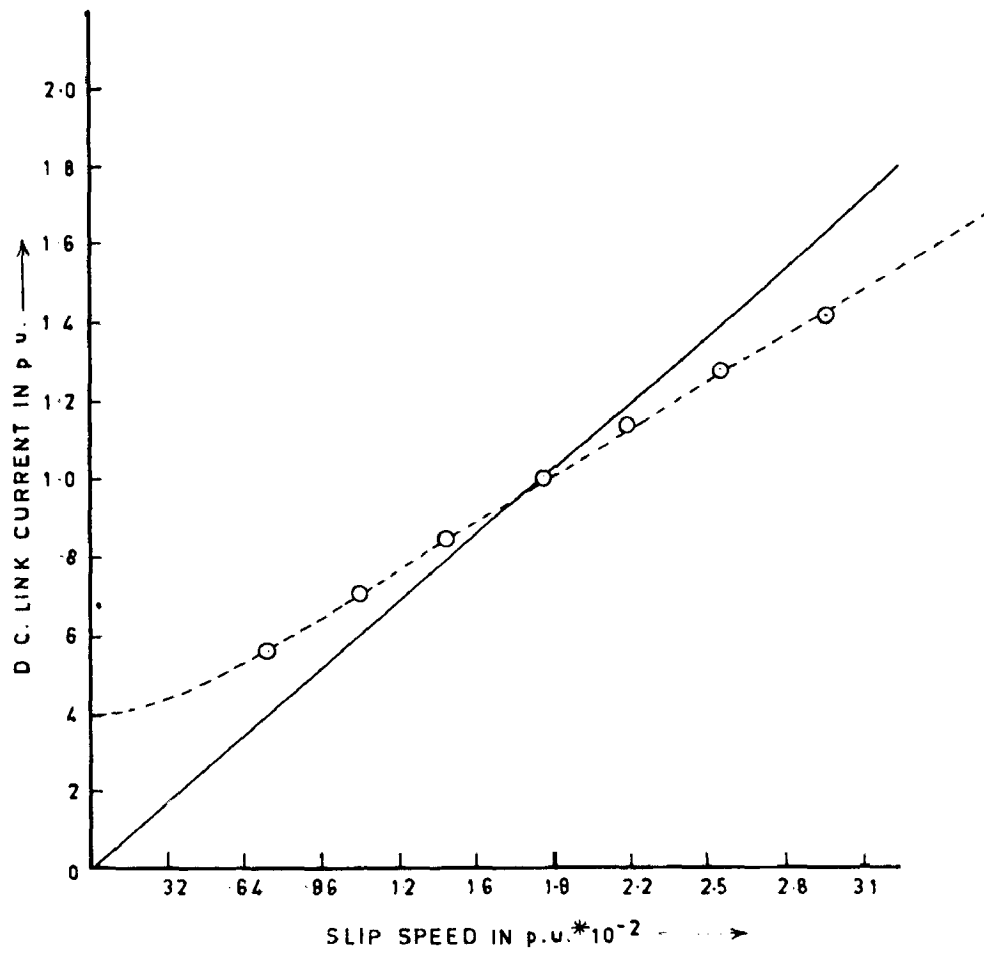


Fig 3.8 SLIP REGULATOR CHARACTERISTICS

## CHAPTER - 4

COORDINATION OF DRIVE PARAMETERS FOR SYSTEM  
STABILITY

In this Chapter a compact expression for the system characteristic equation is derived from small displacement theory and then, by applying the D-partitioning technique, the stability boundaries are determined in the plane of two adjustable parameter of the drive. The open-loop system is unstable while the closed loop system is stable if system parameters are selected properly. The values of these parameters are so chosen that system is not only stable but also possesses a certain minimum degree of stability.

## 4.1 SYSTEM EQUATIONS UNDER SMALL DISPLACEMENT THEORY

The small displacement theory was initially employed in the analysis of stability of electric machines by Park [24, 25]. This theory enables one to establish linear relationships between the machine variables for small changes about an operating point. The small displacement equations are not valid for large excursion of the variables; however these relationships offer a means of investigating system stability when used in conjunction with the D-partitioning technique [26, 27].

The following additional assumption, in addition of those in the mathematical model is made for applying small displacement theory.

The effect of harmonics is ignored i.e. the effect of only fundamental current of machine is considered and hence  $g_{qs}^e = 1$ ,  $g_{ds}^e = 0$  [in equations (2.24) and (2.25)].

Using equation (2.21) for all perturbation about steady-state condition

$$V_{RO} = V_{IO} + (R_F + X_{CO}) I_{RO} \quad \dots(4.1)$$

$$V_{RO} + \Delta V_R = V_{IO} + \Delta V_I + (R_F + X_{CO} + p X_F)(I_{RO} + \Delta I_R) \quad \dots(4.2)$$

Subtracting equation (4.1) from equation (4.2) gives

$$\Delta V_R = \Delta V_I + (R_F + X_{CO} + p X_F) \Delta I_R \quad \dots(4.3)$$

Equations (2.26) are rewritten as

$$v_{qs}^e = (\gamma_s + p X_s) i_{qs}^e + p X_m i_{qr}^e + \omega_e X_m i_{dr}^e \quad \dots(4.4)$$

$$0 = p X_m i_{qs}^e + (\gamma_r + p X_r) i_{qr}^e + \omega_{sl} X_r i_{dr}^e \quad \dots(4.5)$$

$$0 = -\omega_{sl} X_m i_{qs}^e - \omega_{sl} X_r i_{qr}^e + (\gamma_r + p X_r) i_{dr}^e \quad \dots(4.6)$$

From equation (4.6)

$$i_{qr}^e = \frac{1}{\omega_{sl} X_r} \left[ -\omega_{sl} X_m i_{qs}^e + (\gamma_r + p X_r) i_{dr}^e \right] \quad \dots(4.7)$$

Substituting the expression for  $\omega_{sl} i_{qr}^e$  in equations (4.4) and (4.5) from equation (4.7) yield

$$\omega_{sl} v_{qs}^e = \omega_{sl} \left[ \gamma_s + p \left( X_s - \frac{X_m}{X_r} \right) \right] i_{qs}^e + \left( \omega_{sl} \omega_e X_m + \frac{p X_m \gamma_r}{X_r} + p^2 X_m \right) i_{dr}^e \quad \dots(4.8)$$

$$0 = \omega_{s\ell} \left[ -\frac{\gamma_r x_m}{x_r} \right] i_{qs}^e + \left[ \omega_{s\ell}^2 x_r + \frac{\gamma_r^2}{x_r} + p(2 \gamma_r) + p^2 x_r \right] i_{dr}^e \quad \dots (4.9)$$

Substituting  $g_{qs}^e = 1$  and  $g_{ds}^e = 0$  in equations (2.23) to (2.25) as the effect of harmonics in machine variables have been neglected.

$$V_I = v_{qs}^e \quad \dots (4.10)$$

$$i_{qs}^e = I_R \quad \dots (4.11)$$

$$i_{ds}^e = 0 \quad \dots (4.12)$$

From equations (2.21), (4.10) and (4.11)

$$V_R = v_{qs}^e + (R_F + X_{CO} + p X_F) i_{qs}^e \quad \dots (4.13)$$

From equation (4.13)

$$v_{qs}^e = V_R - (R_F + X_{CO} + p X_F) i_{qs}^e \quad \dots (4.14)$$

Substituting the expression for  $v_{qs}^e$  from equation (4.14) in equation (4.8) results in the following equation and rewriting equation (4.9)

$$\omega_{s\ell} V_R = \omega_{s\ell} \left[ \gamma_s + R_F + X_{CO} + p(X_F + X_s - \frac{x_m^2}{x_r}) \right] i_{qs}^e + \left( \omega_{s\ell} \omega_e x_m + p \frac{x_m \gamma_r}{x_r} + p^2 x_m \right) i_{dr}^e \quad \dots (4.15)$$

$$0 = -\frac{\gamma_r x_m \omega_{s\ell}}{x_r} i_{qs}^e + \left[ \omega_{s\ell}^2 x_r + \frac{\gamma_r^2}{x_r} + p(2 \gamma_r) + p^2 x_r \right] i_{dr}^e \quad \dots (4.16)$$

Certain terms involving fixed value of machine variables have been renamed as follows -

$$\begin{aligned} r_s + R_F + X_{CO} &= R, & \frac{X_m r_r}{X_r} &= R_A, & \frac{r_r^2}{X_r} &= R_B, & 2 r_r &= R_C, \\ X_F + X_S - \frac{X_m^2}{X_r} &= X & & & & & & \dots(4.17) \end{aligned}$$

Substituting for various expressions as defined in equations (4.17) in equations (4.15) and (4.16) results in

$$\omega_{sl} V_R = \omega_{sl} (R + pX) i_{qs}^e + (\omega_{sl} \omega_e X_m + p R_A + p^2 X_m) i_{dr}^e \dots(4.18)$$

$$0 = -\omega_{sl} R_A i_{qs}^e + (\omega_{sl}^2 X_r + R_B + p R_C + p^2 X_r) i_{dr}^e \dots(4.19)$$

Small-perturbation equations about steady-state operating point and the steady-state equations as defined from equations (4.18) and (4.19) are given below -

$$\begin{aligned} (\omega_{sl0} + \Delta\omega_{sl})(V_{R0} + \Delta V_R) &= (\omega_{sl0} + \Delta\omega_{sl})(R + pX)(i_{qso}^e + \Delta i_{qs}^e) \\ &+ [(\omega_{sl0} + \Delta\omega_{sl})(\omega_{e0} + \Delta\omega_e) X_m + \\ &p R_A + p^2 X_m] [i_{dro}^e + \Delta i_{dr}^e] \dots(4.20) \end{aligned}$$

$$\omega_{sl0} V_{R0} = \omega_{sl0} R i_{qso}^e + \omega_{sl0} \omega_{e0} X_m i_{dro}^e \dots(4.21)$$

$$\begin{aligned} 0 &= -(\omega_{sl0} + \Delta\omega_{sl}) R_A (i_{qso}^e + \Delta i_{qs}^e) + [(\omega_{sl0} + \Delta\omega_{sl})^2 X_r + \\ &R_B + p R_C + p^2 X_r] [i_{dro}^e + \Delta i_{dr}^e] \dots(4.22) \end{aligned}$$

$$0 = -\omega_{sl0} R_A i_{qso}^e + (\omega_{sl0}^2 X_r + R_B) i_{dro}^e \dots(4.23)$$

Subtracting equation (4.21) from equation (4.20) and ignoring second order quantities



$$\begin{aligned} \omega_{s\ell 0} \Delta V_R = & \omega_{s\ell 0} (R + pX) \Delta i_{qs}^e + (\omega_{s\ell 0} \omega_{e0} X_m + p R_A + p^2 X_m) \Delta i_{dr}^e \\ & + \omega_{s\ell 0} i_{dro}^e X_m \Delta \omega_e + (R i_{qso}^e + \omega_{e0} i_{dro}^e X_m - \\ & V_{RO}) \Delta \omega_{s\ell} \end{aligned} \quad \dots (4.24)$$

Subtracting equation (4.23) from equation (4.22) and ignoring second-order quantities

$$\begin{aligned} 0 = & -\omega_{s\ell 0} R_A \Delta i_{qs}^e + (\omega_{s\ell 0}^2 X_r + R_B + p R_C + p^2 X_r) \Delta i_{dr}^e + \\ & (2 \omega_{s\ell 0} i_{dro}^e X_r - R_A i_{qso}^e) \Delta \omega_{s\ell} \end{aligned} \quad \dots (4.25)$$

Rewriting equations (3.6) and (2.32)

$$\begin{aligned} T_e &= X_m i_{qs}^e i_{dr}^e \\ &= T_L + 4\pi f_b H p \omega_r \end{aligned} \quad \dots (4.25)$$

Above equations for small perturbations about steady-state operating point and steady-state conditions result in

$$\begin{aligned} T_{e0} + \Delta T_e &= X_m (i_{qso}^e + \Delta i_{qs}^e) (i_{dro}^e + \Delta i_{dr}^e) \\ &= T_{L0} + \Delta T_L + 4\pi f_b H p (\omega_{r0} + \Delta \omega_r) \end{aligned} \quad \dots (4.26)$$

$$\begin{aligned} T_{e0} &= X_m i_{qso}^e i_{dro}^e \\ &= T_{L0} \end{aligned} \quad \dots (4.27)$$

Subtracting equations (4.27) from equations (4.26)

$$\begin{aligned} \Delta T_e &= X_m (i_{qso}^e \Delta i_{dr}^e + \Delta i_{qs}^e i_{dro}^e) \\ &= \Delta T_L + 4\pi f_b H p \omega_r \end{aligned} \quad \dots (4.28)$$

Substituting the expression for  $\Delta \omega_r$  as

$$\Delta \omega_r = \Delta \omega_e - \Delta \omega_{s\ell}$$

in equation (4.28) gives

$$\begin{aligned} \Delta T_e &= X_m (i_{qso}^e \Delta i_{dr}^e + \Delta i_{qs}^e i_{dro}^e) \\ &= \Delta T_L + 4\pi f_b H p (\Delta \omega_e - \Delta \omega_{s\ell}) \end{aligned} \quad \dots(4.29)$$

Rewriting equations (4.24), (2.25) and (4.29) in matrix form

$$\begin{bmatrix} \omega_{s\ell o} (R + pX) & \omega_{s\ell o} \omega_{eo} X_m + pR_A + p^2 X_m & \omega_{s\ell o} i_{dro}^e X_m \\ -\omega_{s\ell o} R_A & \omega_{s\ell o}^2 X_r + R_B + pR_C + p^2 X_r & 0 \\ X_m i_{dro}^e & X_m i_{qso}^e & -4\pi f_b H p \end{bmatrix} \begin{bmatrix} \Delta i_{qs}^e \\ \Delta i_{dr}^e \\ \Delta \omega_e \end{bmatrix} = \begin{bmatrix} \omega_{s\ell o} \\ 0 \\ 0 \end{bmatrix} \Delta V_R$$

$$+ \begin{bmatrix} 0 \\ 0 \\ 1 \end{bmatrix} \Delta T_L - \begin{bmatrix} R i_{qso}^e + \omega_{eo} i_{dro}^e X_m - V_{RO} \\ 2 \omega_{s\ell o} i_{dro}^e X_r - R_A i_{qso}^e \\ 4\pi f_b H p \end{bmatrix} \Delta \omega_{s\ell} \quad \dots(4.30)$$

Further rewriting equations (2.33) to (2.36)

$$I_R^* = K_{sp} (\omega_r^* - \omega_r) \quad \dots(4.31)$$

$$V_R = \frac{K_c (1 + T \omega_b p)}{\omega_b p} (I_R^* - I_R) \quad \dots(4.32)$$

$$\omega_{s\ell} = K_{s\ell} I_R \quad \dots(4.33)$$

$$\omega_e = \omega_r + \omega_{s\ell} \quad \dots(4.34)$$

From equations (4.31) to (4.34) for small perturbations about steady-state operating point

$$\Delta I_R^* = K_{sp} (\Delta \omega_r^* - \Delta \omega_r) \quad \dots(4.35)$$

$$\Delta V_R = \frac{K_c (1 + T \omega_b p)}{\omega_b p} (\Delta I_R^* - \Delta I_R) \quad \dots(4.36)$$

$$\Delta \omega_e = \Delta \omega_r + \Delta \omega_{s\ell} \quad \dots(4.37)$$

$$\Delta \omega_{s\ell} = K_{s\ell} \Delta I_R \quad \dots(4.38)$$

Substituting expression for  $\Delta I_R^*$  from equation (4.35) and for  $\Delta I_R$  from equation (4.11) in equation (4.36)

$$\Delta V_R = \frac{K_c (1 + T \omega_b p)}{\omega_b p} (K_{sp} \Delta \omega_r^* - K_{sp} \Delta \omega_r - \Delta i_{qs}^e) \dots(4.39)$$

Substituting expression for  $\Delta \omega_r$  from equation (4.37) in equation (4.39)

$$\Delta V_R = \frac{K_c (1 + T \omega_b p)}{\omega_b p} [K_{sp} \Delta \omega_r^* - K_{sp} (\Delta \omega_e - \Delta \omega_{s\ell}) - \Delta i_{qs}^e] \dots(4.40)$$

Substituting expression for  $\Delta V_R$  for equation (4.40) in equations (4.30) and rearranging the terms

$$\begin{bmatrix} \frac{\omega_{s\ell 0} [R + p X + K_c (1 + T \omega_b p)]}{\omega_b p} & \frac{\omega_{s\ell 0} \omega_{e 0} X_m + p R_A + p^2 X_m}{p R_A + p^2 X_m} & \frac{\omega_{s\ell 0} [i_{dr 0}^e X_m + K_{sp} K_c (1 + T \omega_b p)]}{\omega_b p} \\ -\omega_{s\ell 0} R_A & \frac{\omega_{s\ell 0}^2 X_r + R_B + p R_C + p^2 X_r}{p R_C + p^2 X_r} & 0 \\ X_m i_{dr 0}^e & X_m i_{qs 0}^e & -4\pi f_b H p \end{bmatrix} \begin{bmatrix} \Delta i_{qs}^e \\ \Delta i_{dr}^e \\ \Delta \omega_e \end{bmatrix}$$

$$\begin{bmatrix} 0 \\ 0 \\ 1 \end{bmatrix} \Delta T_L + \begin{bmatrix} \omega_{s/o} \frac{K_c K_{sp} (1 + T \omega_b p)}{\omega_b p} \\ 0 \\ 0 \end{bmatrix} \Delta \omega_r^* = \begin{bmatrix} R i_{qso} e^{s t} + \omega_{e/o} i_{dro} e^{s t} X_m \\ -V_{RO} - \omega_{s/o} \frac{K_c K_{sp}}{\omega_b p} (1 + T \omega_b p) \\ 2 \omega_{s/o} i_{dro} e^{s t} X_r - R_A i_{qso} e^{s t} \\ 4\pi f_b H p \end{bmatrix} \Delta \omega_{s/o} \quad \dots (4.41)$$

Substituting the expression for  $\Delta I_R$  as  $\Delta i_{qs}^e$  from equation (4.11), the equation (4.38) yields

$$\Delta \omega_{s/o} = K_{s/o} \Delta i_{qs}^e \quad \dots (4.42)$$

Substituting the expression for  $\Delta \omega_{s/o}$  from equation (4.42) in equations (4.41) and rearranging the terms

$$\begin{bmatrix} \omega_{s/o} (R + pX) + K_{s/o} (R i_{qso} e^{s t} + \omega_{e/o} \omega_{s/o} X_m + \omega_{s/o} [i_{dro} e^{s t} X_m + K_{sp} K_c (1 + T \omega_b p)]) \\ \omega_{e/o} i_{dro} e^{s t} X_m - V_{RO} + p R_A + p^2 X_m \\ \frac{\omega_{s/o} K_c (1 + T \omega_b p) (1 - K_{s/o} K_{sp})}{\omega_b p} \\ \omega_{s/o} (-R_A + 2K_{s/o} i_{dro} e^{s t} X_r) - K_{s/o} R_A i_{qso} e^{s t} \\ X_m i_{dro} e^{s t} + K_{s/o} 4\pi f_b H p \end{bmatrix} \begin{bmatrix} \Delta i_{qs}^e \\ \Delta i_{dr}^e \\ \Delta \omega_e \end{bmatrix} = \begin{bmatrix} \omega_{s/o}^2 X_r + R_B + p R_c + p^2 X_r \\ 0 \\ X_m i_{qso} e^{s t} - 4\pi f_b H p \end{bmatrix}$$

$$\begin{bmatrix} 0 \\ 0 \\ 1 \end{bmatrix} \Delta T_L + \begin{bmatrix} \omega_{s/o} \frac{K_c K_{sp} (1 + T \omega_b p)}{\omega_b p} \\ 0 \\ 0 \end{bmatrix} \Delta \omega_r^* \quad \dots (4.44)$$

Defining

$$-R_A \omega_{s/o} + 2 \omega_{s/o} K_{s/l} i_{dro}^e X_r - K_{s/l} R_A i_{qso}^e = A \quad \dots (4.45)$$

$$\omega_{s/o} R + K_{s/l} R i_{qso}^e + K_{s/l} \omega_{eo} i_{dro}^e X_m - K_{s/l} V_{RO} = B \quad \dots (4.46)$$

$$\omega_{s/o} (1 - K_{sp} K_{s/l}) = D \quad \dots (4.47)$$

$$4\pi f_b H p = z_1(p) \quad \dots (4.48)$$

$$\omega_{s/o} \omega_{eo} X_m + p R_A + p^2 X_m = z_2(p) \quad \dots (4.49)$$

$$\omega_{s/o}^2 X_r + R_B + p R_C + p^2 X_r = z_3(p) \quad \dots (4.50)$$

$$\omega_{s/o} p X + B = z_4(p) \quad \dots (4.51)$$

$$X_m i_{dro}^e + K_{s/l} z_1(p) = z_5(p) \quad \dots (4.52)$$

Substituting for various expressions as defined in equations (4.45) to (4.52) in equations (4.44) gives

$$\begin{bmatrix} \frac{K_c(1+T\omega_b p) D}{p \omega_b} + z_4(p) & z_2(p) & \frac{\omega_{s/o} K_c K_{sp}(1+T\omega_b p)}{\omega_b p} + \omega_{s/o} i_{dro}^e X_m \\ A & z_3(p) & 0 \\ z_5(p) & X_m i_{qso}^e & -z_1(p) \end{bmatrix} \begin{bmatrix} \Delta i_{qs}^e \\ \Delta i_{dr}^e \\ \Delta \omega_e \end{bmatrix} \\ = \begin{bmatrix} 0 \\ 0 \\ 1 \end{bmatrix} \Delta T_L + \begin{bmatrix} \frac{\omega_{s/o} K_c K_{sp}(1+T\omega_b p)}{\omega_b p} \\ 0 \\ 0 \end{bmatrix} \Delta \omega_r \quad \dots (4.53)$$

System characteristic equation is as follows

$$\frac{K_c(1+T\omega_b p)}{\omega_b p} \left[ -D z_1(p) z_3(p) + \omega_{s/o} K_{sp} \left\{ A X_m i_{qso}^e - z_5(p) z_3(p) \right\} \right] \\ + \omega_{s/o} i_{dro}^e X_m \left\{ A X_m i_{qso}^e - z_3(p) z_5(p) \right\} \\ - z_1(p) z_3(p) z_4(p) + z_2(p) z_1(p) \lambda = 0 \quad \dots (4.54)$$

Defining

$$A X_m i_{qso}^e - z_5(p) z_3(p) = z_6(p) \quad \dots(4.55)$$

$$-D z_1(p) z_3(p) + K_{sp} \omega_{s/o} \left\{ A X_m i_{qso}^e - z_5(p) z_3(p) \right\} = f_2(p) \quad \dots (4.56)$$

$$\frac{f_2(p)}{\omega_b p} = f_1(p) \quad \dots (4.57)$$

$$z_1(p) \left\{ z_2(p) \lambda - z_3(p) z_4(p) \right\} + \omega_{s/o} i_{dro}^e X_m z_6(p) = f_3(p) \quad \dots (4.58)$$

Substituting for various expression as defined in equations(4.55) to (4.58) in equation (4.54) results in the following system characteristic equation

$$K_c f_1(p) + K_c T f_2(p) + f_3(p) = 0 \quad \dots(4.59)$$

$$\text{or } D(p) = 0 \quad \dots (4.60)$$

Above equation is suitable for stability analysis by the D-partitioning technique. This technique is more than 100 times faster than the root locus method or R.H. criterion. The results are expressed in parameter plane, the convenient coordinate axes being  $K_c$ ,  $K_c T$  which appear linearly in the system characteristic equation. Unlike earlier efforts using this technique by

Lawrenson [28] it may be noted here that it is not necessary to obtain expression for the characteristic equation in a polynomial form. This saves a lot of manual labour and there are less chances of error.

Substituting  $p = -\sigma + j\omega$  the characteristic equation can be split into two real equations

$$K_c f_{1R} + K_c^T f_{2R} + f_{3R} = 0 \quad \dots(4.61)$$

$$K_c f_{1I} + K_c^T f_{2I} + f_{3I} = 0 \quad \dots(4.62)$$

These equations can be solved for  $K_c$  and  $K_c^T$  parameters for any fixed value of  $\sigma$  as the value of  $\omega$  is varied from 0 to  $\infty$

Apart from the above two adjustable drive parameters, one more adjustable parameter is the proportionality gain constant of the speed regulator (i.e.  $K_{sp}$ ) which unfortunately appears in a product form with the other two adjustable parameters in the system characteristic equation. As such, this parameter can not be chosen as a coordinate axis while plotting the stability regions. The stability region are accordingly determined in the plane of  $K_c$ - $K_c^T$  for a certain fixed value of  $K_{sp}$ . Three values of  $K_{sp}$  namely 10, 20 and 50 have been selected in this study.

Since the drive under study is a variable speed drive, four widely varying p.u. operating frequencies have been selected to fix the steady-state operating conditions, these p.u. frequencies being .2, .5, .8 and 1.

### 4.3 COMPUTER RESULTS AND DISCUSSION

In this section theoretical results of stability analysis obtained using D-partitioning technique are presented. The objective is to select sets of controller parameters for which the system is not only stable over a widely varying range of operating speeds but possesses a certain minimum degree of stability as well.

Results have been computed here for rated torque conditions for three different values of  $K_{sp}$  and four different operational frequencies for each value of  $K_{sp}$ . The D-partitioning curves are plotted in plane of  $(K_C - K_C T)$  each time. For convenience of plotting the unit of time in all D-partitioning curves is in second unit.

Fig. 4.2 shows the manner of carrying out D-partitioning in plane of  $K_C - K_C T$ . Also, the probable stable zone for one particular value of operational frequency and  $K_{sp}$  is shown.

To confirm this region to be really a stable region point checks have been made by the Frequency Scanning Technique [26, 27]. Point 'A' from Fig. (4.1) have been selected and corresponding characteristic vector  $D(j\omega)$  for variation in  $\omega$  from  $-\infty$  to  $\infty$  results in frequency scanning trajectories as plotted in Fig. 4.2. For this point origin of  $D(j\omega)$  - plane lies in the inner most region in the sense of shading of the frequency scanning trajectory. Hence the D-partitioning region containing the point 'A' is the stable area.

For relative stability studies  $p$  is substituted as  $-\sigma + j\omega$  in the characteristic equation and then for different



values of  $\sigma$ , D-partitioning is carried out in plane  $K_C - K_C T$ .

Fig. 4.3 shows stable area for one particular operational frequency ( $\omega_e = 1.0$ ) with the value of  $K_{sp}$  equal to 20. As seen in this figure, as  $\sigma$  is increased the relatively more stable region decreases. A stable area corresponding to larger value of  $\sigma$  is contained in areas corresponding to smaller values of  $\sigma$ . Beyond a certain upper limit of  $\sigma$  no area is obtained, thus indicating the largest attainable value of  $\sigma$  (degree of stability) and the corresponding set of adjustable parameters for the chosen structure of the drive under study.

Figs. 4.3, 4.4, 4.5 and 4.6 show relative stability areas for  $K_{sp}$  equal to 20 and operational frequencies 1.0, .8, .5 and .2 p.u. with variation in  $\sigma$ . As operational frequency is decreased stable area decreases. The maximum achievable  $\sigma$  for  $\omega_e = .2$  is less than the maximum  $\sigma$  obtained for  $\omega_e = 1.0$ . Further, the stable area for  $\omega_e = .2$  shifts down towards fourth quadrant of the  $K_C - K_C T$  plane.

Figs. 4.7, 4.8, 4.9 and 4.10 show stable areas for  $K_{sp}$  equal to 10, and for operational frequencies 1.0, .8, .5 and .2 p.u. respectively with varying values of  $\sigma$ . The change of operational frequencies causes similar results as obtained for  $K_{sp}$  equal to 20. However, the stable area is less for the case of  $K_{sp}$  equal to 10 in comparison to the case of  $K_{sp}$  equal to 20 for same degree of stability ( $\sigma$ ).

Figs. 4.11, 4.12, 4.13 and 4.14 show the stable areas for  $K_{sp}$  equal to 50 and operational frequencies 1.0, .8, .5 and .2 p.u. respectively with varying value of  $\sigma$ . The nature of results obtained are as before. However, the stable area is smaller than for the cases with  $K_{sp}$  equal to 10 and 20 for same degree of stability ( $\sigma$ ).

Accordingly it can be concluded that as  $K_{sp}$  is increased stable area decreases for same degree of stability ( $\sigma$ ) and as operational frequency is varied from 1.0 p.u. to .2 p.u. the stable area again decreases for all values of  $K_{sp}$  under taken here for same degree of stability ( $\sigma$ ). Further, the maximum attainable  $\sigma$  is large for high speed case in comparison to that for low speed case at all values of  $K_{sp}$ .

A variable speed drive should give very nearly similar performance for all speeds. Hence, a common set of parameters ( $K_c, K_c T$ ) must be determined by sacrificing maximum  $\sigma$  slightly at large operational frequencies for all values of the gain  $K_{sp}$ .

Figs. 4.15, 4.16 and 4.17 show a common area in between two extreme operational frequencies i.e. 1.0 and .2 p.u. with values of  $K_{sp}$  20, 10 and 50 respectively.

Table below shows selected values of  $K_c - K_c T$  for different values of  $K_{sp}$ . These values of controller parameters will be used in following chapters i.e. for sixth harmonic analysis and transient response.

$K_{sp}$	$K_c$	$K_c T$	$T$ (sec.)	Minimum $\sigma$ ensured ( $\text{sec}^{-1}$ )
10	.3	.015	.05	2.7
20	.2	.01	.05	2.7
50	.1	.01	.1	2.7

#### 4.3 CONCLUSION

In this chapter stability aspects of the rectifier controlled current inverter fed induction motor drive have been discussed. It has been shown earlier in third chapter that the induction motor gets highly saturated in the stable zone of the motor torque-slip characteristic under open-loop conditions. To overcome this the drive is operated in an otherwise unstable zone of the motor torque-slip characteristic employing regulators, namely a proportional speed regulator, a p-i current regulator and a slip regulator. The proportional speed regulator works on speed error and sets the reference d.c. link current. The p-i regulator works on d.c. link current error and controls the d.c. link current by suitably adjusting the voltage of the rectifier. The slip regulator maintains constant air-gap flux in the induction motor by setting slip speed proportional to d.c. link current.

The characteristic equation which describe the behaviour of the drive has been established using the theory of small

displacements to linearize the various nonlinear equations of the drive. The analysis ignores harmonic effect of applied stator current and also ignores inverter commutation period. By applying D-partitioning technique to the characteristic equation the relative stability boundaries have been found out in the plane of  $K_C - K_C T$  gains of the p-i controller with varying values of the proportional gain constant of the speed regulator,  $K_{sp}$ .

The study shows that as  $K_{sp}$  is increased stability boundaries decrease for any operational frequency. Further, as operational frequencies are decreased the stability boundaries again decrease for all values of  $K_{sp}$ .

A stable area corresponding to larger value of  $\sigma$  (degree of stability) is contained in areas corresponding to smaller value of  $\sigma$ . Beyond a certain upper limit of  $\sigma$  no area is obtained, thus indicating the largest attainable value of  $\sigma$  and the corresponding set of adjustable parameters for the chosen structure of the drive understudy.

As operational frequency is decreased, maximum attainable  $\sigma$ , for which system is relatively stable, also decreases.

A variable speed drive should give very nearly similar performance for all speeds. Hence, for each of the three different values of the speed regulator gain ( $K_{sp}$ ) a set of

parameters ( $K_c, K_c T$ ) has been determined, for which system ensures a degree of stability ( $\sigma$ )  $2.7 \text{ sec}^{-1}$  or better for all operational frequencies. Further comparisons between these 3 sets of controller parameters will be carried out in the subsequent chapters with a view for final selection of the parameters.

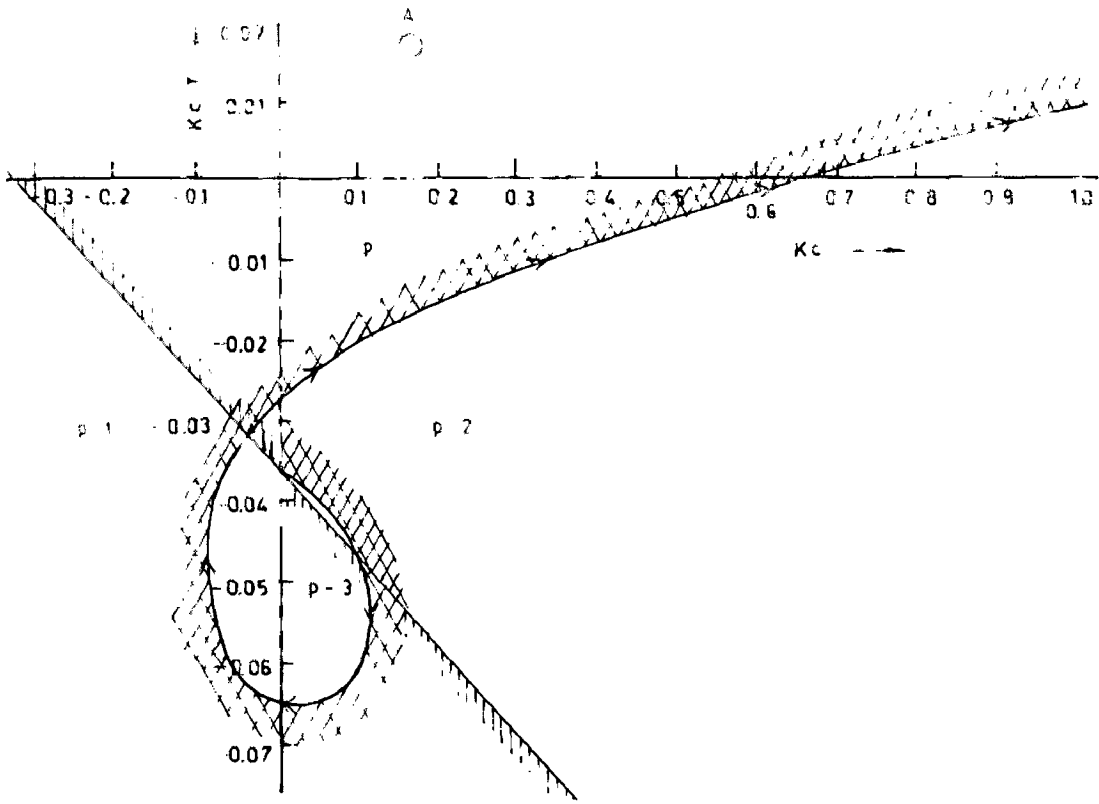


FIG 41 DEPARTIONING TECHNIQUE IN PLANE OF  $K_c - K_c T$  FOR  
 ( $K_{sp} = 20, W_e = 10$ )

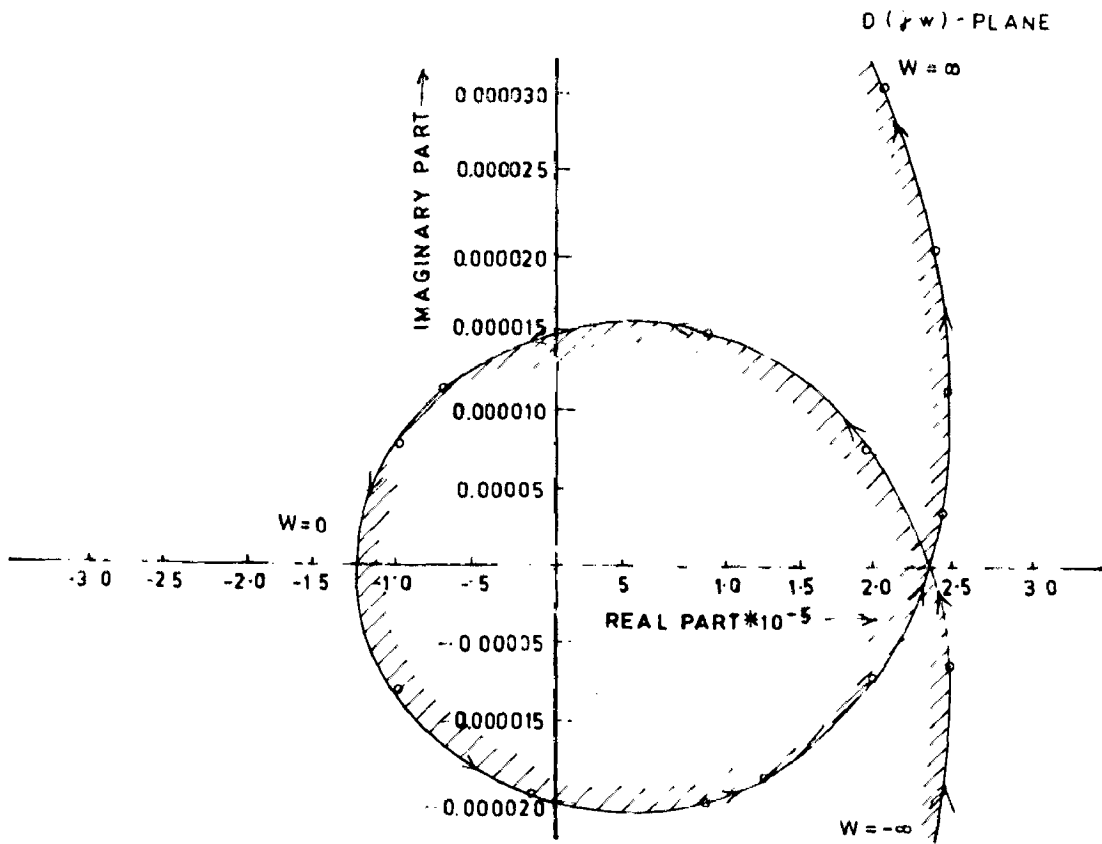


FIG 42 POINT CHECK FOR CONFIRMATION OF STABILITY BY  
 FREQUENCY SCANNING TECHNIQUE

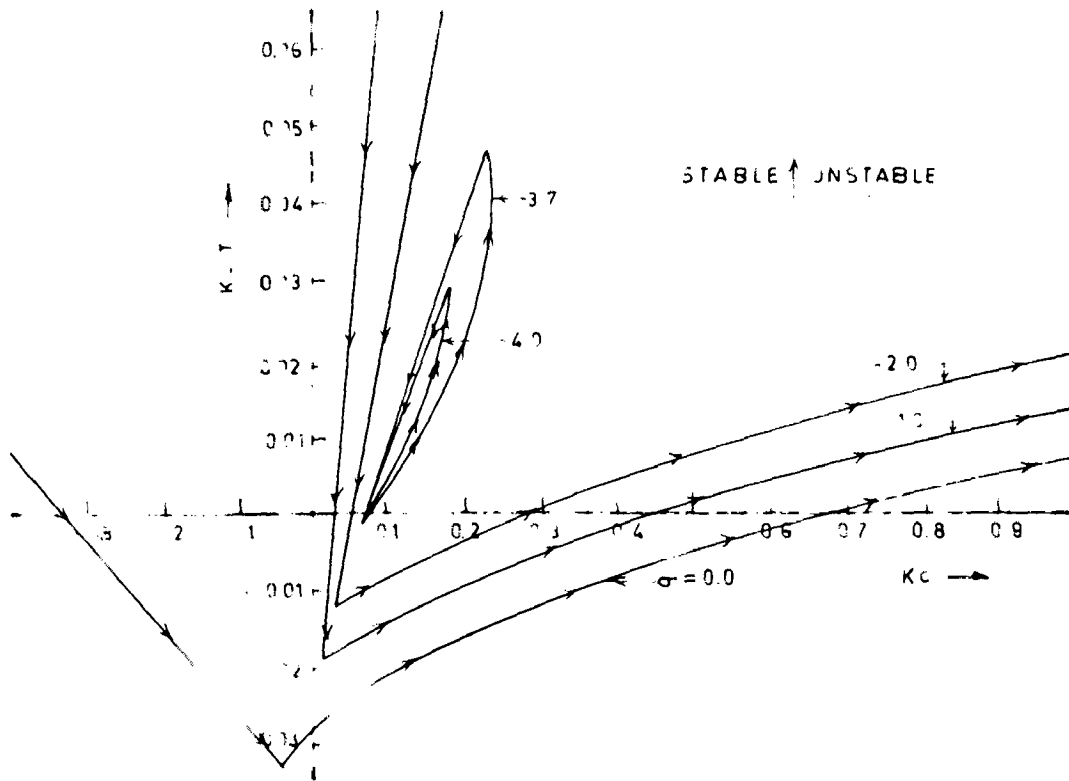


FIG 43 STABILITY REGION IN PLANE OF  $(K_c - K_{cT})$  FOR VARYING DEGREE OF STABILITY  $\sigma$ —( $K_{sp}=20, We=1.0$ )

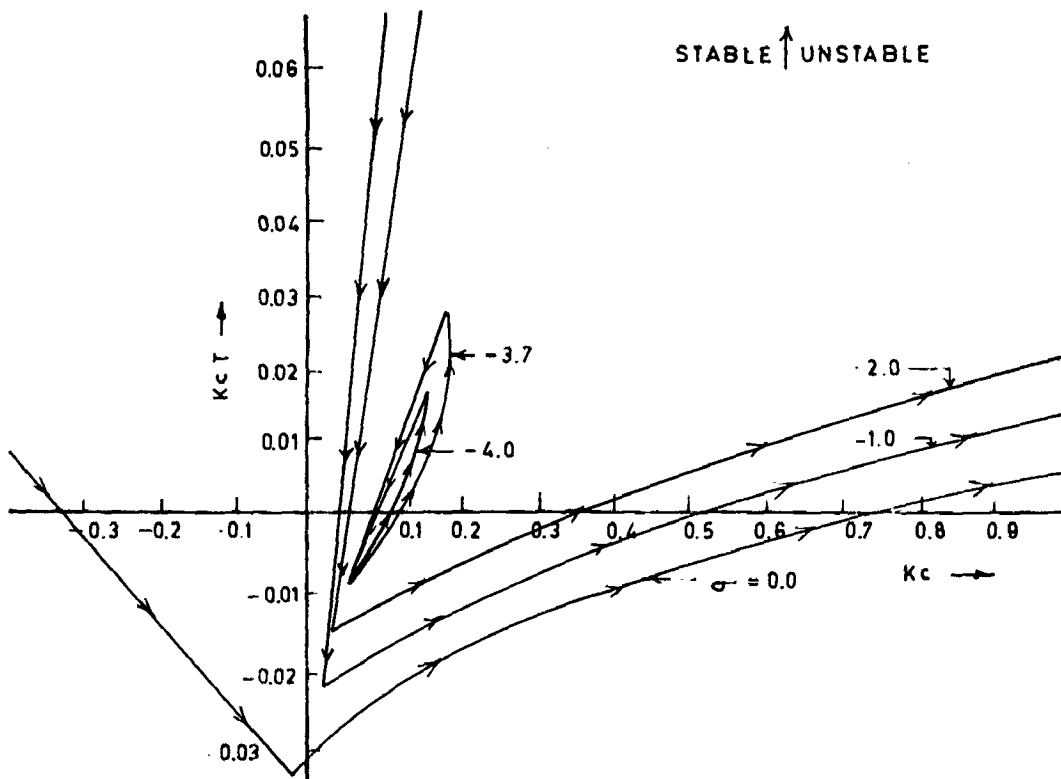


FIG.4.4. STABILITY REGION IN PLANE OF  $(K_c - K_{cT})$  FOR VARYING DEGREE OF STABILITY  $\sigma$ —( $K_{sp}=20, We=0.8$ )

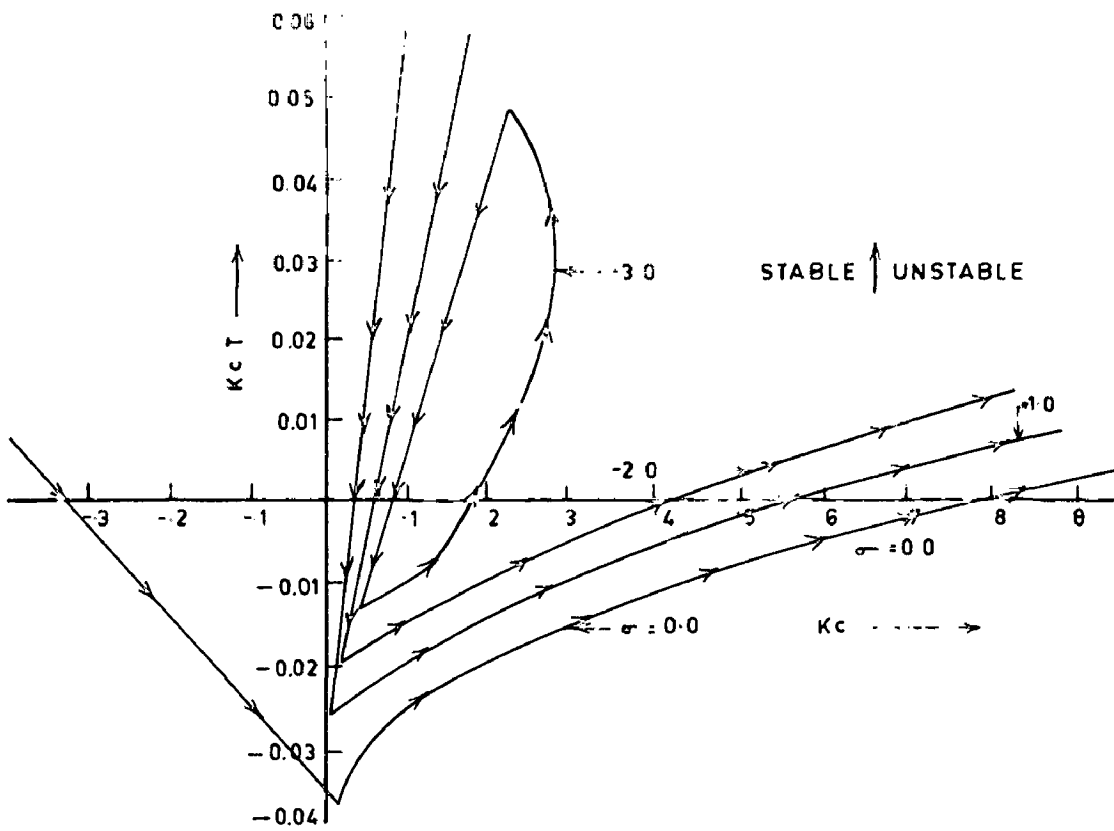


FIG. 45. STABILITY REGION IN PLANE OF  $(K_c - K_{cT})$  FOR VARYING DEGREE OF STABILITY  $\sigma$  ( $K_{sp} = 20, We = 0.50$ )

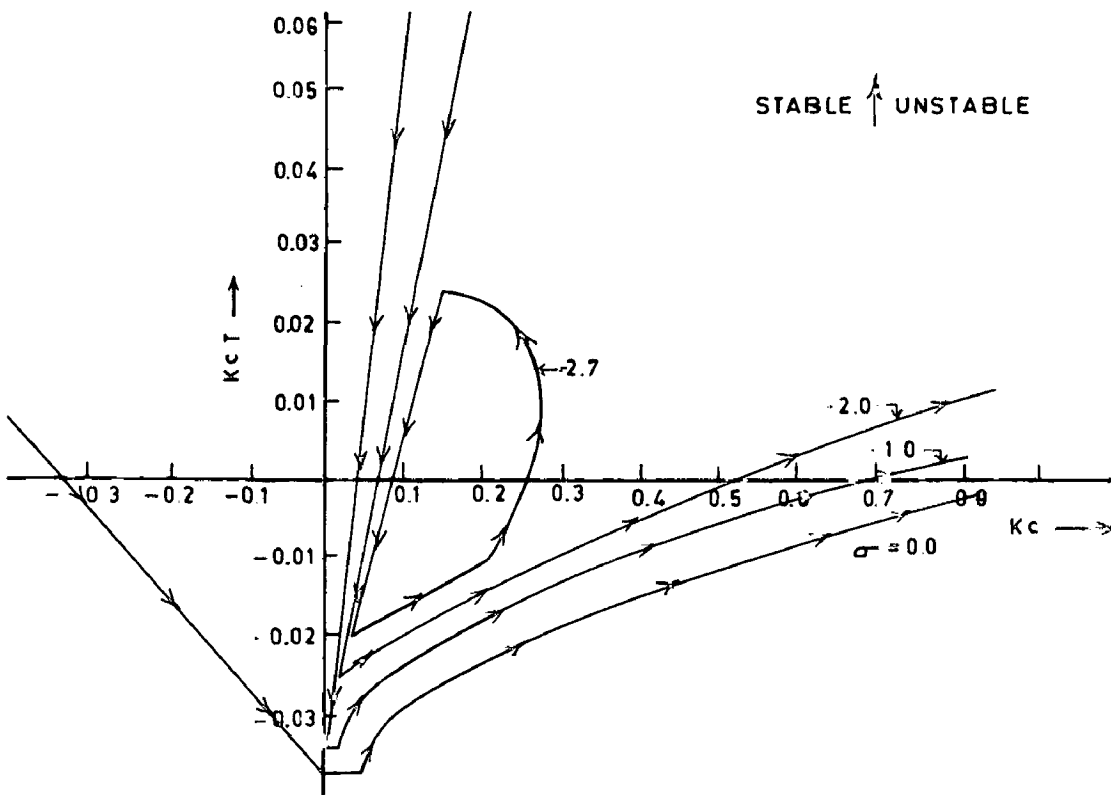


FIG. 46 STABILITY REGION IN PLANE OF  $(K_c - K_{cT})$  FOR VARYING DEGREE OF STABILITY  $\sigma$  ( $K_{sp} = 20, We = 0.20$ )



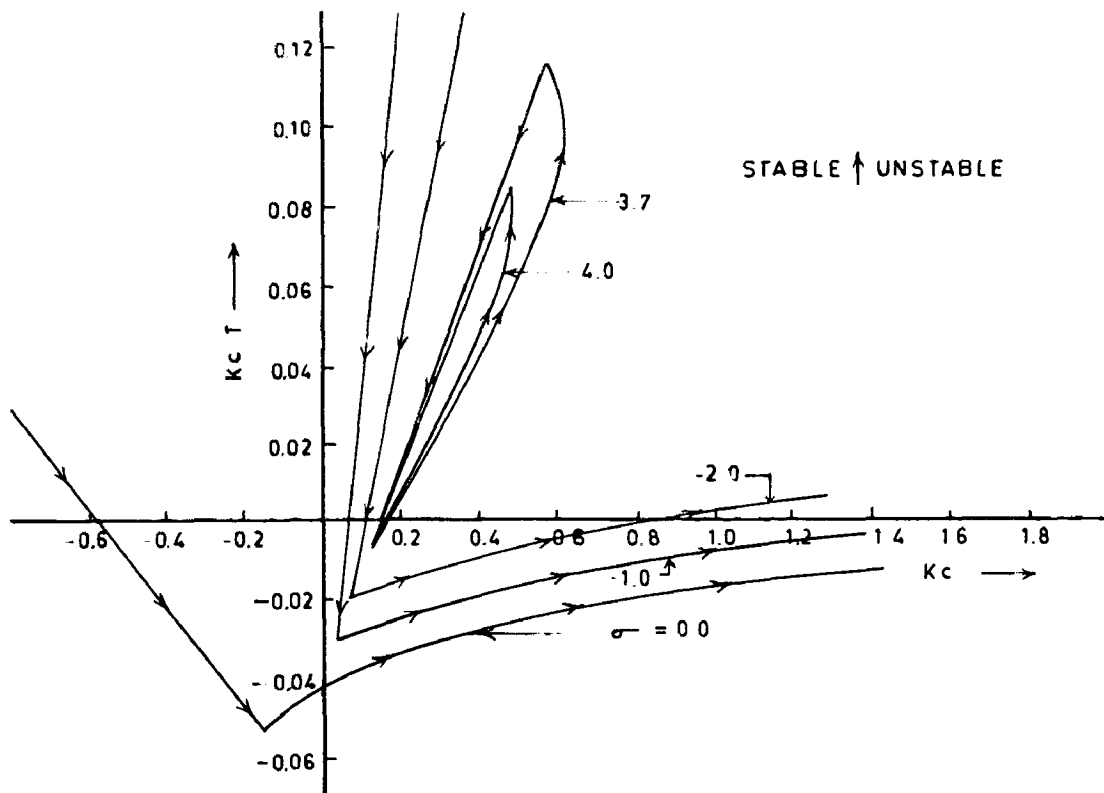


Fig 4.7 STABILITY REGION IN PLANE OF  $K_c$ - $K_c T$  FOR VARYING DEGREE OF STABILITY  $\sigma$  ( $K_{sp} = 10$ ,  $We = 1.0$ )

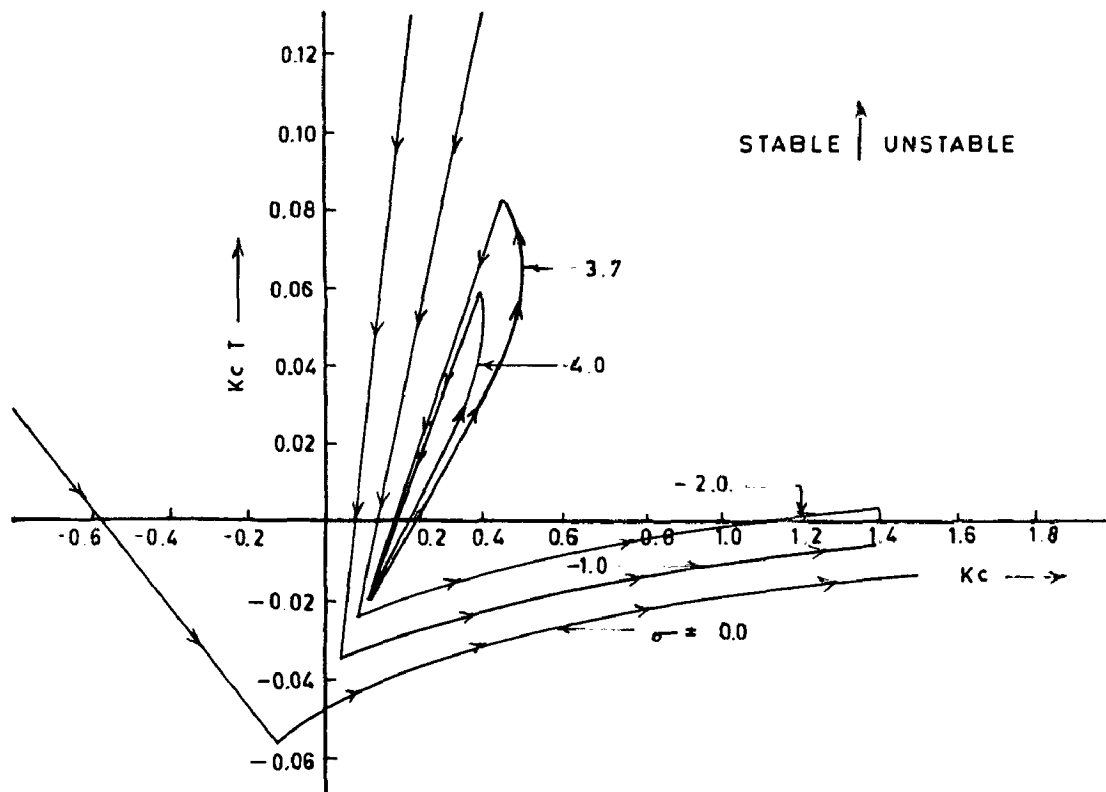


Fig 4.8 STABILITY REGION IN PLANE OF  $K_c$ - $K_c T$  FOR VARYING DEGREE OF STABILITY  $\sigma$  ( $K_{sp} = 10$ ,  $We = 8$ )

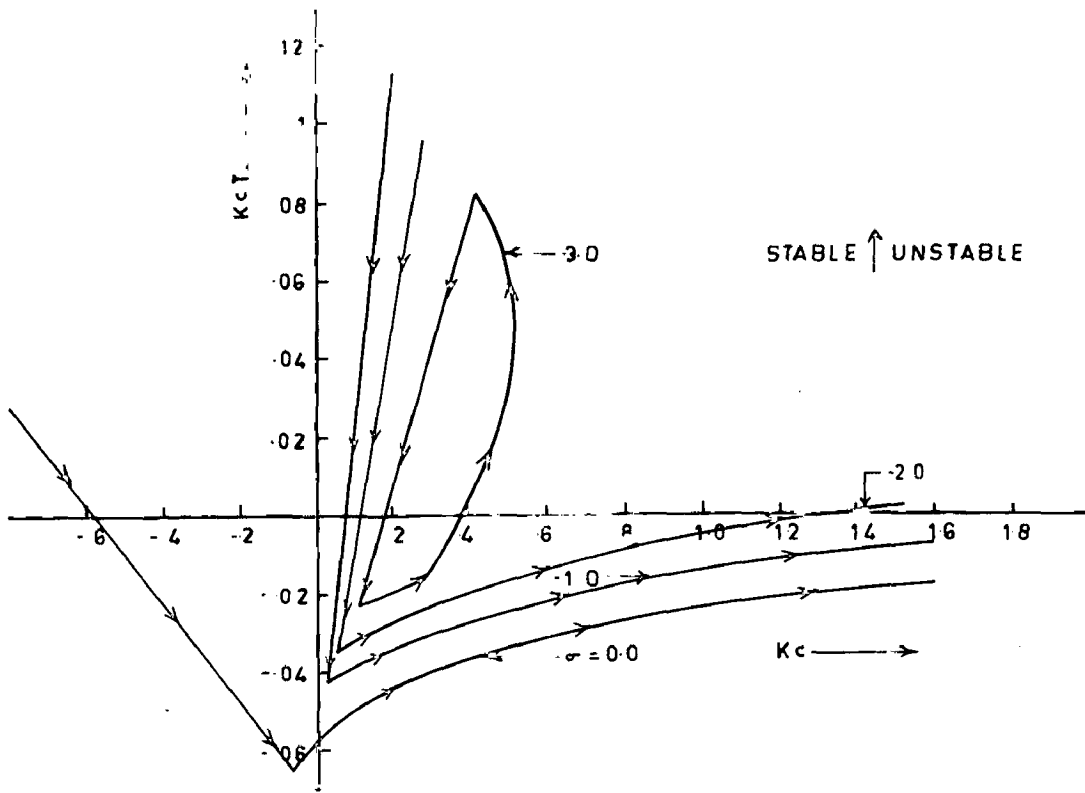


FIG. 49 STABILITY REGION IN PLANE OF  $K_c - K_{cT}$  FOR VARYING DEGREE OF STABILITY  $\sigma$  ( $K_{sp} = 10, We = 0.5$ )

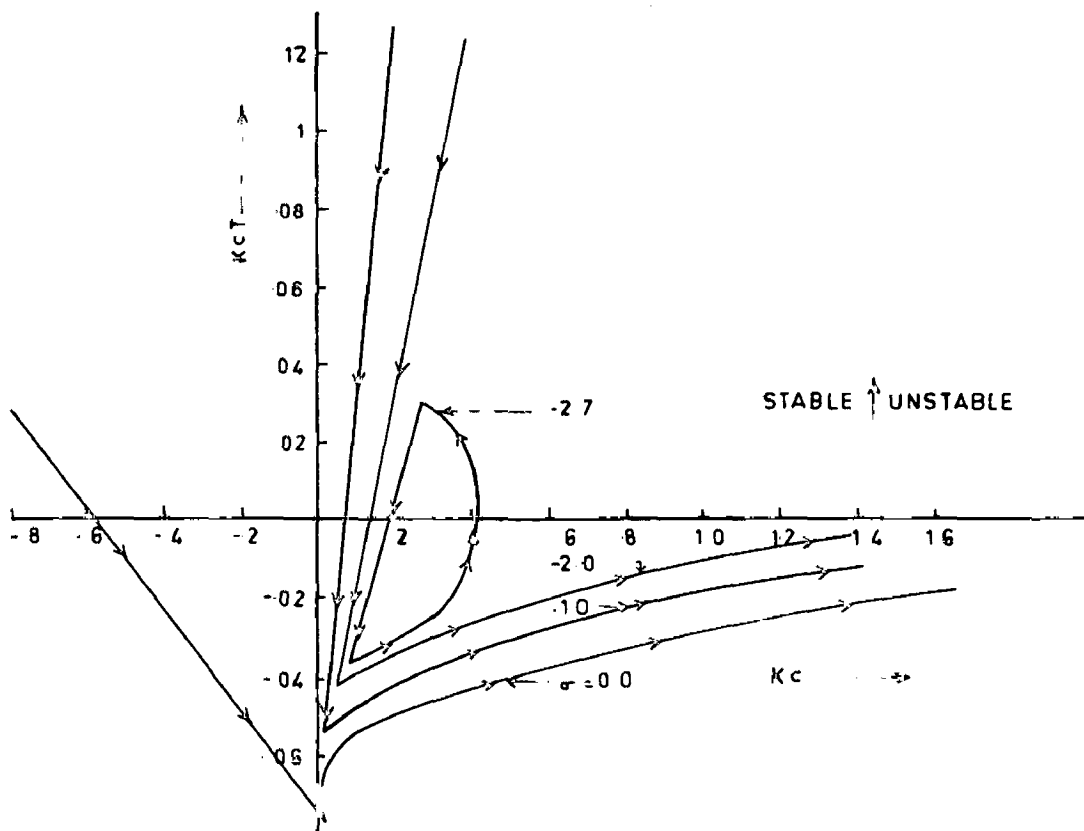


FIG. 410 STABILITY REGION IN PLANE OF  $K_c - K_{cT}$  FOR VARYING DEGREE OF STABILITY  $\sigma$  ( $K_{sp} = 10, We = 0.20$ )

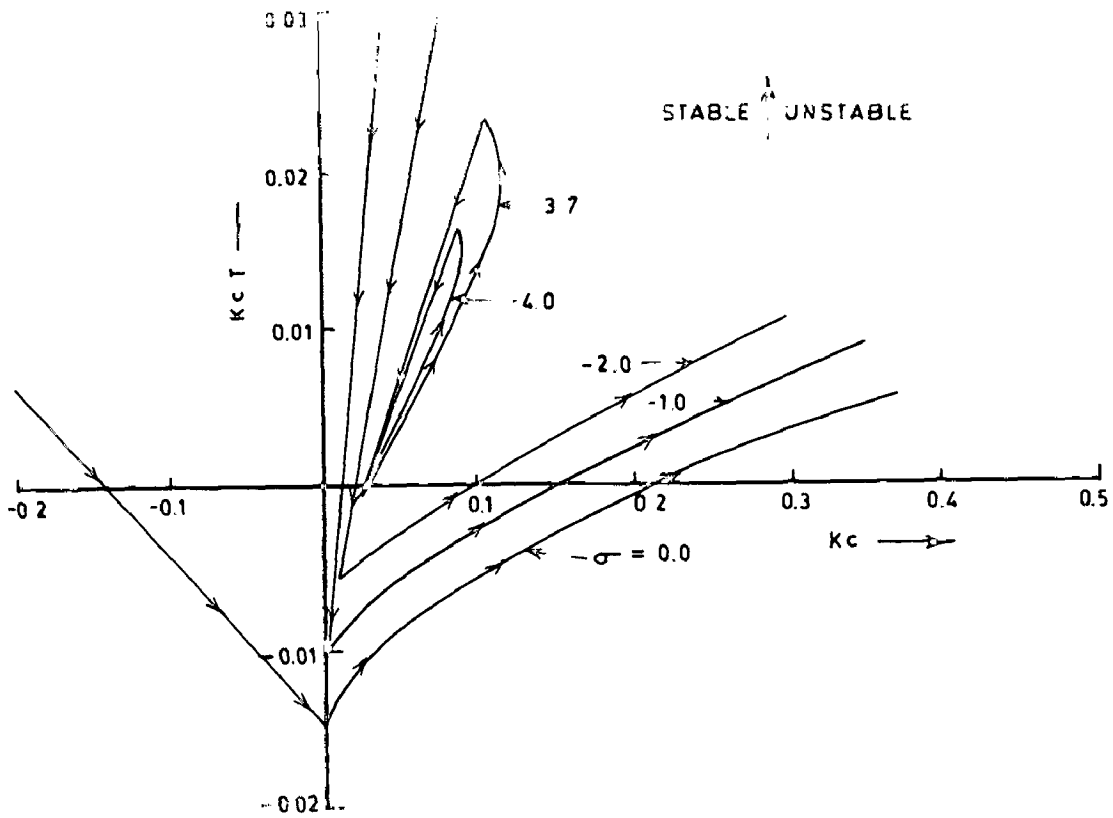


FIG. 4.11 STABILITY REGION IN PLANE OF (  $K_c$ - $K_cT$  ) FOR VARYING DEGREE OF STABILITY  $\sigma$ - (  $K_{sp} = 50$  ,  $We = 1.0$  )

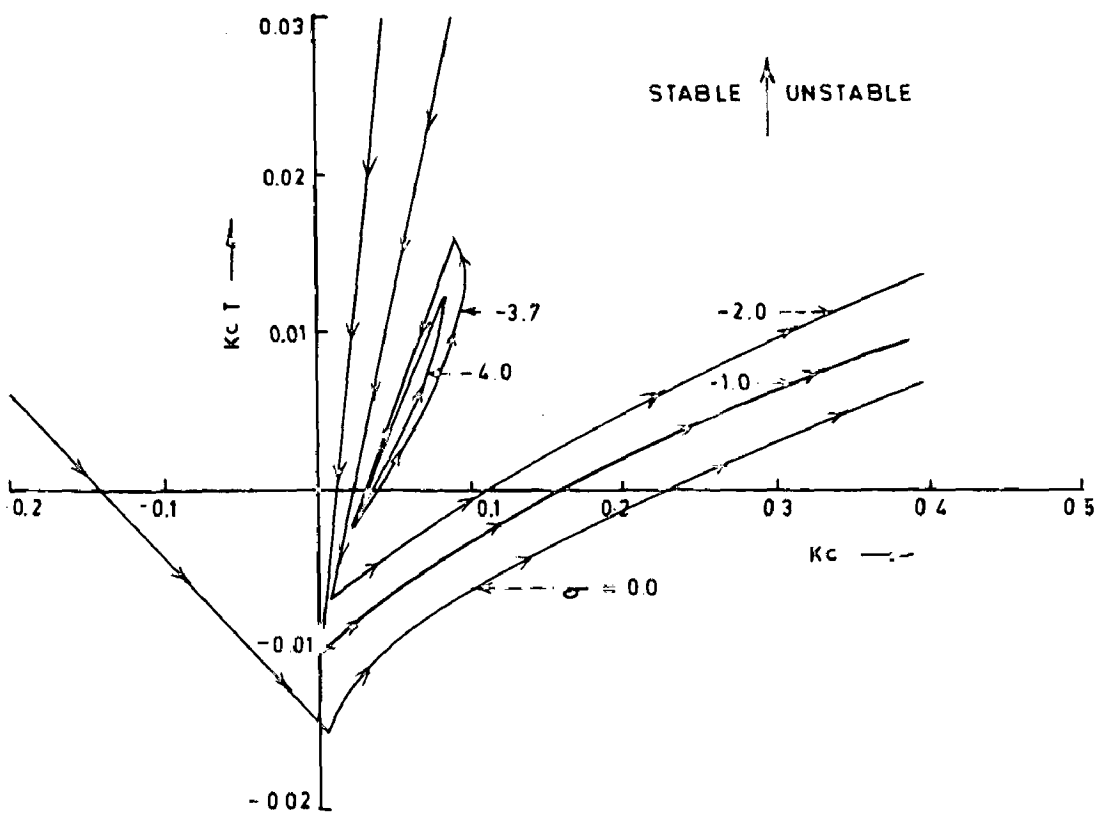


FIG. 4.12 STABILITY REGION IN PLANE OF (  $K_c$ - $K_cT$  ) FOR VARYING DEGREE OF STABILITY  $\sigma$ - (  $K_{sp} = 50$  ,  $We = 8$  )

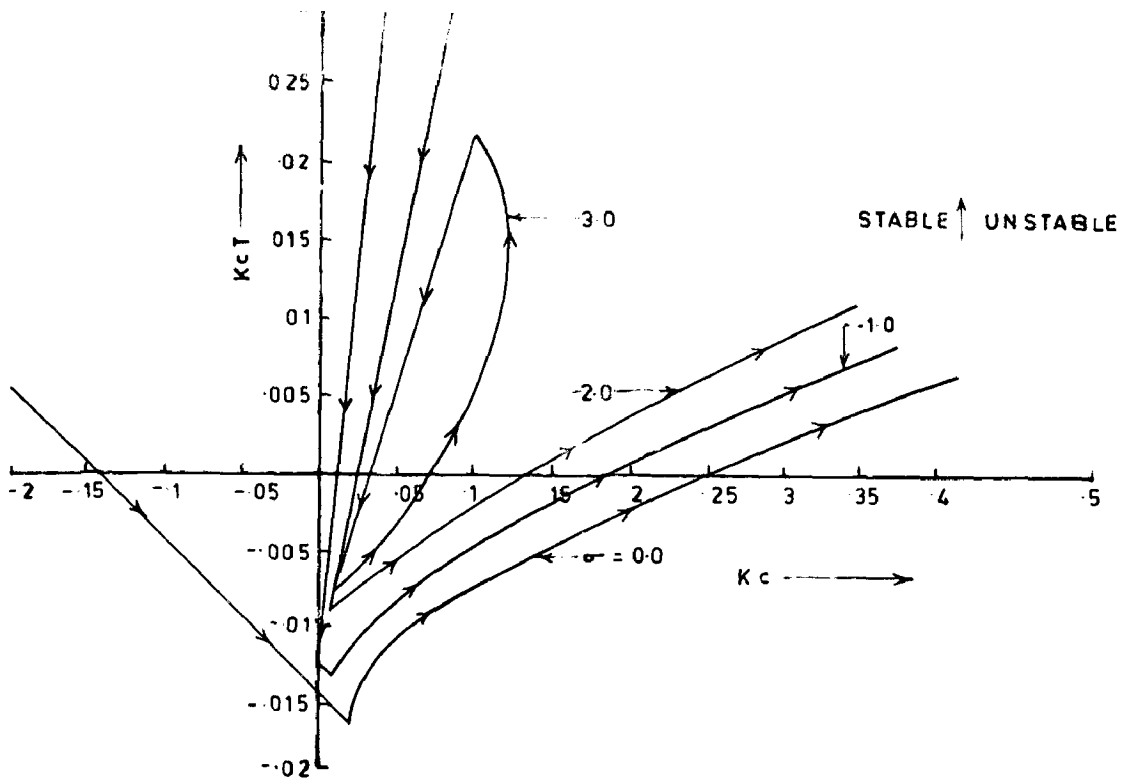


Fig.4.13 STABILITY REGION IN PLANE ( $K_c - K_{cT}$ ) FOR VARYING DEGREE OF STABILITY ( $K_{sp} = 50, We = 50$ )

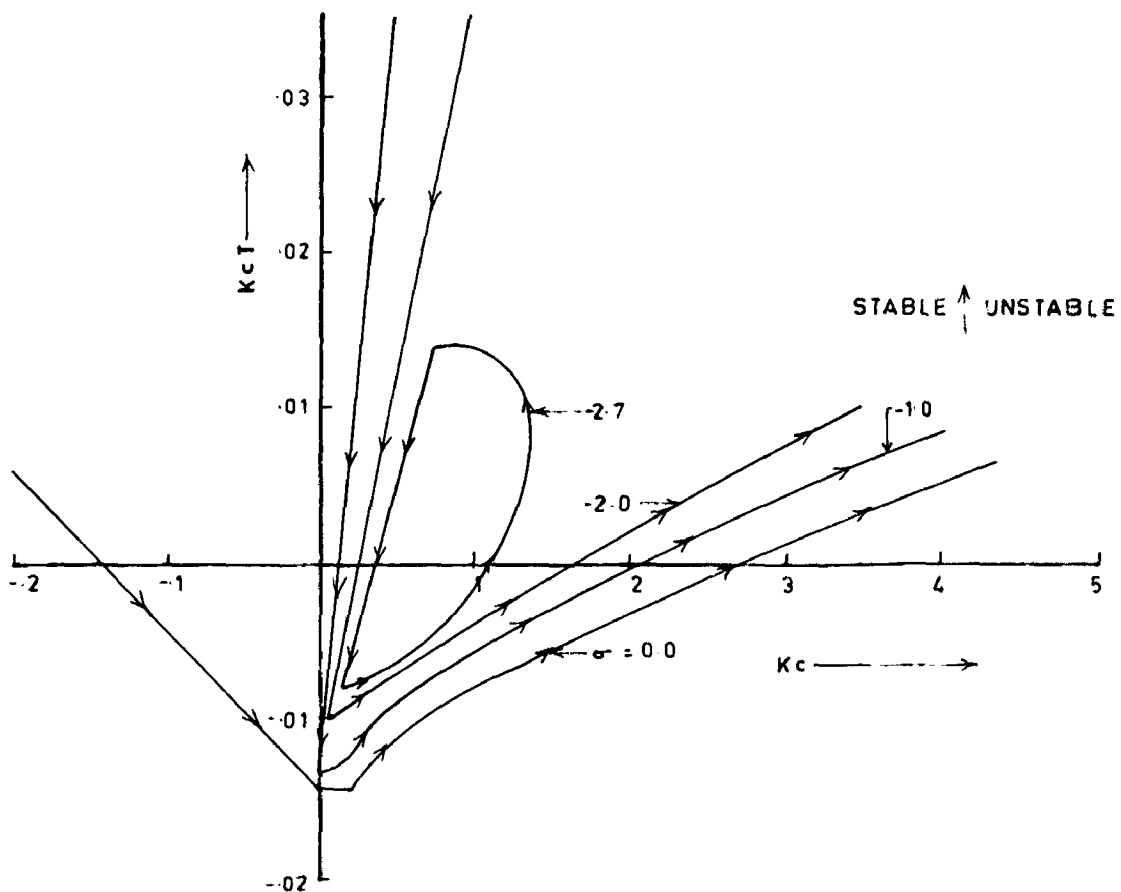


Fig.4.14 STABILITY REGION IN PLANE ( $K_c - K_{cT}$ ) FOR VARYING DEGREE OF STABILITY ( $K_{sp} = 50, We = 20$ )

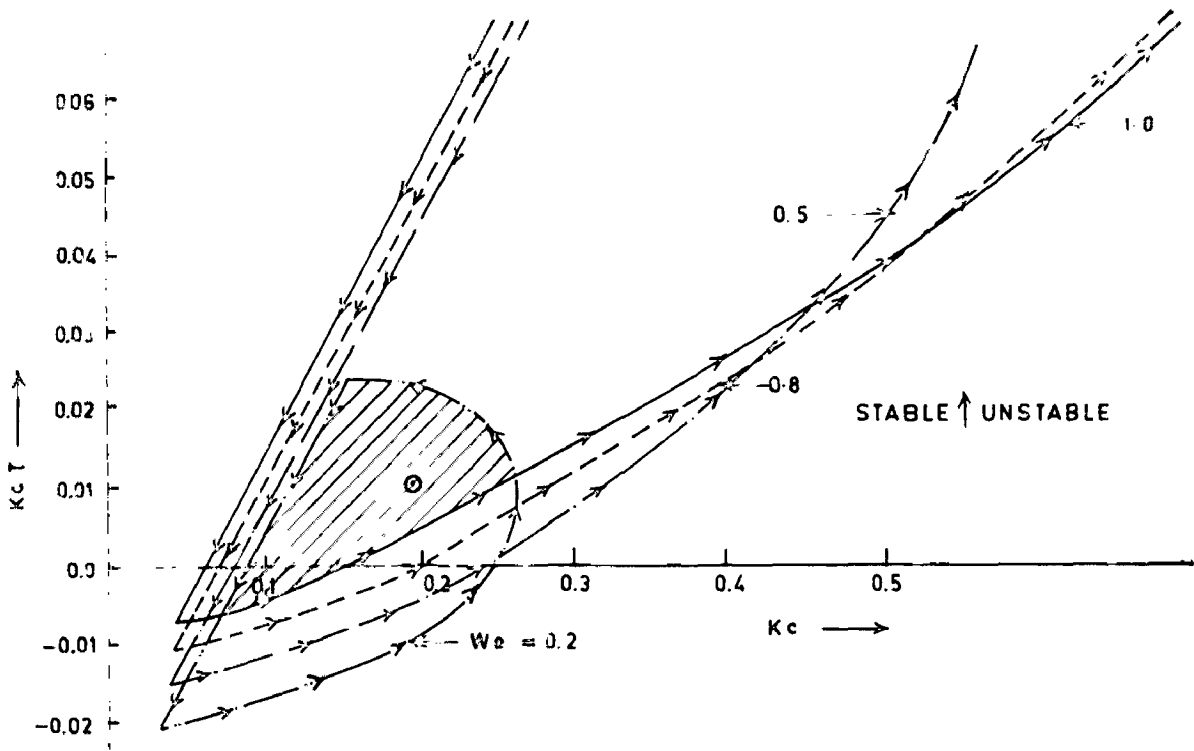


Fig 4-15 REGION OF STABILITY IN THE PLANE OF  $K_c - K_{cT}$  ENSURING  $\sigma \geq 27$  WITH VARIATION IN p.u. OPERATING FREQUENCY ( $K_{sp} = 20$ )

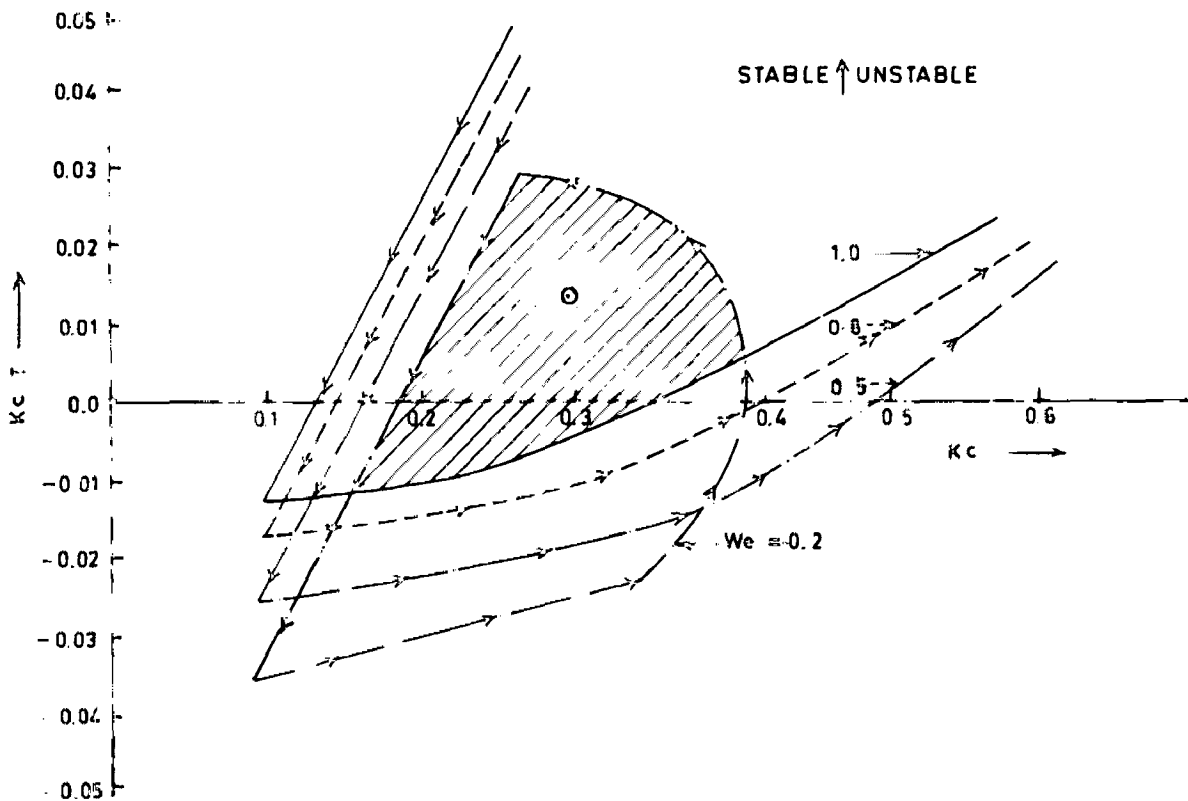


Fig 4-16 REGION OF STABILITY IN THE PLANE OF  $K_c - K_{cT}$  ENSURING  $\sigma \geq 27$  WITH VARIATION IN p.u. OPERATING FREQUENCY ( $K_{sp} = 10$ )

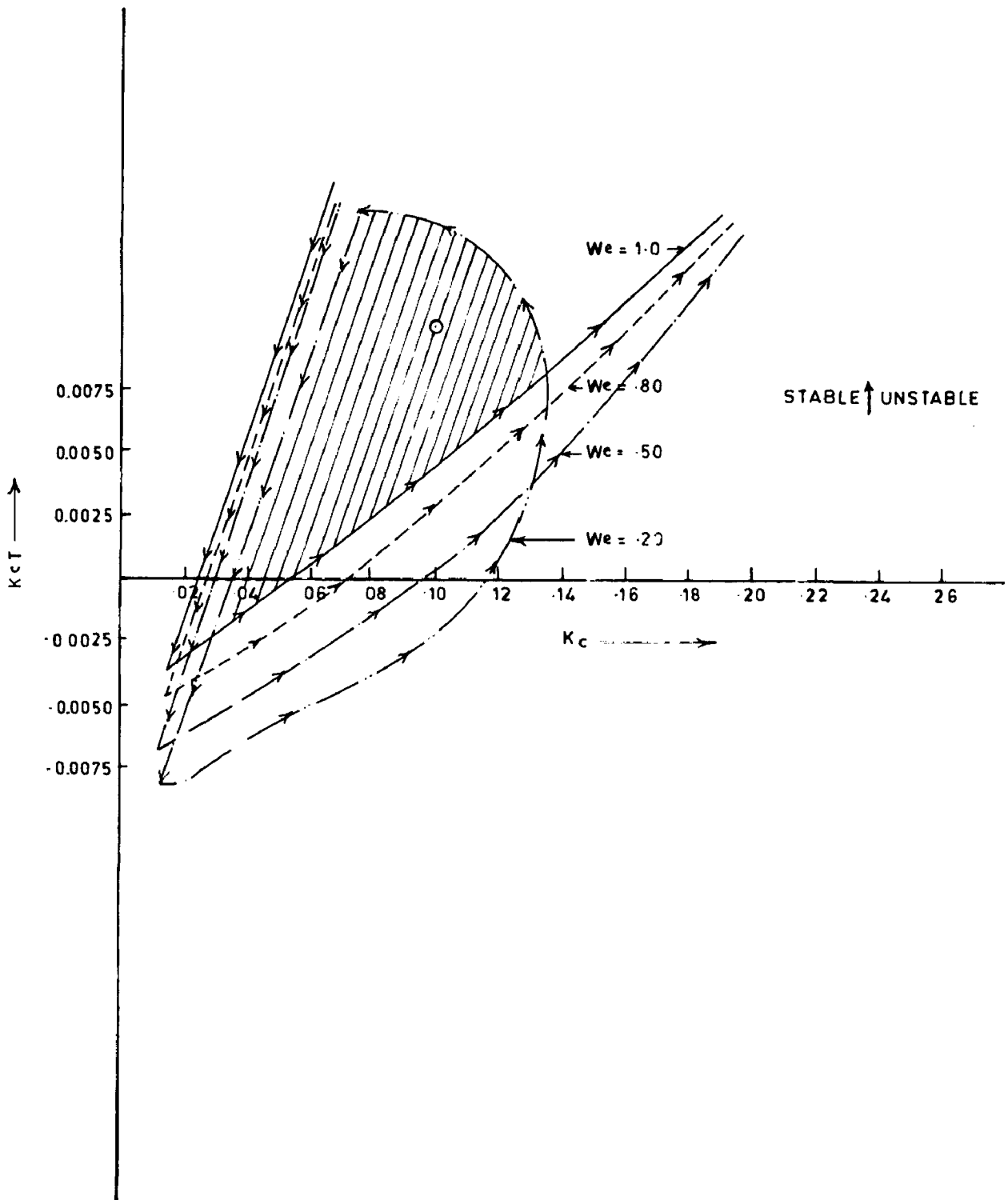


Fig 417 REGION OF STABILITY IN THE PLANE OF  $K_c - K_{cT}$  ENSURING  $\sigma > -2.7$  WITH VARIATION IN  $\rho u$  OPERATING FREQUENCY ( $K_{sp} = 50$ )

## CHAPTER - 5

## THE SIXTH HARMONIC ANALYSIS OF THE DRIVE

Due to the harmonics present in the inverter current, harmonic torques are produced which cause pulsation in the rotor speed. In applications where uniform speed of rotation is mandatory such as machine tool, antenna positioning and other applications it is important to ensure magnitude of these speed oscillations within limits.

An analytical method for calculating the 6th harmonic torques arising from a rectifier controlled-current inverter power source is given. This analysis is general in that it includes effect of steady-state speed variation, voltage fluctuation and current variation. The sixth harmonic pulsations in torque, rotor speed and stator voltage of induction motor have been calculated for three sets of controller parameters and four different p.u. operating frequencies.

## 6.1 MATHEMATICAL EQUATIONS FOR THE SIXTH HARMONIC EFFECTS

First a general set of equations is derived for the drive system to study the 6th harmonic phenomena. Equations (2.3), (2.4), (2.5), (2.7), (2.11), (2.12) and (2.14) comprise a set which completely describes the behaviour of rectifier-inverter induction motor drive. However, due to the infinite series of time varying coefficients in equation (2.3), (2.5) and (2.7) it is desirable to simplify these equations to a set which closely approximates to the actual system response.

At higher inverter frequencies the harmonic content of the applied stator currents and the resulting harmonic voltage have negligible effect on the system performance [12]. At sufficiently low frequencies the harmonic contents begin to influence the system response and can not be neglected. However, unless the inverter frequency is nearly zero, the 5th and 7th harmonics predominate and the effect of the 11th, 13th and higher stator current and voltage harmonics may be neglected [12].

In the synchronously rotating reference frame the 5th and 7th harmonics appear as 6th harmonic quantities. If the static drive system is stable, the fundamental frequency voltage and current consist of a constant component along with 6th, 12th and higher multiples of 6th harmonic. Since 12th and higher harmonics are neglected all variables may be written as the sum of a constant plus a 6th-harmonic component. For example

$$\begin{aligned}
 V_I &= V_{I0} + V_{I6} \\
 &= V_{I0} + V_{I\alpha} \cos 6 \omega_e t + V_{I\beta} \sin 6 \omega_e t \\
 I_I &= I_{I0} + I_{I6} \\
 &= I_{I0} + I_{I\alpha} \cos 6 \omega_e t + I_{I\beta} \sin 6 \omega_e t \\
 T_e &= T_{e0} + T_{e6} \\
 &= T_{e0} + T_{e\alpha} \cos 6 \omega_e t + T_{e\beta} \sin 6 \omega_e t \\
 \omega_r &= \omega_{r0} + \omega_{r6} \\
 &= \omega_{r0} + \omega_{r\alpha} \cos 6 \omega_e t + \omega_{r\beta} \sin 6 \omega_e t
 \end{aligned}
 \quad \left. \vphantom{\begin{aligned} V_I \\ I_I \\ T_e \\ \omega_r \end{aligned}} \right\} \dots (5.1)$$



and so forth for  $v_{qs}^e$ ,  $v_{ds}^e$ ,  $i_{qs}^e$ ,  $i_{ds}^e$ ,  $i_{qr}^e$ ,  $i_{dr}^e$ ,  $I_R$ ,  $\omega_{s\ell}$  and  $\omega_e$ . Rewriting equation (2.26)

$$\begin{bmatrix} v_{qs}^e \\ v_{ds}^e \\ 0 \\ 0 \end{bmatrix} = \begin{bmatrix} \gamma_s + pX_s & \omega_e X_s & pX_m & \omega_e X_m \\ -\omega_e X_s & \gamma_s + pX_s & -\omega_e X_m & pX_m \\ pX_m & \omega_{s\ell} X_m & \gamma_r + pX_r & \omega_{s\ell} X_r \\ -\omega_{s\ell} X_m & pX_m & -\omega_{s\ell} X_r & \gamma_r + pX_r \end{bmatrix} \begin{bmatrix} i_{qs}^e \\ i_{ds}^e \\ i_{qr}^e \\ i_{dr}^e \end{bmatrix} \quad \dots(5.2)$$

Substituting various expression from equations (5.1) in equations (5.2) yields a set of equations containing only d.c., 6th and 12th harmonic terms. Equating terms of the same frequency yields three sets of equations. one set containing d.c. terms only, a second set containing 6th harmonic terms, and the third set involving only 12th harmonic quantities. Since only the 6th harmonic torque is of interest in this development, the set of equations containing the 12th terms will not be considered.

From equations (5.2) and equations (5.1) the set of relations involving the d.c. terms are as follows -

$$\begin{bmatrix} v_{qso}^e \\ v_{dso}^e \\ 0 \\ 0 \end{bmatrix} = \begin{bmatrix} \gamma_s & \omega_{e0} X_s & 0 & \omega_{e0} X_m \\ -\omega_{e0} X_s & \gamma_s & -\omega_{e0} X_m & 0 \\ 0 & \omega_{s\ell 0} X_m & \gamma_r & \omega_{s\ell 0} X_r \\ -\omega_{s\ell 0} X_m & 0 & -\omega_{s\ell 0} X_r & \gamma_r \end{bmatrix} \begin{bmatrix} i_{qso}^e \\ i_{dso}^e \\ i_{qro}^e \\ i_{dro}^e \end{bmatrix} +$$

$$\frac{1}{2} \begin{bmatrix} 0 & 0 & X_s & X_s & 0 & 0 & \omega_{e\alpha} & \omega_{e\beta} \\ & & \omega_{e\alpha} & \omega_{e\beta} & & & X_m & X_m \\ -X_s & -\omega_{e\beta} & & & -X_m & -X_m & & \\ \omega_{e\alpha} & X_s & 0 & 0 & \omega_{e\alpha} & \omega_{e\beta} & 0 & 0 \\ 0 & 0 & \omega_{s\alpha} & \omega_{s\beta} & 0 & 0 & \omega_{s\alpha} & \omega_{s\beta} \\ & & X_m & X_m & & & X_r & X_r \\ -\omega_{s\alpha} & -\omega_{s\beta} & & & -\omega_{s\alpha} & -\omega_{s\beta} & & \\ X_m & X_m & 0 & 0 & X_r & X_r & 0 & 0 \end{bmatrix} \begin{bmatrix} i_{q\alpha}^e \\ i_{q\beta}^e \\ i_{d\alpha}^e \\ i_{d\beta}^e \\ i_{q\alpha}^e \\ i_{q\beta}^e \\ i_{d\alpha}^e \\ i_{d\beta}^e \end{bmatrix}$$

... (5.3)

$$\omega_{s\alpha} = \omega_{e\alpha} - \omega_{r\alpha}$$

... (5.4)

$$T_{eo} = X_m \left[ i_{q\alpha}^e i_{d\beta}^e - i_{d\alpha}^e i_{q\beta}^e + \frac{1}{2} (i_{q\alpha}^e i_{d\alpha}^e + i_{q\beta}^e i_{d\beta}^e - i_{d\alpha}^e i_{q\alpha}^e - i_{d\beta}^e i_{q\beta}^e) \right]$$

... (5.5)

$$T_{eo} - T_{Lo} = 0$$

... (5.6)

Rewriting equations (2.3), (2.7) and (2.11) in p.u.

$$i_{qs}^e = I_R \left[ 1 - \frac{2}{35} \cos 6 \omega_e t - \frac{2}{143} \cos 12 \omega_e t \dots \right]$$

... (5.7)

$$i_{ds}^e = I_R \left[ -\frac{12}{35} \sin 6 \omega_e t - \frac{24}{143} \sin 12 \omega_e t \dots \right]$$

... (5.8)

$$V_I = v_{qs}^e \left[ 1 - \frac{2}{35} \cos 6 \omega_e t - \frac{2}{143} \cos 12 \omega_e t \dots \right]$$

$$+ v_{ds}^e \left[ -\frac{12}{35} \sin 6 \omega_e t - \frac{24}{143} \sin 12 \omega_e t \dots \right]$$

... (5.9)

$$V_R = V_I + (R_F + X_{CO} + p X_F) I_R$$

... (5.10)

Hence,

$$i_{qso}^e = I_{RO} - \frac{1}{35} I_{R\alpha} \quad \dots(5.11)$$

$$i_{dso}^e = -\frac{6}{35} I_{R\beta} \quad \dots(5.12)$$

$$V_{RO} = V_{IO} + (R_F + X_{CO}) I_{RO} \quad \dots(5.13)$$

$$V_{IO} = v_{qso}^e - \frac{1}{35} v_{qsa}^e - \frac{6}{35} v_{ds\beta}^e \quad \dots(5.14)$$

The zero-suffix quantities and the magnitude of the 6th harmonic quantities together make up the steady-state operating point. However for normal operation the magnitude of quantities (steady-state) is much larger than the magnitude of the 6th harmonic quantities which do not contribute appreciably to the average values of the system variables. This fact has been noted by other investigators [12]. Hence, equations(5.3), (5.11) to (5.14) may be expressed approximately as -

$$\begin{bmatrix} v_{qso}^e \\ v_{dso}^e \\ 0 \\ 0 \end{bmatrix} = \begin{bmatrix} r_s & \omega_{eo} X_s & 0 & \omega_{eo} X_m \\ -\omega_{eo} X_s & r_s & \omega_{eo} X_m & 0 \\ 0 & \omega_{sfo} X_m & r_r & \omega_{sfo} X_r \\ \omega_{sfo} X_m & 0 & -\omega_{sfo} X_r & r_r \end{bmatrix} \begin{bmatrix} i_{qso}^e \\ i_{dso}^e \\ i_{qro}^e \\ i_{dro}^e \end{bmatrix} \quad \dots(5.15)$$

$$T_{eo} = X_m [i_{qso}^e i_{dro}^e - i_{dso}^e i_{qro}^e] \quad \dots(5.16)$$

$$i_{qso}^e = I_{RO} \quad \dots(5.17)$$

$$i_{dso}^e = 0 \quad \dots(5.18)$$

$$V_{IO} = v_{qso}^e \quad \dots(5.19)$$

$$V_{RO} = V_{IO} + (R_F + X_{CO}) I_{RO} \quad \dots(5.20)$$

Upon simplification, the steady-state constant quantities (d.c. term) can be expressed as -

$$\begin{bmatrix} V_{RO} \\ v_{dso}^e \\ 0 \\ 0 \end{bmatrix} = \begin{bmatrix} r_s + R_F + X_{CO} & \omega_{eo} X_s & 0 & \omega_{eo} X_m \\ -\omega_{eo} X_s & r_s & -\omega_{eo} X_m & 0 \\ 0 & 0 & \omega_{sfo} X_m & r_r \\ -\omega_{sfo} X_m & 0 & -\omega_{sfo} X_r & r_r \end{bmatrix} \begin{bmatrix} i_{qso}^e \\ 0 \\ i_{qro}^e \\ i_{dro}^e \end{bmatrix} \quad \dots(5.21)$$

$$T_{eo} = X_m i_{qso}^e i_{dro}^e \quad \dots(5.22)$$

It is clear that equations(5.21) and equation (5.22) formulate an algebraic set of equations which establishes the average value of all variables. Although these equations are approximate, they are sufficiently accurate to describe the average value of the converter and machine variables.

Equating terms for the 6th harmonic from equations (5.1) and (5.2), yields

$$\begin{bmatrix} v_{qs6}^e \\ v_{ds6}^e \\ 0 \\ 0 \end{bmatrix} = \begin{bmatrix} r_s + pX_s & \omega_{eo} X_s & p X_m & \omega_{eo} X_m & X_s i_{dso}^e + X_m i_{dro}^e & 0 \\ -\omega_{eo} X_s & r_s + p X_s & -\omega_{eo} X_m & p X_m & -(X_s i_{qso}^e + X_m i_{qro}^e) & 0 \\ p X_m & \omega_{sfo} X_m & r_r + p X_r & \omega_{sfo} X_r & 0 & X_m i_{dso}^e + X_r i_{dro}^e \\ -\omega_{sfo} X_m & p X_m & -\omega_{sfo} X_r & r_r + p X_r & 0 & -(X_m i_{qso}^e + X_r i_{qro}^e) \end{bmatrix} \begin{bmatrix} i_{qs6}^e \\ i_{ds6}^e \\ i_{qr6}^e \\ i_{dr6}^e \\ \omega_{e6} \\ \omega_{s/6} \end{bmatrix} \quad \dots(5.23)$$

$$T_{e6} = X_m \left[ i_{qso}^e i_{dr6}^e + i_{dro}^e i_{qs6}^e - i_{qro}^e i_{ds6}^e - i_{dso}^e i_{qr6}^e \right] \quad \dots(5.24)$$

$$T_{L6} = 0 \quad \dots(5.25)$$

Rewriting equation (2.14)

$$T_e = T_L + 4\pi f_b H p (\omega_r) \quad \dots(5.26)$$

The expression for the 6th harmonic speed pulsation is given by

$$\omega_{r6} = \frac{1}{4\pi f_b H p} \frac{1}{p} T_{e6} \quad \dots(5.27)$$

From equations (5.7), (5.8) and (5.9)

$$i_{qs6}^e = -\frac{2}{35} I_{RO} \cos 6 \omega_e t + I_{R6} \quad \dots(5.28)$$

$$i_{ds6}^e = -\frac{12}{35} I_{RO} \sin 6 \omega_e t \quad \dots(5.29)$$

$$V_{I6} = -\frac{2}{35} v_{qso}^e \cos 6 \omega_e t + v_{qs6}^e - \frac{12}{35} v_{dso}^e \sin 6 \omega_e t \quad \dots(5.30)$$

Rewriting equations (2.23) to (2.36)

$$I_R^* = K_{sp} (\omega_r^* - \omega_r) \quad \dots(5.31)$$

$$V_R = \frac{K_c (1 + T \omega_b p)}{p \omega_b} (I_R^* - I_R) \quad \dots(5.32)$$

$$\omega_{sl} = k_{sl} I_R \quad \dots(5.33)$$

$$\omega_e = \omega_r + \omega_{sl} \quad (\text{for motor operation}) \quad \dots(5.34)$$

The expressions for concerned 6th harmonic variation are as

follows -

$$I_{R6}^* = -K_{sp} \omega_{r6} \quad \dots(5.35)$$

$$V_{R6} = \frac{K_c (1 + T \omega_{bp})}{\omega_{bp}} (I_{R6}^* - I_{R6}) \quad \dots(5.36)$$

$$\omega_{s/6} = K_{s/} I_{R6} \quad \dots(5.37)$$

$$\omega_{e6} = \omega_{r6} + \omega_{s/6} \quad \dots(5.38)$$

The four forcing functions, namely  $\frac{2}{35} I_{R0} \cos 6 \omega_e t$ ,  $\frac{12}{35} I_{R0} \sin 6 \omega_e t$ ,  $\frac{2}{35} v_{qso}^e \cos 6 \omega_e t$ ,  $\frac{12}{35} v_{dso}^e \sin 6 \omega_e t$  are of the same frequency. Thus all variables in the steady-state will be of this frequency and hence phasors may be employed for these harmonic variables. Therefore, if  $\cos 6 \omega_e t$  is replaced by a unit phasor (1),  $\sin 6 \omega_e t$  will be replaced by  $-j$  and  $p$  by  $j 6 \omega_{e0}$ . Defining

$$\psi_{qro} = X_m i_{qso}^e + X_r i_{qro}^e \quad \dots(5.39)$$

$$\psi_{dro} = X_m i_{dso}^e + X_r i_{dro}^e \quad \dots(5.40)$$

$$\psi_{qso} = X_s i_{qso}^e + X_m i_{qro}^e \quad \dots(5.41)$$

$$\psi_{dso} = X_s i_{dso}^e + X_m i_{dro}^e \quad \dots(5.42)$$

The equations (5.23) gives after some simplification

$$\begin{bmatrix} \overline{i_{qs6}^e} \\ \overline{i_{ds6}^e} \\ 0 \\ 0 \end{bmatrix} = \begin{bmatrix} \gamma_s + j6 \omega_{e0} X_s & \omega_{e0} X_s & j6 \omega_{e0} X_m & \omega_{e0} X_m & \psi_{dso} & 0 \\ \omega_{e0} X_s & \gamma_s + j6 \omega_{e0} X_s & -\omega_{e0} X_m & j6 \omega_{e0} X_m & -\psi_{qso} & 0 \\ j6 \omega_{e0} X_m & \omega_{e0} X_s & \gamma_r + j6 \omega_{e0} X_r & \omega_{e0} X_r & 0 & \psi_{dro} \\ -\omega_{e0} X_m & j6 \omega_{e0} X_m & -\omega_{e0} X_r & \gamma_r + j6 \omega_{e0} X_r & 0 & -\psi_{qro} \end{bmatrix} \begin{bmatrix} \overline{i_{qs6}^e} \\ \overline{i_{ds6}^e} \\ \overline{i_{qr6}^e} \\ \overline{i_{dr6}^e} \\ \overline{\omega_{e6}} \\ \overline{\omega_{s/6}} \end{bmatrix} \quad \dots(5.43)$$

Further, from equations (5.24), (5.27) to (5.30) and (5.35) to (5.38)

$$\overline{T_{e6}} = X_m \left[ \overline{i_{qso}^e} \overline{i_{dr6}^e} + \overline{i_{dro}^e} \overline{i_{qs6}^e} - \overline{i_{qro}^e} \overline{i_{ds6}^e} - \overline{i_{dso}^e} \overline{i_{qr6}^e} \right] \quad \dots(5.44)$$

$$\overline{\omega_{r6}} = -j \frac{1}{24\pi f_b H \omega_{e0}} \overline{T_{e6}} \quad \dots(5.45)$$

$$\overline{i_{qs6}^e} = -\frac{2}{35} I_{R0} + \overline{I_{R6}} \quad \dots(5.46)$$

$$\overline{i_{ds6}^e} = j \frac{12}{35} I_{R0} \quad \dots(5.47)$$

$$\overline{V_{I6}} = -\frac{2}{35} v_{qso}^e + j \frac{12}{35} v_{dso}^e + \overline{v_{qs6}^e} \quad \dots(5.48)$$

$$\overline{I_{R6}^*} = -K_{sp} \overline{\omega_{r6}} \quad \dots(5.49)$$

$$\overline{V_{R6}} = \left( -\frac{j K_c}{6\omega_b \omega_{e0}} + K_c T \right) (\overline{I_{R6}^*} - \overline{I_{R6}}) \quad \dots(5.50)$$

$$\overline{\omega_{s\ell 6}} = K_{s\ell} \overline{I_{R6}} \quad \dots(5.51)$$

$$\overline{\omega_{e6}} = \overline{\omega_{r6}} + \overline{\omega_{s\ell 6}} \quad \dots(5.52)$$

$$\overline{V_{R6}} = \overline{V_{I6}} + (j6 \omega_{e0} X_F + R_F + X_{CO}) \overline{I_{R6}} \quad \dots(5.53)$$

Substituting the expression for  $\overline{I_{R6}^*}$  equation (5.49) in equation (5.50)

$$\overline{V_{R6}} = \left( -\frac{j K_c}{6\omega_b \omega_{e0}} + K_c T \right) (-K_{sp} \overline{\omega_{r6}} - \overline{I_{R6}}) \quad \dots(5.54)$$

From equations (5.48), (5.53) and (5.46)

$$\overline{v_{qs6}^e} = \overline{V_{I6}} + \frac{2}{35} v_{qso}^e - j \frac{12}{35} v_{dso}^e \quad \dots(5.55)$$

$$\overline{V_{I6}} = \overline{V_{R6}} (j6 \omega_{e0} X_F + R_F + X_{CO}) \overline{I_{R6}} \quad \dots (5.56)$$

$$\overline{I_{R6}} = \overline{i_{qs6}}^e + \frac{2}{35} \overline{I_{R0}} \quad \dots (5.57)$$

Using equations (5.54), (5.56) and (5.57), equation (5.55) can be written as

$$\begin{aligned} \overline{v_{qs6}}^e = & - \left( -\frac{jK_c}{6\omega_b \omega_{e0}} + K_c T \right) K_{sp} \overline{w_{r6}} \left( -\frac{jK_c}{6\omega_b \omega_{e0}} + K_c T + j6 \omega_{e0} X_F + \right. \\ & \left. R_F + X_{CO} \right) \left( \overline{i_{qs6}}^e + \frac{2}{35} \overline{I_{R0}} \right) + \frac{2}{35} \overline{v_{qso}}^e - j \frac{12}{35} \overline{v_{dso}}^e \end{aligned} \quad \dots (5.58)$$

substituting for  $\overline{T_{e6}}$  from equations (5.44) in equation (5.45)

$$\begin{aligned} \overline{w_{r6}} = & - \frac{j}{24\pi f_b H \omega_{e0}} X_m \left[ \overline{i_{qso}}^e \overline{i_{dr6}}^e + \overline{i_{dro}}^e \overline{i_{qs6}}^e - \overline{i_{qro}}^e \overline{i_{ds6}}^e - \right. \\ & \left. \overline{i_{dso}}^e \overline{i_{qr6}}^e \right] \quad \dots (5.59) \end{aligned}$$

Using equations (5.18), the above equation becomes

$$\overline{w_{r6}} = \frac{-j}{24\pi f_b \omega_{e0}} X_m \left[ \overline{i_{qso}}^e \overline{i_{dr6}}^e + \overline{i_{dro}}^e \overline{i_{qs6}}^e - \overline{i_{qro}}^e \overline{i_{ds6}}^e - \right] \quad \dots (5.60)$$

Substitution of above expression for  $\overline{w_{r6}}$  in equation (5.58)

results in

$$\begin{aligned} \overline{v_{qs6}}^e = & \left( -\frac{jK_c}{6\omega_b \omega_{e0}} + K_c T \right) \frac{jK_{sp} X_m}{24\pi f_b \omega_{e0}} \left( \overline{i_{qso}}^e \overline{i_{dr6}}^e + \overline{i_{dro}}^e \overline{i_{qs6}}^e - \right. \\ & \left. \overline{i_{qro}}^e \overline{i_{ds6}}^e \right) - \left( \overline{i_{qs6}}^e + \frac{2}{35} \overline{I_{R0}} \right) \left( -\frac{jK_c}{6\omega_b \omega_{e0}} + K_c T + j6 \omega_{e0} X_F + \right. \\ & \left. R_F + X_{CO} \right) + \frac{2}{35} \overline{v_{qso}}^e - j \frac{12}{35} \overline{v_{dso}}^e \quad \dots (5.61) \end{aligned}$$



From equations (5.51) and (5.57)

$$\overline{\omega_{s\ell 6}} = K_{s\ell} (\overline{i_{qs6}}^e + \frac{2}{35} I_{RO}) \quad \dots(5.62)$$

expressions for  $\overline{\omega_{r6}}$  and  $\overline{\omega_{s\ell 6}}$  from equations (5.60) and (5.62) respectively in equation (5.52) and defining

$$K_T = \frac{X_m}{24\pi f_b H \omega_{eo}} \quad \dots (5.63)$$

One gets

$$\overline{\omega_{r6}} = (K_{s\ell} - j K_T i_{dro}^e) \overline{i_{qs6}}^e + \frac{2}{35} I_{RO} K_{s\ell} - j K_T (i_{qso}^e \overline{i_{dr6}}^e - i_{qro}^e \overline{i_{ds6}}^e) \quad \dots(5.64)$$

Utilising equations (5.62) and equation (5.64), equations (5.43) gives

$$\begin{bmatrix} \overline{v_{qs6}}^e \\ \overline{v_{ds6}}^e \\ 0 \\ 0 \end{bmatrix} = \begin{bmatrix} \gamma_s + j6\omega_{eo} X_s + \psi_{dso} (K_{s\ell} - jK_T) i_{dro}^e & \omega_{eo} X_s + j K_T i_{qro}^e \psi_{dso} & j6\omega_{eo} X_m & \omega_{eo} X_m - jK_T \psi_{dso} i_{qso}^e \\ -\omega_{eo} X_s - \psi_{qso} (K_{s\ell} - jK_T) i_{dro}^e & \gamma_s + j6\omega_{eo} X_s - \omega_{eo} X_m & j6\omega_{eo} X_m + jK_T \psi_{qso} i_{qro}^e & \psi_{qso} i_{qso}^e \\ j6\omega_{eo} X_m + \psi_{dro} K_{s\ell} & \omega_{s\ell 0} X_m & \gamma_r + j6\omega_{eo} X_r & \omega_{s\ell 0} X_r \\ -\omega_{s\ell 0} X_m - \psi_{qro} K_{s\ell} & j6\omega_{eo} X_m - \omega_{s\ell 0} X_r & \gamma_r + j6\omega_{eo} X_r & \omega_{eo} X_r \end{bmatrix} \begin{bmatrix} \overline{i_{qs6}}^e \\ \overline{i_{ds6}}^e \\ \overline{i_{qr6}}^e \\ \overline{i_{dr6}}^e \end{bmatrix}$$

$$+ \begin{bmatrix} \frac{2}{35} I_{RO} K_{s\ell} \psi_{dso} \\ -\frac{2}{35} I_{RO} K_{s\ell} \psi_{qso} \\ \frac{2}{35} K_{s\ell} I_{RO} \psi_{dro} \\ -\frac{2}{35} K_{s\ell} I_{RO} \psi_{qro} \end{bmatrix} \dots (5.65)$$

Substituting the expression for  $\overline{v_{qs6}^e}$  from equation (5.61) in equation (5.65) and rearranging the terms

$$\begin{bmatrix} \frac{2}{35}(\overline{v_{qso}^e} - j6\overline{v_{dso}^e}) \\ \overline{v_{ds6}^e} \\ 0 \\ 0 \end{bmatrix} = \begin{bmatrix} r_s + j6\omega_{eo} X_s + \psi_{dso}(K_{s\ell} - jK_T) & \omega_{eo} X_s + jK_T & j6\omega_{eo} X_m - jK_T & \omega_{eo} X_m - jK_T \\ \psi_{dro}(-jK_c) + jK_{sp}K_T & i_{qro} \psi_{dso} + X_m & \psi_{dso} i_{qso}^e & \psi_{dso} i_{qso}^e \\ K_c T - jK_{sp}K_T & (-\frac{jK_c}{6\omega_b \omega_{eo}} + jK_{sp}K_T) & -jK_{sp}K_T & -jK_{sp}K_T \\ i_{dro}^e(-\frac{jK_c}{6\omega_b \omega_{eo}} + K_c T) + j6\omega_{eo} X_F + R_F + X_{CO} & (-\frac{jK_c}{6\omega_b \omega_{eo}} + K_c T) & i_{qso}^e \frac{jK_c}{6\omega_b \omega_{eo}} + K_c T & i_{qso}^e \frac{jK_c}{6\omega_b \omega_{eo}} + K_c T \end{bmatrix} \begin{bmatrix} \overline{i_{qs6}^e} \\ \overline{i_{ds6}^e} \\ \overline{i_{qr6}^e} \\ \overline{i_{dr6}^e} \end{bmatrix}$$

$$\begin{bmatrix} \psi_{dro} K_{s\ell} & r_s + j6\omega_{eo} X_s - \psi_{qso} & -\omega_{eo} X_m & j6\omega_{eo} X_m + jK_T \psi_{qso} \\ j6\omega_{eo} X_m + \psi_{dro} K_{s\ell} & jK_T i_{qro}^e & \psi_{qso} & jK_T \psi_{qso} \\ -\omega_{s\ell 0} X_m - \psi_{qro} K_{s\ell} & \omega_{s\ell 0} X_m & \gamma_r + j6\omega_{eo} X_r & \omega_{s\ell 0} X_r \\ -\omega_{s\ell 0} X_m - \psi_{qro} K_{s\ell} & j6\omega_{eo} X_m & -\omega_{s\ell 0} X_r & \gamma_r + j6\omega_{eo} X_r \end{bmatrix}$$

$$\begin{aligned}
 & + \left[ \begin{array}{c} \frac{jK_c}{6\omega_b \omega_{eo}} + K_c T + j6 \omega_{eo} X_F + R_F + X_{CO} + K_{s\ell} \psi_{dso} \\ - K_{s\ell} \psi_{qro} \\ K_{s\ell} \psi_{dro} \\ - K_{s\ell} \psi_{qro} \end{array} \right] \left[ \frac{2}{35} I_{RO} \right] \dots(5.66)
 \end{aligned}$$

Defining

$$Z_A = K_{s\ell} - j K_T i_{dro} \dots(5.67)$$

$$Z_B = - \frac{j K_c}{6 \omega_b \omega_{eo}} + K_c T \dots(5.68)$$

$$Z = j 6 \omega_{eo} \dots(5.69)$$

and substituting using these new constants in equation (5.69)

one gets

$$\begin{bmatrix} \frac{2}{35} (v_{qso} e^-) \\ j6 v_{dso} e^- \\ \\ v_{ds6} e^- \\ 0 \\ 0 \end{bmatrix} = \begin{bmatrix} \gamma_s + R_F + X_{CO} + \omega_{eo} X_s + jK_T & Z X_m & \omega_{eo} X_m - j K_T \\ Z(X_s + X_F) + \psi_{dso} Z_A + Z_B & i_{qro} e \psi_{dso} + j K_{sp} K_T & \psi_{dso} i_{qso} e - j K_{sp} K_T \\ -j K_{sp} K_T & i_{qro} e Z_B & i_{qso} e Z_B \\ i_{dro} e Z_B & -\omega_{eo} X_s - \psi_{qso} Z_A & \gamma_s + Z X_s - \omega_{eo} X_m & Z X_m + j K_T \\ -\omega_{eo} X_s - \psi_{qso} Z_A & j K_T i_{qro} e & \psi_{qso} & i_{qso} e \psi_{qso} \\ Z X_m + \psi_{dro} & \omega_{s\ell} X_m & r_r + Z X_r & \omega_{s\ell} X_r \\ K_{s\ell} & -\omega_{s\ell} X_m - Z X_m & -\omega_{s\ell} X_r & \gamma_r + Z X_r \\ -\omega_{s\ell} X_m - Z X_m & \psi_{qro} K_{s\ell} & & \end{bmatrix} \begin{bmatrix} i_{qs6} e^- \\ i_{ds6} e^- \\ i_{qr6} e^- \\ i_{dr6} e^- \end{bmatrix}$$

$$+ \begin{bmatrix} Z_B + Z X_F + R_F + X_{CO} + K_{s\ell} \psi_{dso} \\ - K_{s\ell} \psi_{qso} \\ K_{s\ell} \psi_{dro} \\ - K_{s\ell} \psi_{qro} \end{bmatrix} \begin{bmatrix} \frac{2}{35} I_{RO} \end{bmatrix} \dots (5.70)$$

Substitution of alternate expression for  $I_{RO}$  from equation (5.17) and  $\overline{i_{ds6}}$  from equation (5.47) in equation (5.70) results in

$$\begin{bmatrix} \frac{2}{35} (v_{qso} e^{-j6} v_{dso} e^j) \\ \overline{v_{ds6}} e \\ 0 \\ 0 \end{bmatrix} = \begin{bmatrix} r_s + R_F + X_{CO} + \omega_{e0} X_s + j K_T Z X_m & \omega_{e0} X_m - j K_T \\ Z(X_s + X_F) + \psi_{dso} Z_A + Z_B & \psi_{dso} i_{qso} e^{-j6} \\ j K_{sp} K_T & j K_{sp} K_T i_{qso} e^{-j6} \\ i_{dro} e^{-j6} Z_B & i_{qro} e^{-j6} Z_B \\ -\omega_{e0} X_s - \psi_{qso} Z_A & \gamma_s + Z X_s - \omega_{e0} X_m & Z X_m + j K_T \\ j K_T i_{qro} e^{-j6} & \psi_{qso} i_{qso} e^{-j6} \\ Z X_m + \psi_{dro} K_{s\ell} & \omega_{s\ell 0} X_m & \gamma_r + Z X_r & \omega_{s\ell 0} X_r \\ -\omega_{s\ell 0} X_m - \psi_{qro} K_{s\ell} & Z X_m & -\omega_{s\ell 0} X_r & \gamma_r + Z X_r \end{bmatrix} \begin{bmatrix} \overline{i_{qs6}} e \\ j \frac{12}{35} i_{qso} e^{-j6} \\ \overline{i_{qr6}} e \\ \overline{i_{dr6}} e \end{bmatrix}$$

$$+ \begin{bmatrix} Z_B + Z X_F + R_F + X_{CO} + K_{s\ell} \psi_{dso} \\ - K_{s\ell} \psi_{qso} \\ K_{s\ell} \psi_{dro} \\ - K_{s\ell} \psi_{qro} \end{bmatrix} \begin{bmatrix} \frac{2}{35} i_{qso} e^{-j6} \end{bmatrix} \dots (5.71)$$

Rewriting equations (5.71)

$$\begin{aligned} & \left[ r_s + R_F + X_{CO} + z(X_S + X_F) + \psi_{dso} z_A + z_B - j K_{sp} K_T i_{dro}^e z_B \right] \overline{i_{qs6}^e} \\ & + z X_m \overline{i_{qr6}^e} + (\omega_{eo} X_m - j K_T \psi_{dso} i_{qso}^e - j K_{sp} K_T i_{qso}^e z_B) \\ & \overline{i_{dr6}^e} = 2/35 (v_{qso}^e - j6 v_{dso}^e) - (z_B + z X_F + R_F + X_{CO} + \\ & K_{sf} \psi_{dso}) \frac{2}{35} i_{qso}^e - (\omega_{eo} X_s + j K_T i_{qro}^e \psi_{dso} + j K_{sp} K_T \\ & i_{qro}^e z_B) j \frac{12}{35} i_{qso}^e \quad \dots(5.72) \end{aligned}$$

$$\begin{aligned} & (z X_m + \psi_{dro} K_{sf}) \overline{i_{qs6}^e} + (r_r + z X_r) \overline{i_{qr6}^e} + \omega_{sfo} X_r \overline{i_{dr6}^e} \\ & = - \frac{2}{35} K_{sf} \psi_{dro} i_{qso}^e - j \frac{12}{35} i_{qso}^e \omega_{sfo} X_m \quad \dots(5.73) \end{aligned}$$

$$\begin{aligned} & -(\omega_{sfo} X_m - \psi_{qro} K_{sf}) \overline{i_{qs6}^e} - \omega_{sfo} X_r \overline{i_{qr6}^e} + (r_r + z X_r) \overline{i_{dr6}^e} \\ & = \frac{2}{35} K_{sf} \psi_{qro} i_{qso}^e - j z X_m \frac{12}{35} i_{qso}^e \quad \dots(5.74) \end{aligned}$$

$$\begin{aligned} \overline{v_{ds6}^e} & = (-\omega_{eo} X_s - \psi_{qso} z_A) \overline{i_{qs6}^e} + (r_s + z X_s - j K_T i_{qro}^e \psi_{qso}) \\ & j \frac{12}{35} i_{qso}^e - \omega_{eo} X_m \overline{i_{qr6}^e} + (z X_m + j K_T \psi_{qso} i_{qso}^e) \\ & \overline{i_{dr6}^e} - \frac{2}{35} K_{sf} \psi_{qso} i_{qso}^e \quad \dots (5.75) \end{aligned}$$

Equations (5.72) to (5.74) can be solved for  $\overline{i_{qs6}^e}$ ,  $\overline{i_{qr6}^e}$  and  $\overline{i_{dr6}^e}$ . Once  $\overline{i_{qs6}^e}$ ,  $\overline{i_{qr6}^e}$ , and  $\overline{i_{dr6}^e}$  are known then from equation (5.75)  $\overline{v_{ds6}^e}$  can also be computed.

Substituting values of  $\overline{i_{qs6}^e}$ ,  $\overline{i_{qr6}^e}$ ,  $\overline{i_{dr6}^e}$  and  $\overline{v_{ds6}^e}$  in equations (5.44), (5.60) and (5.61) the 6th harmonic torque, speed and voltage pulsations can be calculated respectively.

A computer programme is written to compute all the sixth harmonic variables i.e. 6th harmonic rotor speed, 6th harmonic torque, 6th harmonic stator voltage, 6th harmonic rotor current and 6th harmonic stator current, under steady-state operation of the drive with full load torque output for four different values of p.u. operating frequencies and three sets of controller parameters.

### 5.3 RESULT AND DISCUSSION

In this section theoretical results, obtained through the computer, concerning the harmonic analysis of inverter-fed induction motor drive are discussed. The computer programme is given in Appendix (IV).

The variation in 6th harmonic rotor speed, 6th harmonic torque and 6th harmonic stator voltage as function of the average load torque for different p.u. operating speeds ranging from .2 to 1.0 has been studied and the relevant graphs are plotted.

#### 5.3.1 The Sixth-Harmonic Rotor-Speed Vs Average Load Torque

The rotor speed harmonics, in stable zone of the torque slip characteristic are more in comparison to rotor-speed harmonics in unstable zone of the torque slip characteristic of the induction motor. As p.u. operating frequency is decreased rotor-speed harmonics increases in the entire slip range as shown in Fig. 5.1.

Thus, for small speeds, rotor speed harmonics are more in comparison to rotor-speed harmonics at high speeds. There is not much difference between rotor-speed harmonics at any p.u. frequency of operation in unstable zone of torque slip characteristic but there is considerable difference in the magnitude of rotor-speed harmonic in stable zone of torque slip characteristic for all p.u. frequency of operation.

### 5.3.2. The Sixth-Harmonic Load Torque vs Average Load Torque

Torque harmonics in stable zone are more in comparison to torque harmonics in unstable zone of the torque slip characteristic of the induction motor for any p.u. frequency of operation. Also, the sixth harmonic torque almost remain unaffected with variation in the p.u. operating frequency as shown in Fig. 5.2.

### 5.3.3. The Sixth-Harmonic Voltage vs Average Load Torque

In stable zone of the torque slip characteristic of the induction motor, voltage harmonics are more compared to in the unstable zone for a particular p.u. operating frequency. As the p.u. operating frequency is decreased voltage harmonics in the entire slip range decreases as shown in Fig. 5.3.

Thus, for high speeds, voltage harmonics are more while for low speeds voltage harmonics are less. In stable zone voltage harmonics are mere in comparison to voltage harmonics in unstable zone of torque slip characteristic of Induction motor.

The sixth-harmonic rotor and stator currents are constant for the entire slip range and also there is almost no change caused by variation in the p.u. operating frequency.

#### 5.3.4 The Effect of Change of Controller Parameters ( $K_{sp}, K_c, T$ )

A variation in the controller parameters has negligible effect on all the sixth harmonic quantities.

#### 5.4 CONCLUSION

In this chapter analytical method for determining the sixth-harmonic torque, speed stator voltage and currents pulsations of an Induction motor drive when supplied from a rectifier controlled current inverter source has been set forth.

The sixth-harmonic torque pulsations remain same for all p.u. operating frequencies. Torque harmonics are small in unstable zone of the torque slip characteristic of the Induction motor. There is negligible change in rotor speed sixth harmonic component as p.u. for operating frequency is varied in unstable zone of the torque slip characteristic of the Induction motor. Sixth harmonic rotor speed oscillations are small in unstable zone for all p.u. frequency of operation. The sixth harmonic voltage pulsations are large under high speed operation and small at low speed operation of the drive.

Change in controller parameters does not deteriorate the drive performance as far as the torque and speed harmonic pulsations are concerned.



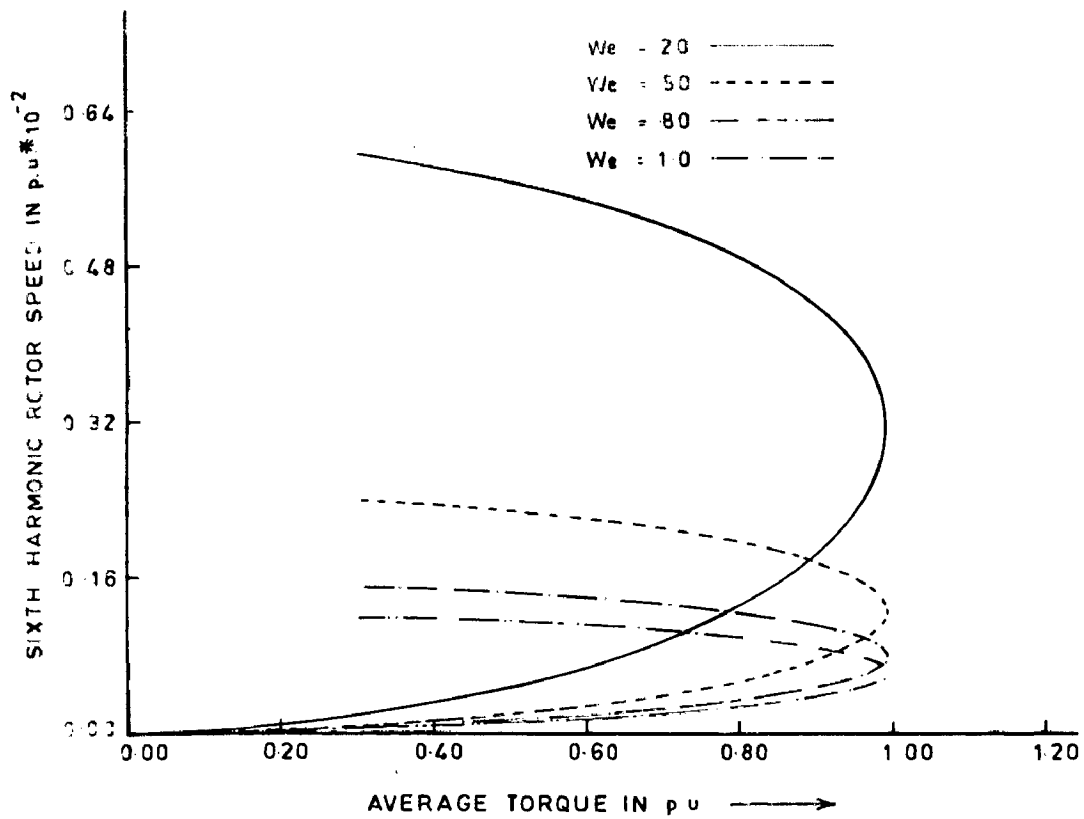


Fig.5.1 VARIATION OF SIXTH HARMONIC ROTAR SPEED AT DIFFERENT OPERATIONAL FREQUENCIES

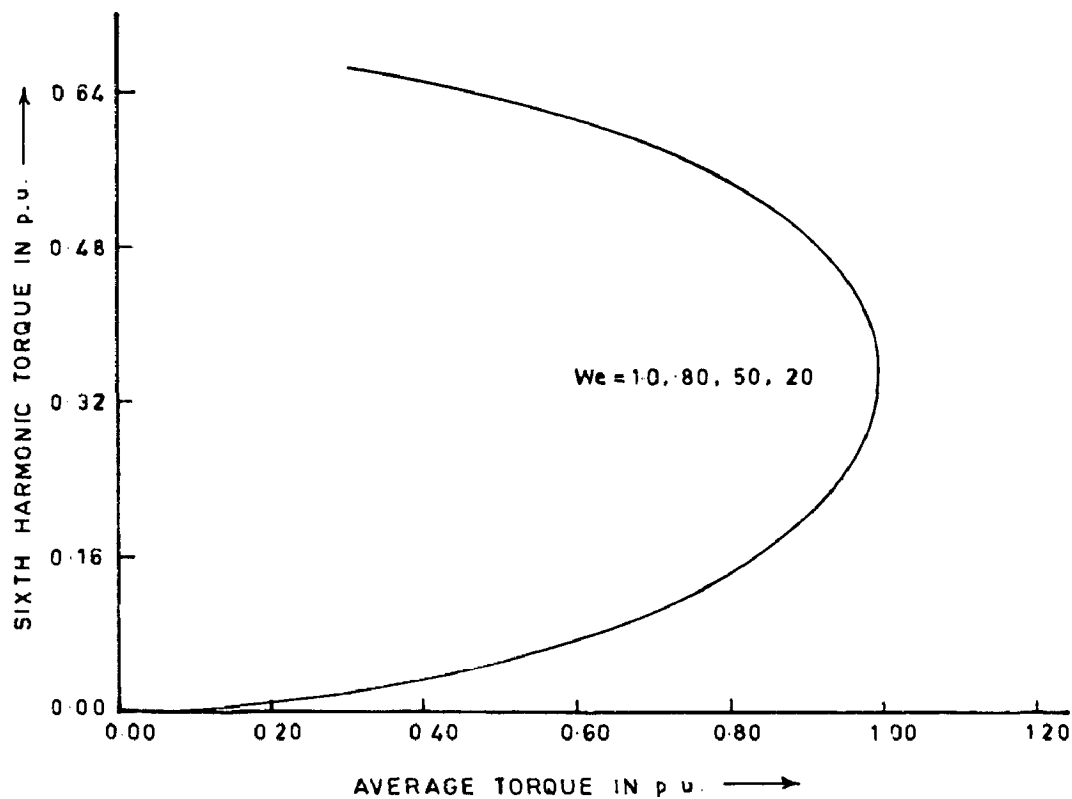


Fig 5.2 VARIATION OF SIXTH HARMONIC TORQUE WITH LOAD TORQUE AT DIFFERENT OPERATIONAL FREQUENCIES

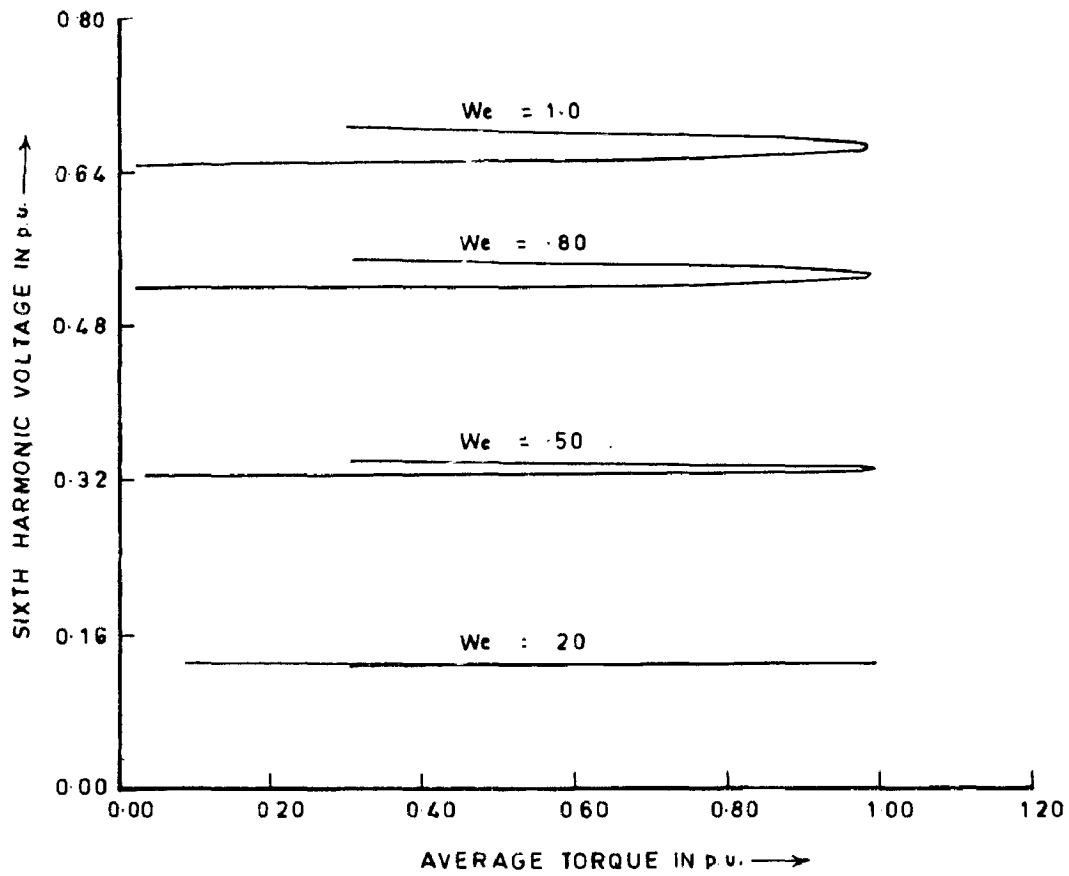


Fig. 5.3 VARIATION OF 1 M SIXTH HARMONIC STATOR VOLTAGE WITH LOAD TORQUE AT DIFFERENT OPERATIONAL FREQUENCIES

## CHAPTER - 6

## THE TRANSIENT ANALYSIS OF THE DRIVE

In this chapter transient response of rectifier controlled current inverter fed induction motor is studied for the three sets of controller parameters (obtained from chapter - 4). All the equation, describing the drive transients behaviour, are converted into five 1st order differential equations. These first order differential equations are solved by fourth order Runga Kutta method. The various aspects of the drive studied are (i) starting from rest (ii) sudden change in reference speed setting and (iii) reversal in direction of rotation of the induction motor.

## 6.1 STATE SPACE EQUATIONS

Following additional assumption, in addition to those in the mathematical modelling, is made to derive the state space equations of the drive.

The effect of harmonics is neglected. Thus only fundamental component of a.c. is considered. So from equations (2.24)

$$\text{and (2.25)} \quad g_{ds}^e = 0, \quad g_{qs}^e = 1 \quad \dots(6.1)$$

Rewriting equation (2.26)

$$\begin{bmatrix} v_{qs}^e \\ v_{ds}^e \\ 0 \\ 0 \end{bmatrix} = \begin{bmatrix} \gamma_s + p X_s & \omega_e X_s & p X_m & \omega_e X_m \\ -\omega_e X_s & \gamma_s + p X_s & \omega_e X_m & p X_m \\ p X_m & \omega_{sl} X_m & \gamma_r + p X_r & \omega_{sl} X_r \\ -\omega_{sl} X_m & p X_m & -\omega_{sl} X_r & \gamma_r + p X_r \end{bmatrix} \begin{bmatrix} i_{qs}^e \\ i_{ds}^e \\ i_{qr}^e \\ i_{dr}^e \end{bmatrix} \quad \dots(6.2)$$

Substituting value of  $g_{ds}^e$  and  $g_{qs}^e$  from equation (6.1) in equation (2.33) to (2.25) yields

$$V_I = v_{qs}^e \quad \dots(6.3)$$

$$i_{qs}^e = I_R \quad \dots(6.4)$$

$$i_{ds}^e = 0 \quad \dots(6.5)$$

The ds equation in equation (6.1) below has been omitted since  $i_{ds}^e$  is identically zero

$$\begin{bmatrix} v_{qs}^e \\ 0 \\ 0 \end{bmatrix} = \begin{bmatrix} r_s & 0 & \omega_e X_m \\ 0 & r_r & \omega_{sl} X_r \\ -\omega_{sl} X_m & -\omega_{sl} X_r & r_r \end{bmatrix} \begin{bmatrix} i_{qs}^e \\ i_{qr}^e \\ i_{dr}^e \end{bmatrix} + p \begin{bmatrix} X_s & X_m & 0 \\ X_m & X_r & 0 \\ 0 & 0 & X_r \end{bmatrix} \begin{bmatrix} i_{qs}^e \\ i_{qr}^e \\ i_{dr}^e \end{bmatrix} \quad \dots(6.6)$$

Rewriting equation (2.21)

$$V_R = V_I + (R_F + X_{CO} + p X_F) I_R \quad \dots(6.7)$$

substitution of value of  $V_I$  and  $I_R$  from equation (6.3) and (6.4) in equation (6.7) results in

$$V_R = v_{qs}^e + (R_F + X_{CO} + p X_F) i_{qs}^e \quad \dots(6.8)$$

Substituting the expression for  $v_{qs}^e$  from equation (6.8) in equation (6.6) and rearranging the terms

$$\begin{bmatrix} V_R \\ 0 \\ 0 \end{bmatrix} = \begin{bmatrix} r_s + R_F + X_{CO} & 0 & \omega_e X_m \\ 0 & r_r & \omega_{sl} X_r \\ -\omega_{sl} X_m & -\omega_{sl} X_r & r_r \end{bmatrix} \begin{bmatrix} i_{qs}^e \\ i_{qr}^e \\ i_{dr}^e \end{bmatrix} + p \begin{bmatrix} X_s + X_F & X_m & 0 \\ X_m & X_r & 0 \\ 0 & 0 & X_r \end{bmatrix} \begin{bmatrix} i_{qs}^e \\ i_{qr}^e \\ i_{dr}^e \end{bmatrix} \quad \dots(6.9)$$

Defining

$$\gamma_s + R_F + X_{CO} = R \quad \dots (6.10)$$

$$X_s + X_F = X \quad \dots (6.11)$$

Substituting the new constants from equations (6.10) and (6.11) in equations (5.9) yields

$$\begin{bmatrix} V_R \\ 0 \\ 0 \end{bmatrix} = \begin{bmatrix} R & 0 & \omega_e X_m \\ 0 & \gamma_r & \omega_s X_r \\ -\omega_s X_m & -\omega_s X_r & \gamma_r \end{bmatrix} \begin{bmatrix} i_{qs}^e \\ i_{qr}^e \\ i_{dr}^e \end{bmatrix} + p \begin{bmatrix} X & X_m & 0 \\ X_m & X_r & 0 \\ 0 & 0 & X_r \end{bmatrix} \begin{bmatrix} i_{qs}^e \\ i_{qr}^e \\ i_{dr}^e \end{bmatrix} \quad \dots (6.12)$$

Writing above equation in 1st order differential form with operator  $p$  defined as  $(\cdot)$  one gets

$$\begin{bmatrix} i_{qs}^{\cdot e} \\ i_{qr}^{\cdot e} \\ i_{dr}^{\cdot e} \end{bmatrix} = \begin{bmatrix} X & X_m & 0 \\ X_m & X_r & 0 \\ 0 & 0 & X_r \end{bmatrix}^{-1} \begin{bmatrix} R & 0 & \omega_e X_m \\ 0 & \gamma_r & \omega_s X_r \\ -\omega_s X_m & -\omega_s X_r & \gamma_r \end{bmatrix} \begin{bmatrix} i_{qs}^e \\ i_{qr}^e \\ i_{dr}^e \end{bmatrix} + \begin{bmatrix} X & X_m & 0 \\ X_m & X_r & 0 \\ 0 & 0 & X_r \end{bmatrix}^{-1} \begin{bmatrix} V_R \\ 0 \\ 0 \end{bmatrix} \quad \dots (6.13)$$

or

$$\begin{bmatrix} i_{qs}^{\cdot e} \\ i_{qr}^{\cdot e} \\ i_{dr}^{\cdot e} \end{bmatrix} = -\frac{1}{X X_r - X_m^2} \begin{bmatrix} R X_r & -X_m \gamma_r & \omega_e X_m X_r - \omega_s X_r X_m \\ -X_m R & X \gamma_r & -\omega_e X_m^2 + \omega_s X_r X \\ -\frac{\omega_s X_m}{X_r} (X X_r - X_m^2) & -\frac{\omega_s X_r}{X_r} (X X_r - X_m^2) & \frac{\gamma_r}{X_r} (X X_r - X_m^2) \end{bmatrix} \begin{bmatrix} i_{qs}^e \\ i_{qr}^e \\ i_{dr}^e \end{bmatrix}$$

$$+ \frac{1}{X X_r - X_m^2} \begin{bmatrix} X_r & -X_m & 0 \\ -X_m & X & 0 \\ 0 & 0 & \frac{X X_r - X_m^2}{X_r} \end{bmatrix} \begin{bmatrix} V_R \\ 0 \\ 0 \end{bmatrix} \quad \dots(6.14)$$

Rewriting equation (6.14)

$$i_{qs}^{.e} = \frac{1}{(X X_r - X_m^2)} \left[ -R X_r i_{qs}^e + X_m r_r i_{qr}^e - (\omega_e X_m X_r - \omega_{sl} X_r X_m) i_{dr}^e + X_r V_R \right] \quad \dots (6.15)$$

$$i_{qr}^{.e} = \frac{1}{(X X_r - X_m^2)} \left[ X_m R i_{qs}^e - X r_r i_{qr}^e + (\omega_e X_m^2 - \omega_{sl} X_r X) i_{dr}^e - X_m V_R \right] \quad \dots(6.16)$$

$$i_{dr}^{.e} = \frac{1}{X_r} (\omega_{sl} X_m i_{qs}^e + \omega_{sl} X_r i_{qr}^e - r_r i_{dr}^e) \quad \dots (6.17)$$

Rewriting equation (2.27)

$$T_e = X_m i_{qs}^e i_{dr}^e \quad \dots (6.18)$$

Rewriting equation (2.32)

$$T_e = T_L + 4\pi f_b H p \omega_r \quad \dots (6.19)$$

From equations (6.18) and (6.19)

$$p \omega_r = \frac{1}{4\pi f_b H} (X_m i_{qs}^e i_{dr}^e - T_L)$$

or

$$\dot{\omega}_r = \frac{1}{4\pi f_b H} (X_m i_{qs}^e i_{dr}^e - T_L) \quad \dots (6.20)$$

Rewriting equations (2.33) to (2.36)

$$I_R^* = K_{sp} (\omega_r^* - \omega_r) \quad \dots (6.21)$$

$$V_R = K_C \frac{(1 + T \omega_b p)}{\omega_b p} (I_R^* - I_R) \quad \dots (6.22)$$

$$\omega_{sl} = K_{sl} I_R \quad \dots (6.23)$$

$$\omega_e = \omega_r + \omega_{sl} \quad \dots (6.24)$$

Rewriting equation (6.22)

$$p V_R = \frac{K_C}{\omega_b} (1 + T \omega_b p) (I_R^* - I_R)$$

or

$$\dot{V}_R = \frac{K_C}{\omega_b} (I_R^* - I_R) + K_C T (\dot{I}_R^* - \dot{I}_R) \quad \dots (6.25)$$

Equations (6.15), (6.16), (6.17), (6.20) and (6.25) are the five first-order differential equations describing the transient behaviour of the drive. These equations are solved with the help of fourth-order Runge Kutta numerical integration method under different modes of operation of the drive.

## 6.2 RESULT AND DISCUSSION

In this chapter the transient response of rectifier controlled-current inverter fed induction motor drive is studied for various conditions as given below. The computer programme is given in Appendix V. Load characteristic is assumed fan type with static frictional torque and given by following expression

$$T_L = T_{LO} + G (\omega_r)^2$$

Table 6.1 - TABLE - 6.1

(a) Starting from rest to reference speed

(i) Reference Speed Setting 0.2

$K_{sp}$	$K_e$	T	Rotor Speed		D.C.link current final value (p.u.)	Torque final value (p.u.)
			Final value (p.u.)	Settling time(sec.)		
(1)	(2)	(3)	(4)	(5)	(6)	(7)
10	0.3	0.05	0.16506	1.226	0.34941	0.11795
20	0.2	0.05	0.18227	1.229	0.35461	0.12189
50	0.1	0.1	0.19284	1.927	0.35802	0.12451

(ii) Reference Speed Setting 0.5

10	0.3	0.05	0.45134	0.9108	0.48658	0.23425
20	0.2	0.05	0.47489	1.156	0.50215	0.24863
50	0.1	0.1	0.48975	1.997	0.51228	0.25807

(iii) Reference Speed 1.0

10	0.3	0.05	0.90931	1.962	0.90686	0.64492
20	0.2	0.05	0.95199	2.627	0.96009	0.69727
50	0.1	0.1	0.98007	5.780	0.99656	0.73302



Table 6.1(contd.)

(b) Sudden Change in Reference Speed Setting

(i) Change in Speed Reference from 0.2 to 0.5 p.u.

(1)	(2)	(3)	(4)	(5)	(6)	(7)
10	0.3	0.05	0.45134	0.7006	0.48658	0.23425
20	0.2	0.05	0.47489	0.8057	0.50215	0.24863
50	0.1	0.1	0.48975	1.366	0.51228	0.25807

(ii) Change in Speed Reference from 1.0 to 0.2 p.u.

10	0.3	0.05	0.16506	2.662	0.34941	0.11795
20	0.2	0.05	0.18227	3.258	0.35461	0.12189
50	0.1	0.1	0.19284	3.382	0.35802	0.12451

(c) Reversal of Direction of Rotation of the Motor

(1) Changes in Speed Reference from 0.8 to -0.8

10	0.3	0.05	-0.72899	4.449	0.71013	-0.45022
50	0.1	0.1	-0.78468	3.678	0.76620	-0.50578

where

$T_{LO}$  = static friction torque p.u.

$\omega_r$  = induction motor rotor speed in p.u.

G = constant

The value of G in present case is 0.66.

For three sets of controller parameters the transient response of the drive is calculated. The various modes of operation of drive are -

- (i) for starting from rest to reference speed settings of .2, .5 and 1.0 p.u. speed
- (ii) sudden change from one steady-state speed to another steady-state speed in both up and down directions.
- (iii) reversal of direction of rotation of the motor.

The transient performance of the drive is illustrated in Figs. 6.1 to 6.30 and Table 6.1 shows the performance at a glance.

#### 6.2.1 Starting from Rest

Figs. 6.1, 6.2 and 6.3 show the transient behaviour in rotor speed for three chosen sets of controller parameters under .2, .5, 1.0 p.u. reference speed setting respectively. Among the three sets of controller parameters set with high  $K_{sp}$  (i.e. 50) is noted to possess more oscillatory speed response at lower reference speed setting. For any low speed setting case the drive with controller parameters set having high  $K_{sp}$  (i.e. 50) is noted to have larger pickup time, higher overshoot and larger

settling time in the speed response. At higher speed setting the speed response characteristic is monotonic in nature, the pick up time and the settling time being always larger for the set of controller parameters with larger  $K_{sp}$  (i.e. 50).

For any reference speed setting the drive is noted to have larger steady-state error in speed for set of controller parameters with smallest  $K_{sp}$  (i.e. 10).

Figs. 6.4, 6.5 and 6.6 show the transient behaviour in d.c. link current for three chosen sets of controller parameters under .2, .5, 1.0 p.u. reference speed setting respectively. The response is noted to be oscillatory in nature, the oscillation persist for long duration with the set of controller parameters having larger  $K_{sp}$  (i.e. 50) especially at lower reference speed settings. The overshoot in current is larger for the set of controller parameters with smallest  $K_{sp}$  (i.e. 10) under all reference speed settings. The instant of overshoot is earlier for controller parameters having smallest  $K_{sp}$  (i.e. 10) and at no time overshoot exceeds a value of about 1.2 p.u.

Figs. 6.7, 6.8 and 6.9 show the torque transient for three chosen set of controller parameters under .2, .5 and 1.0 p.u. reference speed setting respectively. The torque transients behaviour in a manner similar to current transients. Even under the highest speed setting the transient torques are found to be appreciably less, a set of controller parameters with high  $K_{sp}$  (i.e. 50) appears to have better performance in this regard.

### 6.2.2 Sudden Change in Reference Speed Setting

Figs. 6.10, 6.11 and 6.12 show the drive performance under the three sets of controller parameters for sudden change in reference speed setting from .2 to .5 p.u. The speed transients indicate larger overshoot and settling time for controller parameters with high  $K_{sp}$  (i.e. 50). The settling time being almost double for controller parameters with high  $K_{sp}$  (i.e. 50) in comparison to that for controller parameters with smallest  $K_{sp}$  (i.e. 10). The current and torque transients are small for controller parameters with high  $K_{sp}$  (i.e. 50). However the difference in overshoots under extreme cases (controller parameters with high  $K_{sp}$  and controller parameters with low  $K_{sp}$ ) is not much.

Figs. 6.13, 6.14, 6.15, 6.16, 6.17, 6.18, 6.19, 6.20, 6.21 shows the drive performance under the three sets of controller parameters for sudden change in reference speed setting from 1.0 to .2 p.u. speed. Best drive performance is noted for the set of controller parameters with smallest,  $K_{sp}$  (i.e. 10) while the case for controller parameters with  $K_{sp}$  equal to 20 is worst. For the case of controller parameters with smallest  $K_{sp}$  (i.e. 10) is noted to settle earliest, with least value of overshoot in current and torque transients while the case of controller parameters with  $K_{sp}$  equal to 20 appears to worst in all respect.

### 6.2.3 Reversal in Direction of Rotation

Figs. 6.22, 6.23, 6.24, 6.25, 6.26, 6.27, 6.28, 6.29, 6.30 shows drive performance under the three sets of controller parameters for sudden change in reference speed setting from .8 to -.8 p.u. speed. The drive is found to exhibit sustained oscillations for the case with the controller parameters set having  $K_{sp}$  equal to 20. Among the other two cases the controller parameters set with  $K_{sp}$  equal to 50 appears to be settle slightly earlier as far as the speed transients are concerned. However the associated current and torque transients for this case are slightly on the higher side.

### 6.3 CONCLUSION

An analytical method for determining the transient performance of the induction motor drive fed from rectifier controlled-current inverter source has been set forth in this chapter.

For three sets of controller parameters, the transient performance of the drive is calculated under three different conditions i.e. starting sudden change in speed reference setting and reversal in direction of rotation of motor.

For the set of controller parameters with smallest  $K_{sp}$  (i.e. 10) settling time is smallest under all modes of operation except for the case of reversal in direction of motor when the settling time is slightly larger than that for the best set ( $K_{sp} = 50$ ).

Overshoots in torque and currents are more for set of controller parameter with smallest  $K_{sp}$  (i.e. 10) for all cases in which new reference speed setting is more than previous one (i.e. up speeds). Overshoot and undershoots in current, torque and speed are largest for set of controller parameters with  $K_{sp}$  equal to 50 for down-speed cases (i.e. reference speed setting is changed suddenly from high value to a low value).

The torque, speed and current transients are more oscillatory in nature for down-speed cases.

The steady-state error is more for the set of controller parameters with smallest  $K_{sp}$  (i.e. 10).

From the point of view of settling time in speed the set of parameters with

$$K_{sp} = 10 \quad K_c = .3, \quad T = 0.05$$

appears to be the best choice of the controller parameters for various modes of operation excluding sudden reversal in the direction of rotation of the motor. For this latter case the drive performance from the point of view of settling time in speed is only marginally poor in comparison to the best set of parameters (i.e. with  $K_{sp} = 50$ ).

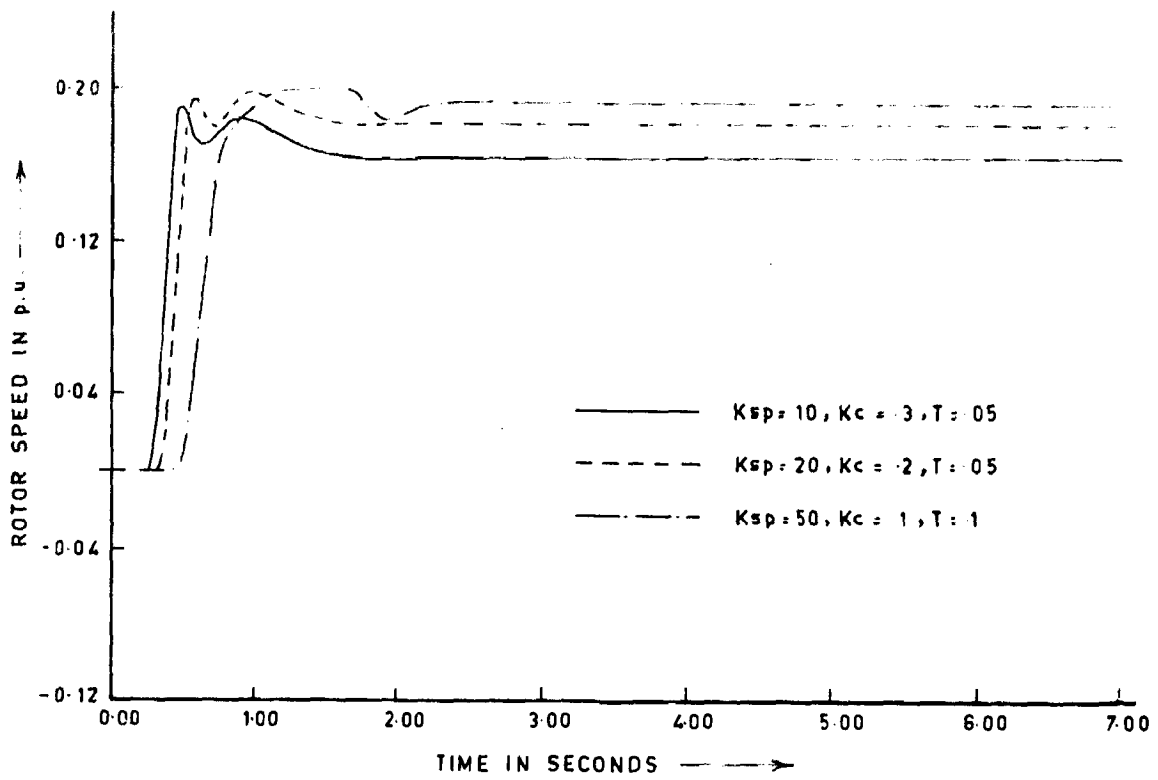


Fig.6.1 ROTOR SPEED TRANSIENTS FOR STARTING FROM REST WITH SPEED REFERENCE 0.2 p.u.

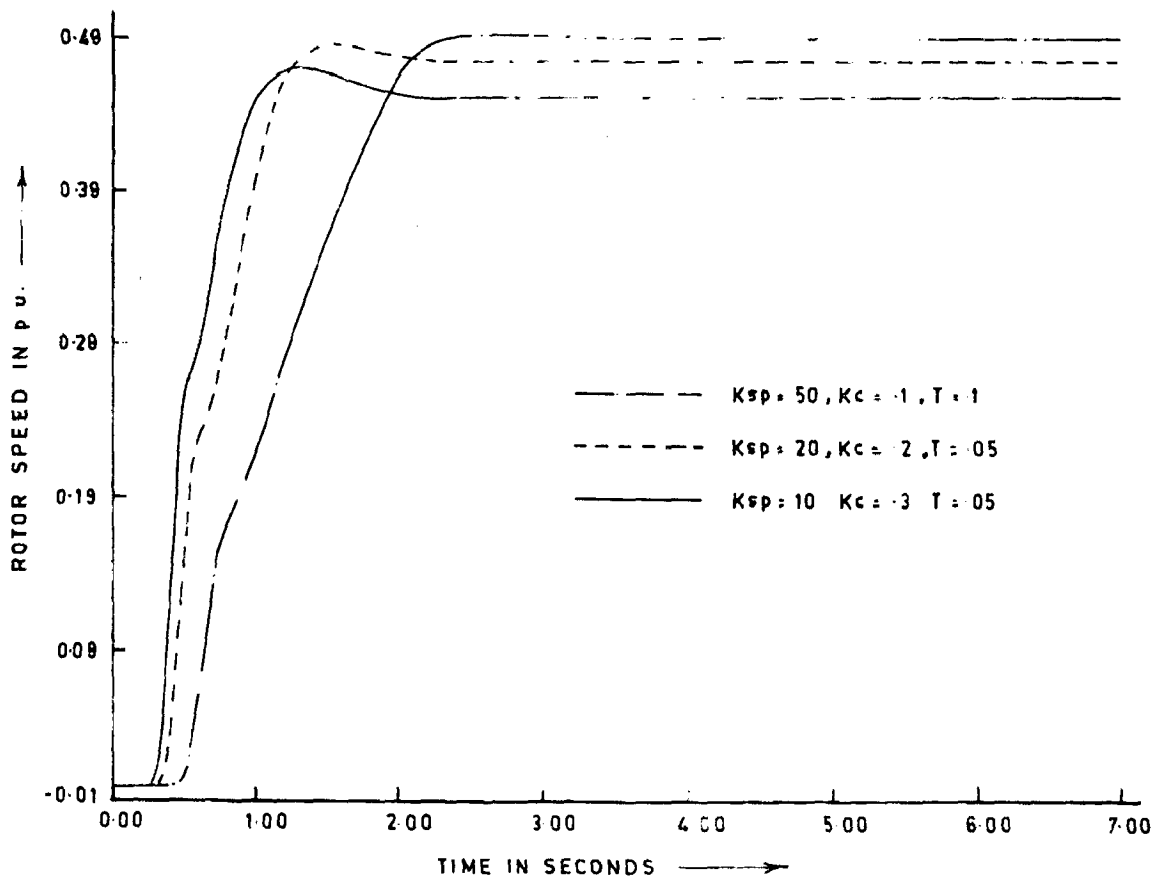


Fig.6.2 ROTOR SPEED TRANSIENTS FOR STARTING FROM REST WITH SPEED REFERENCE 0.5 p.u.

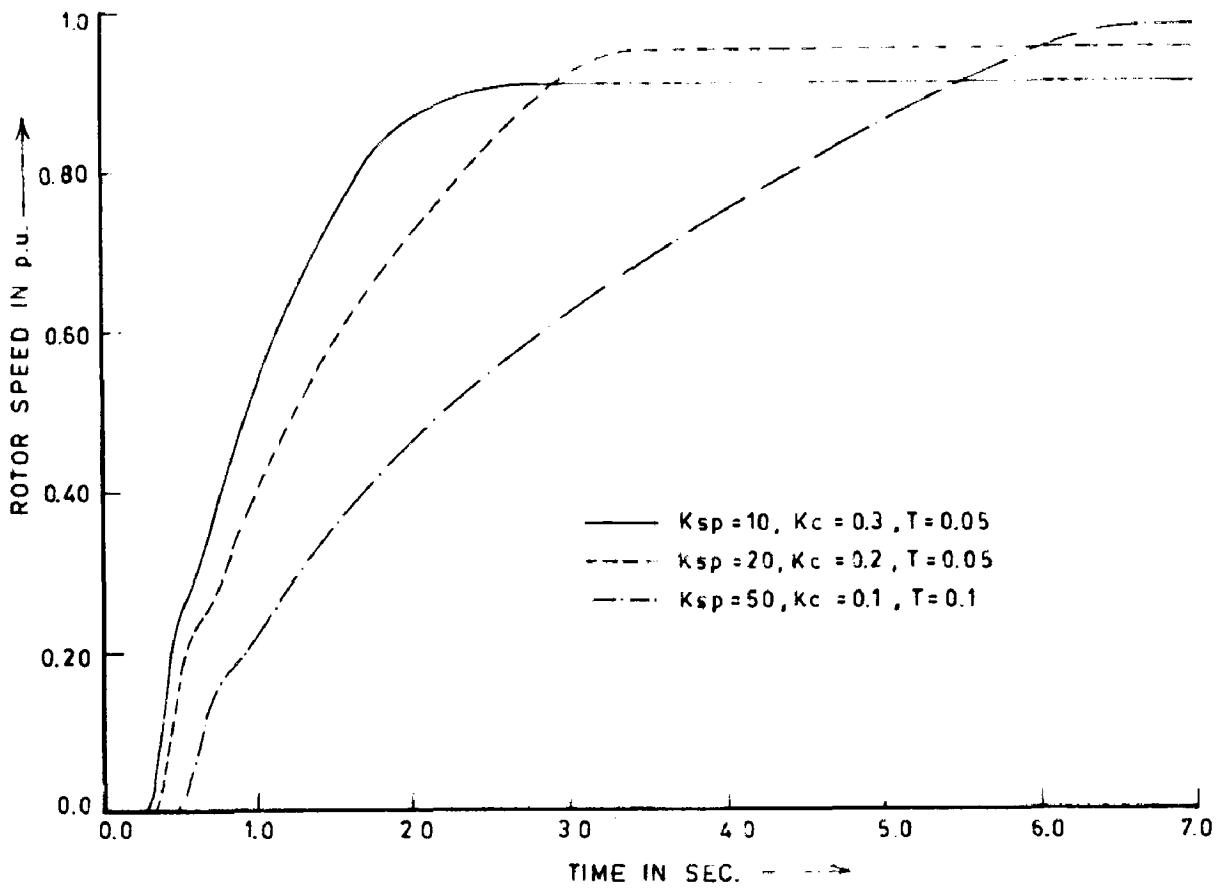


FIG 6.3. ROTOR SPEED TRANSIENT FOR STARTING FROM REST WITH SPEED REFERENCE 1.0 p.u.

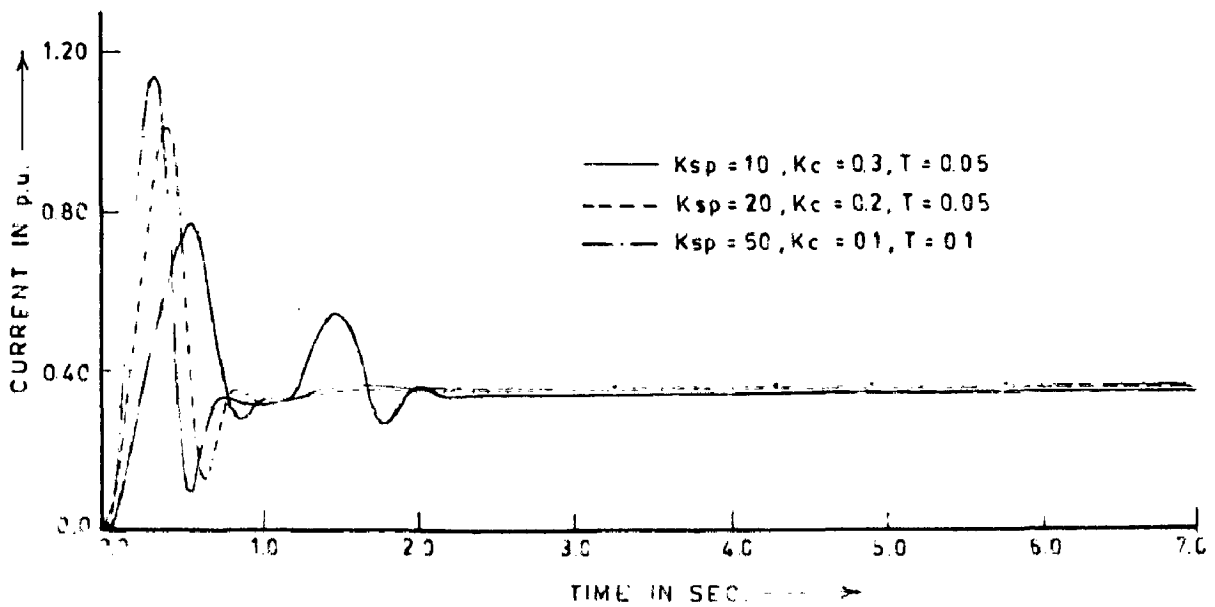


FIG.6.4 D.C. LINK CURRENT TRANSIENT FOR STARTING FROM REST WITH SPEED REFERENCE 0.2 p.u.



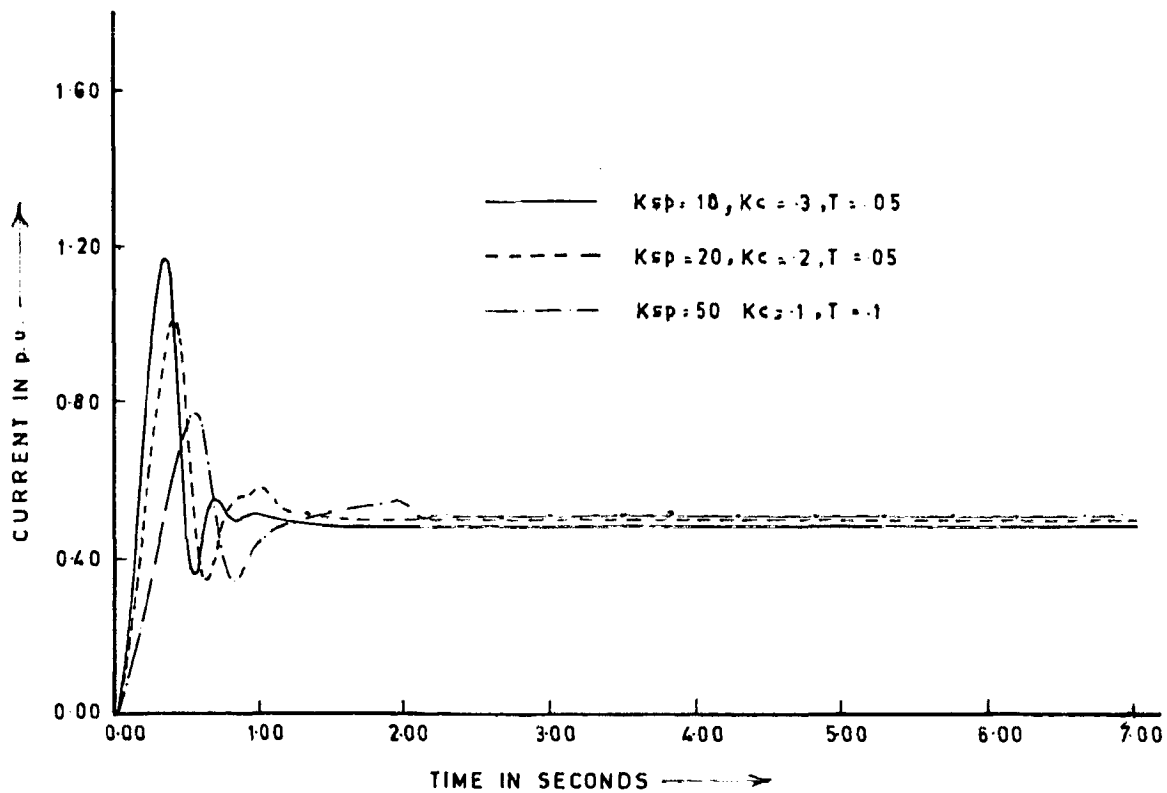


Fig.6.5 D.C. LINK CURRENT TRANSIENT FOR STARTING FROM REST WITH SPEED REFERENCE 5 p.u.

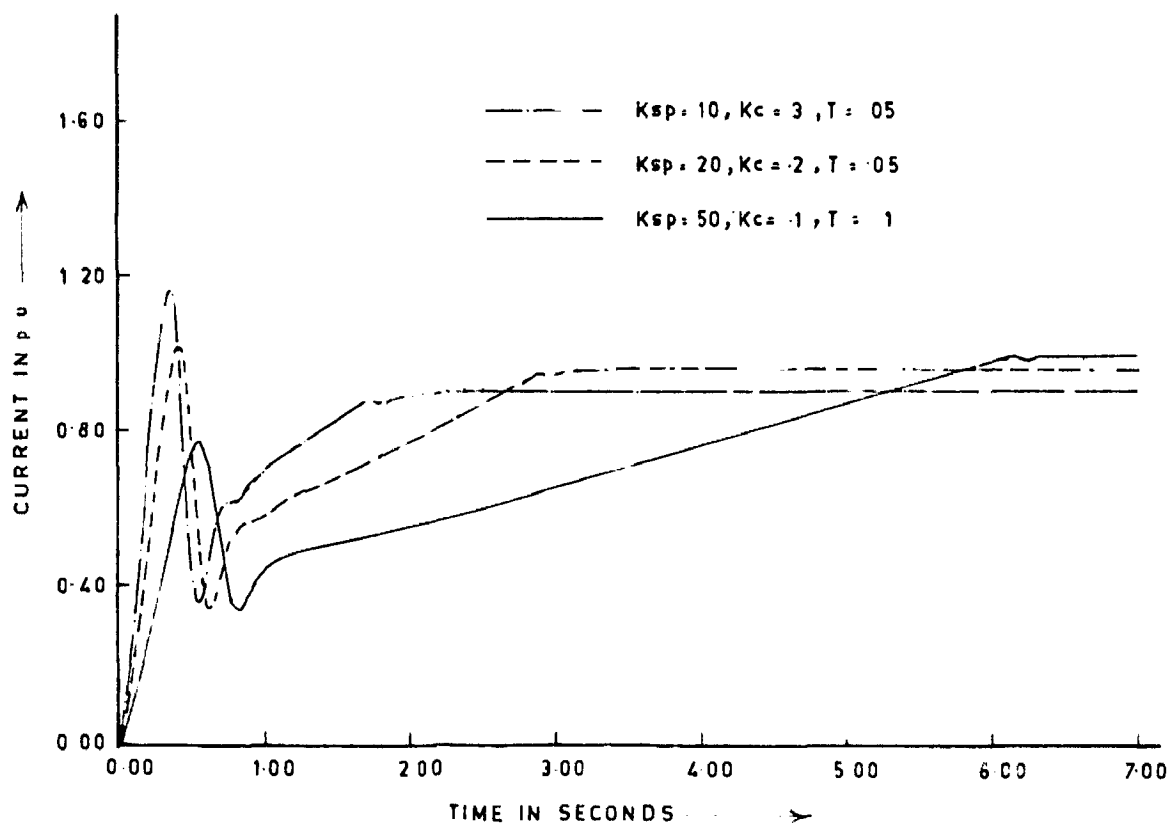


Fig.6.6 D.C. LINK CURRENT TRANSIENT FOR STARTING FROM REST WITH SPEED REFERENCE 10 p.u.

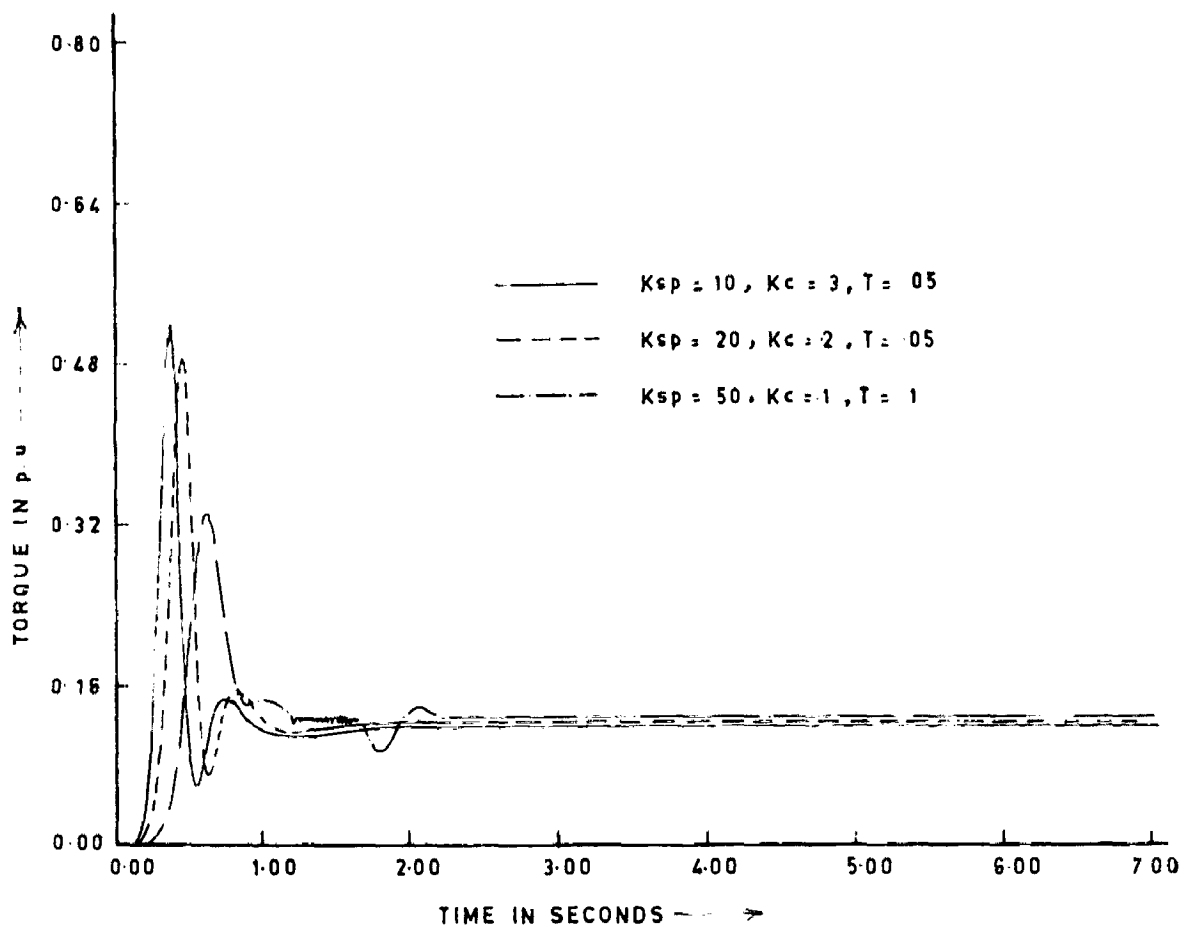


Fig 67 TORQUE TRANSIENTS FOR STARTING FROM REST WITH SPEED REFERENCE 2 p u

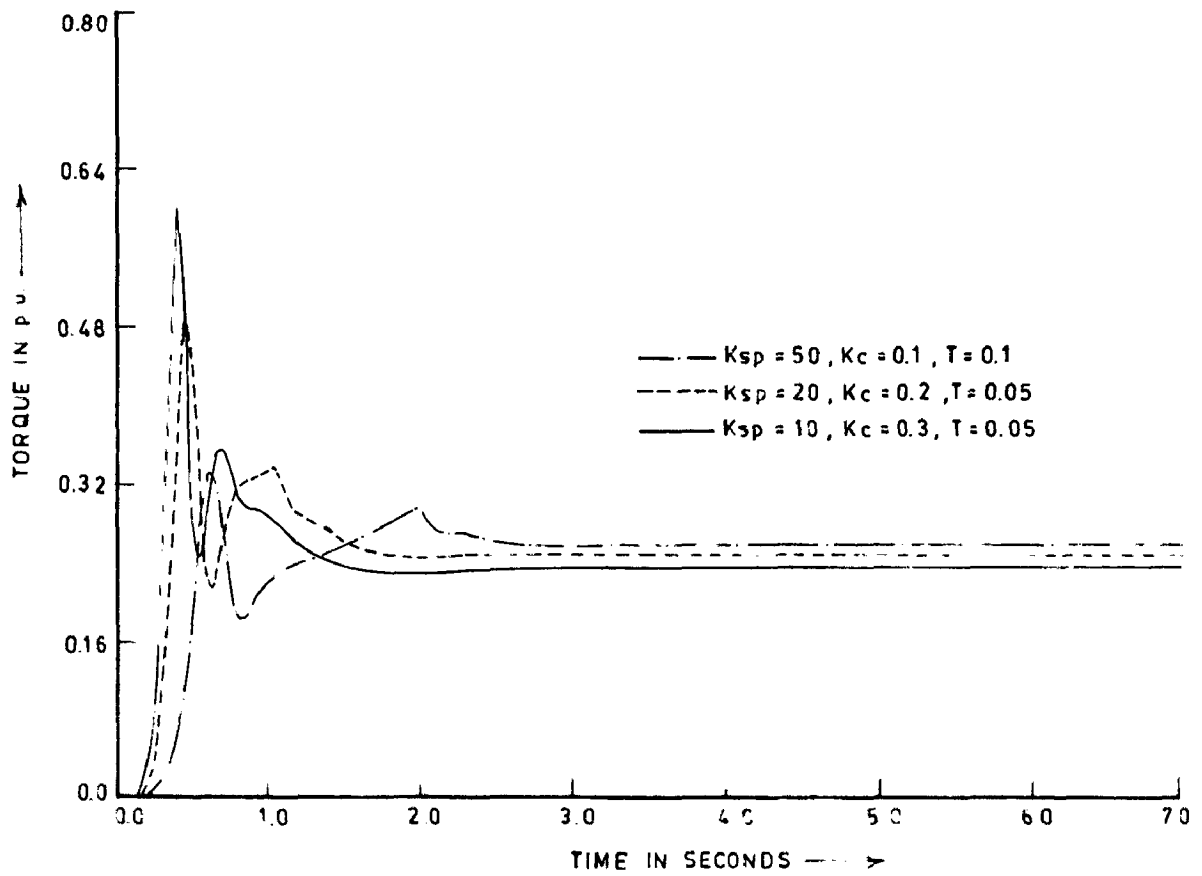


FIG 6.8. TORQUE TRANSIENT FOR STARTING FROM REST WITH SPEED REFERENCE 0.5 pu

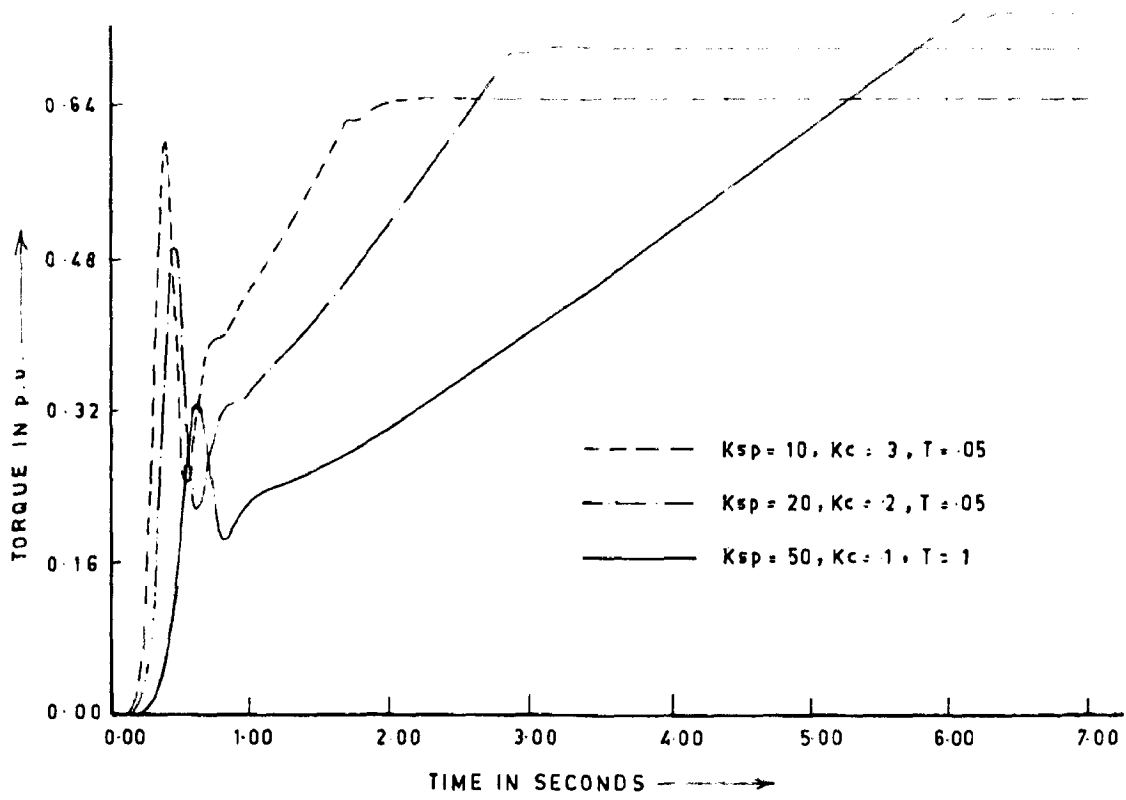


Fig. 6.9 TORQUE TRANSIENTS FOR STARTING FROM REST WITH SPEED REFERENCE 10 p.u.

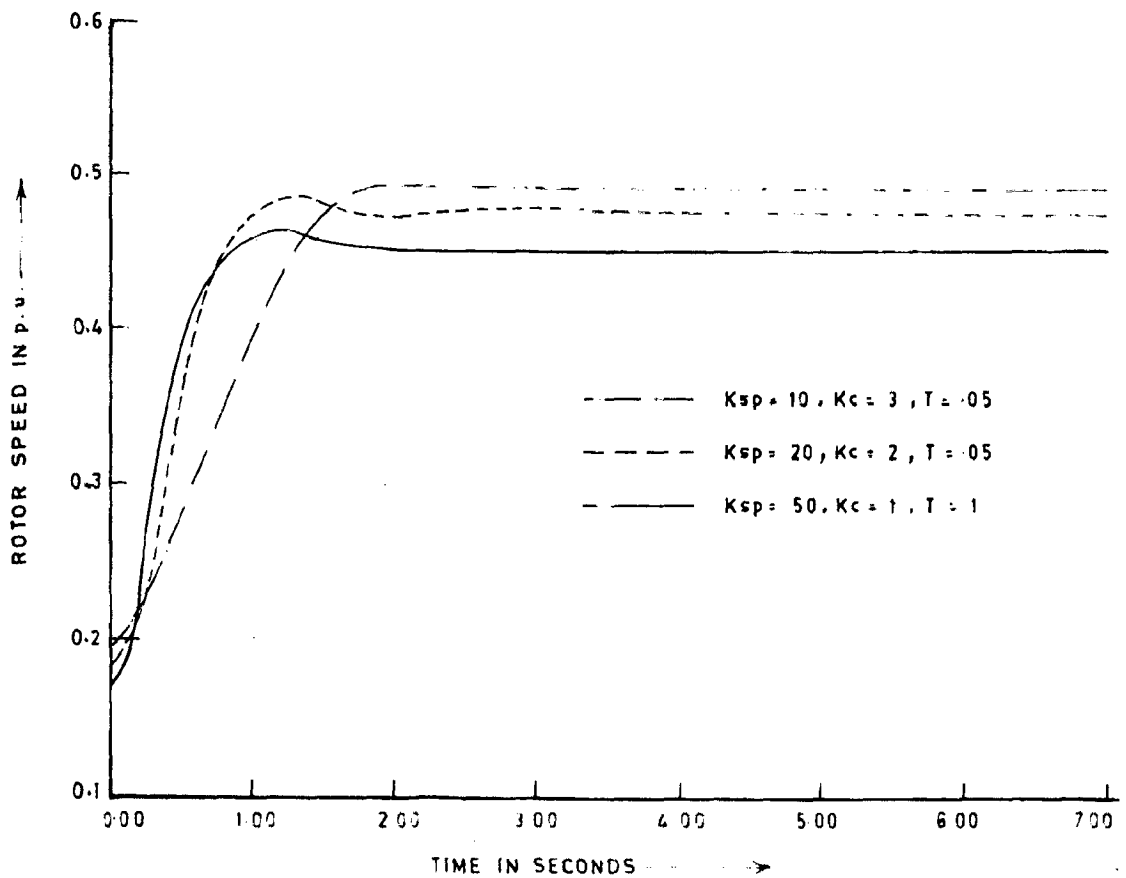


Fig. 6.10 ROTOR SPEED TRANSIENT FOR STEP CHANGE IN SPEED REFERENCE FROM 2 p.u. TO 5 p.u.

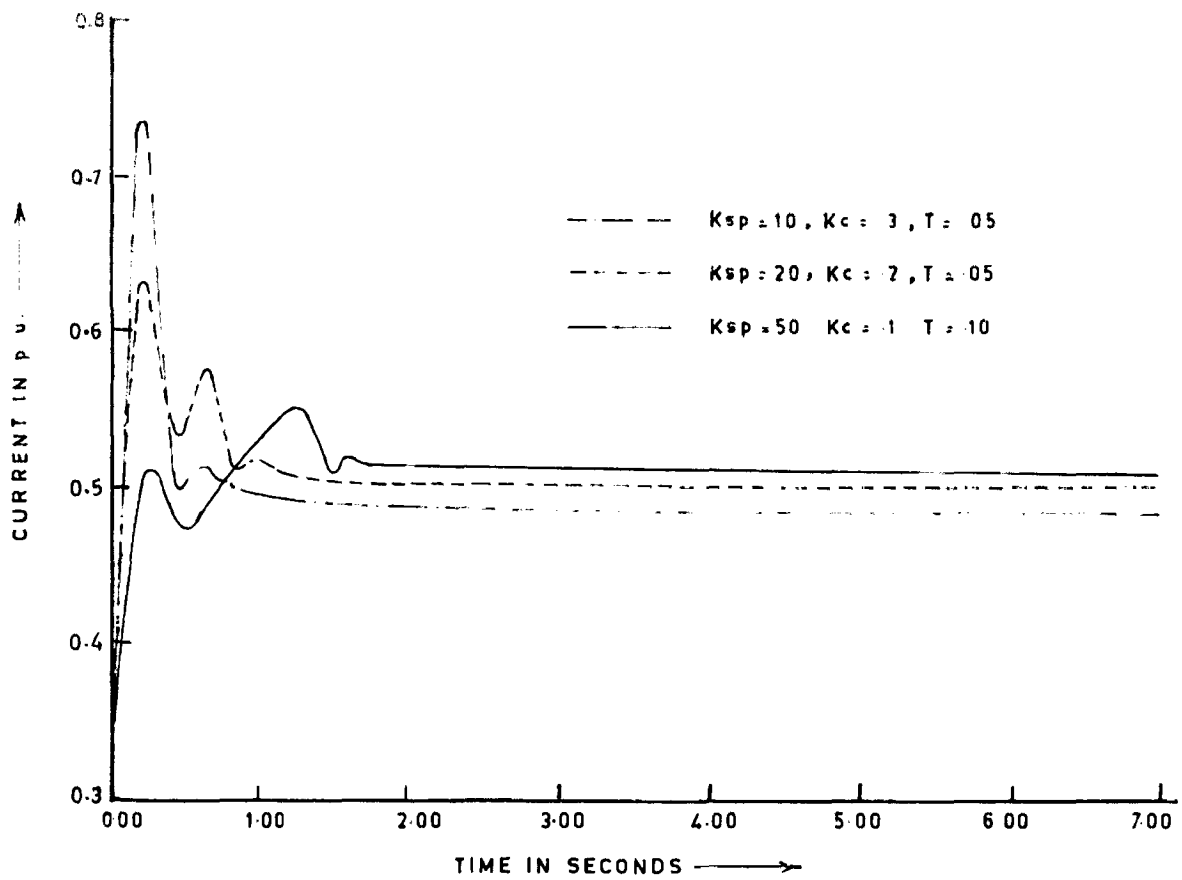


Fig. 6-11 D.C. LINK CURRENT TRANSIENT FOR STEP CHANGE IN SPEED REFERENCE FROM 2 p.u. TO 5 p.u.

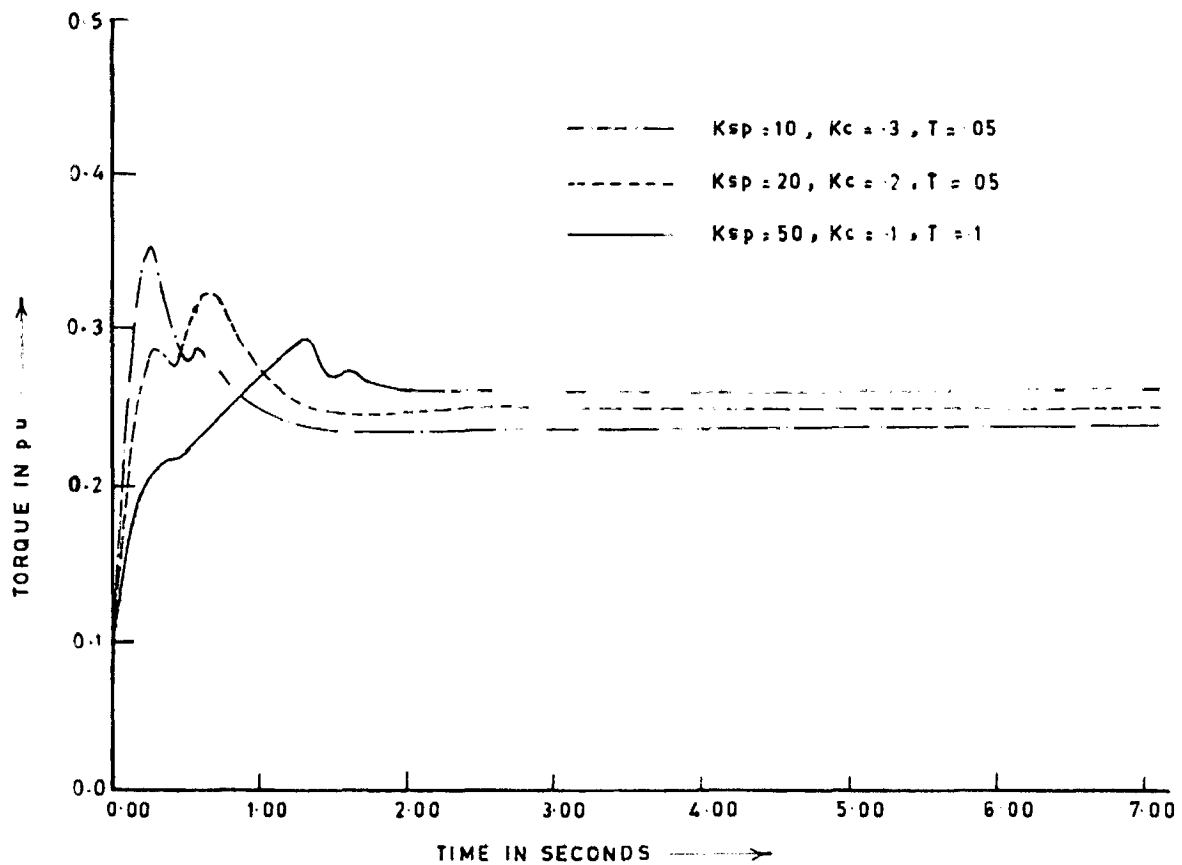


Fig. 6-12 TORQUE TRANSIENT FOR STEP CHANGE IN SPEED REFERENCE FROM 2 p.u. TO 5 p.u.

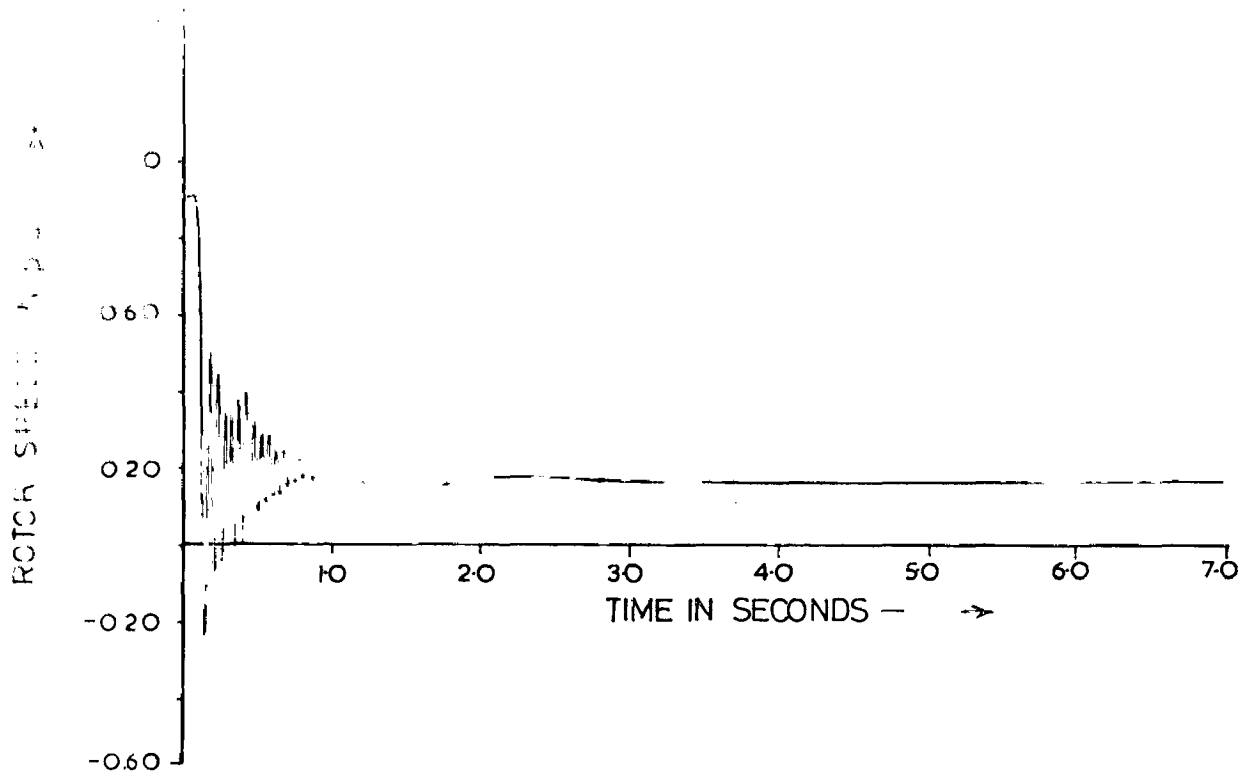


FIG.6.13 ROTOR SPEED TRANSIENT FOR STEP CHANGE IN SPEED REFERENCE FROM 1.0 p.u. TO 0.2 p.u. ( $K_{sp}=10$ ,  $K_c=0.3$ ,  $T=0.05$ )

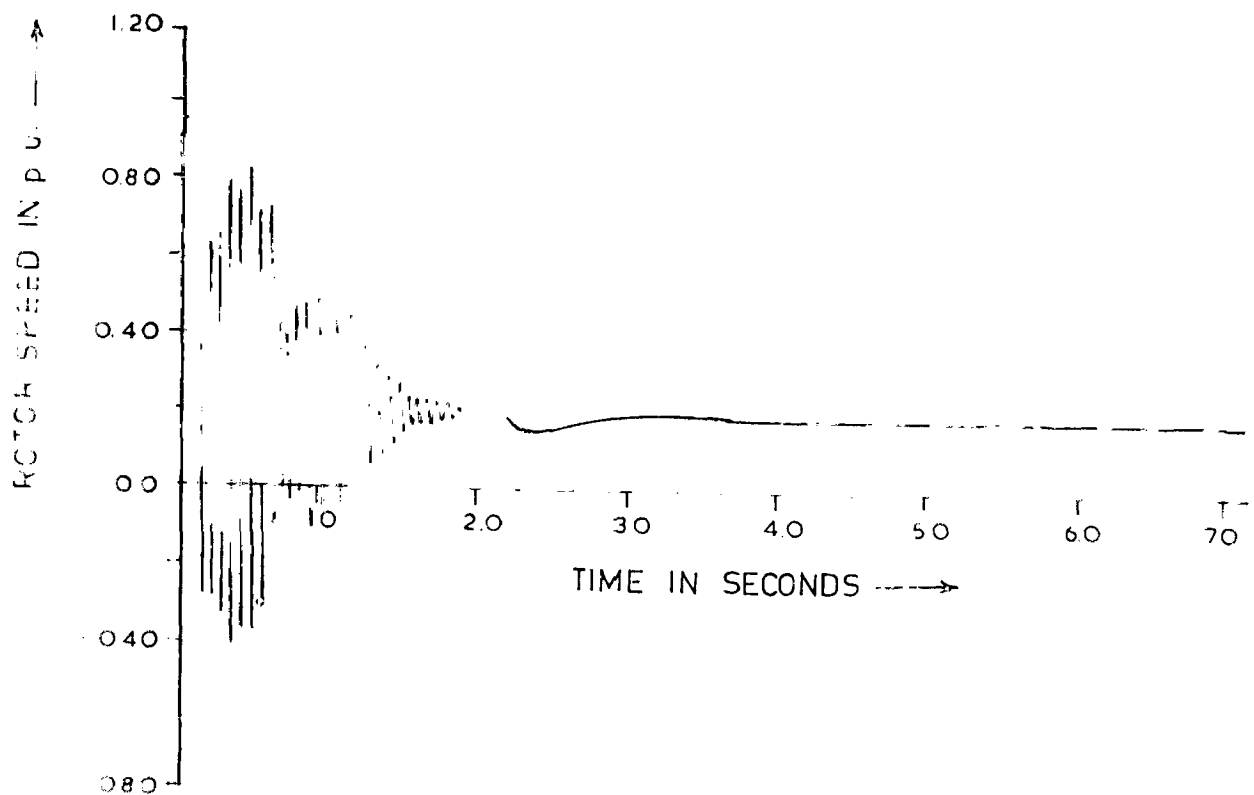


FIG 6.14. ROTOR SPEED TRANSIENT FOR STEP CHANGE IN SPEED REFERENCE FROM 1.0 p.u. TO 0.2 p.u. ( $K_{sp}=20$ ,  $K_c=0.2$ ,  $T=0.05$ )

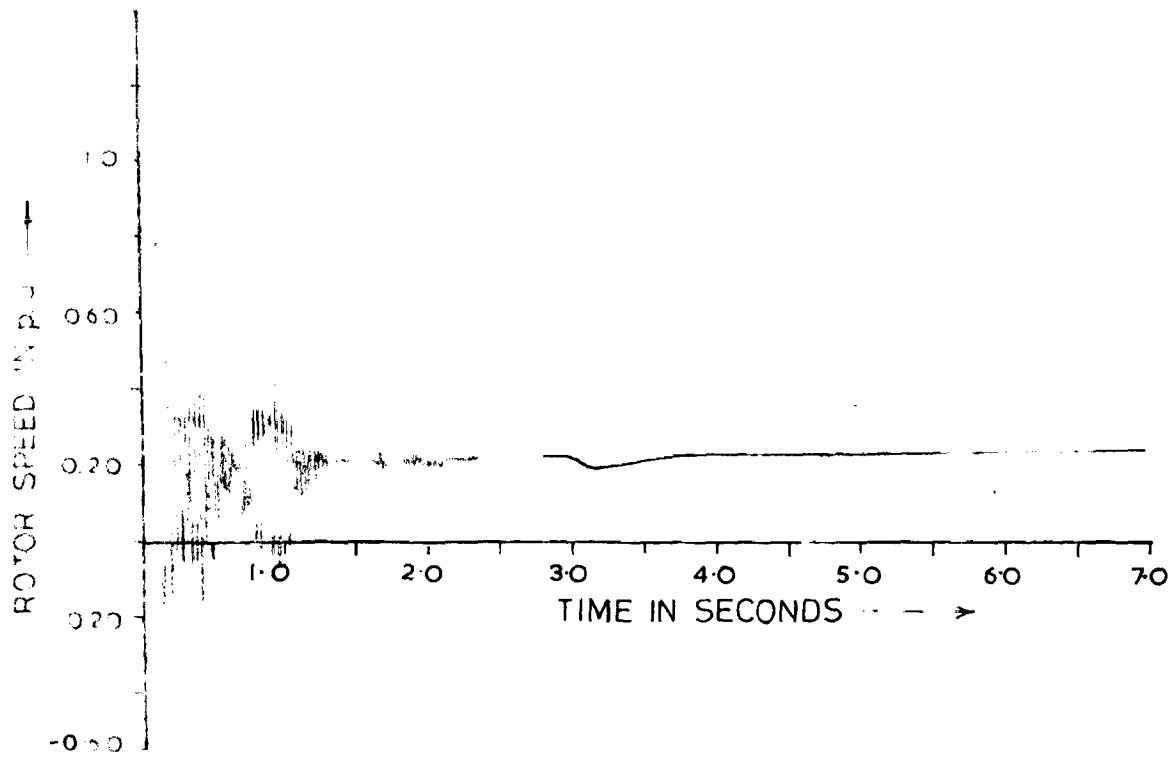


FIG. 6.15 ROTOR SPEED TRANSIENT FOR STEP CHANGE IN SPEED REFERENCE FROM 1.0 p.u. TO 0.2 p.u. ( $K_{sp}=50$ ,  $K_c=0.10$ ,  $T=0.10$ )

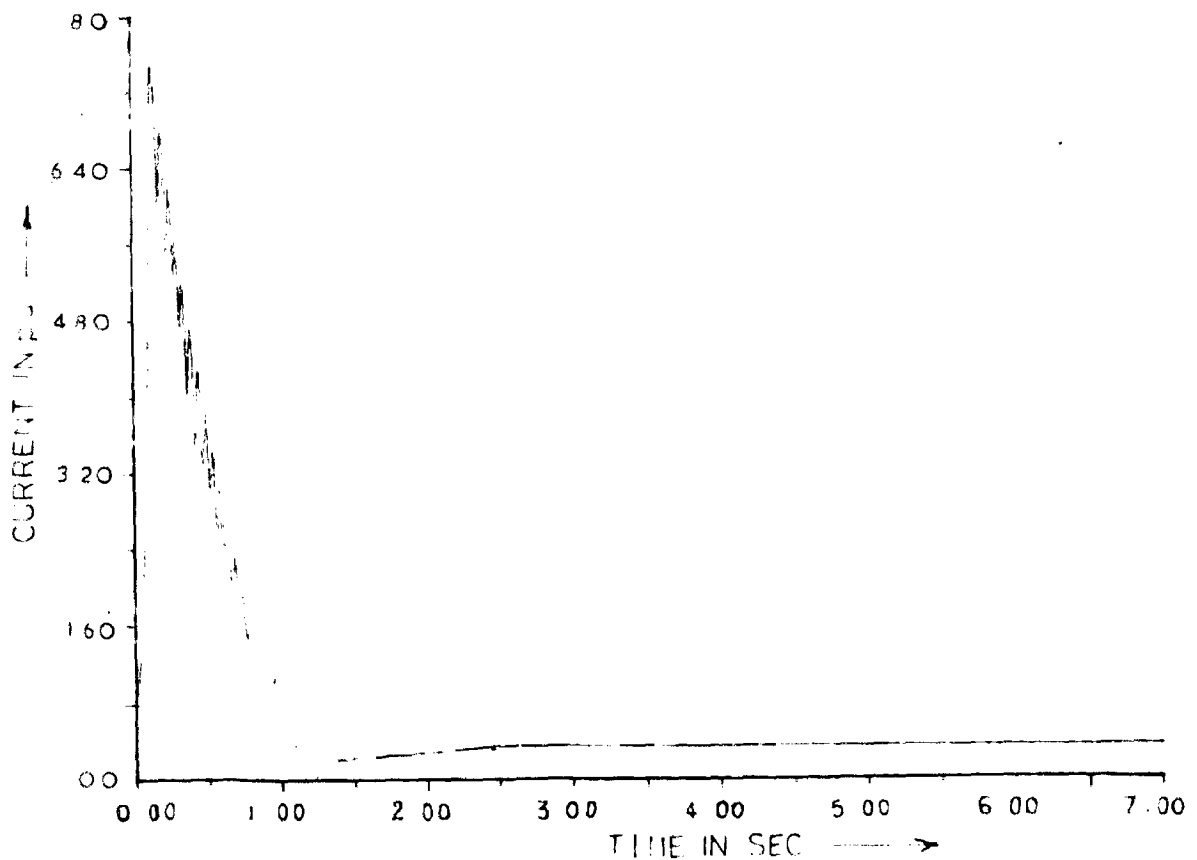


FIG. 6.16 D.C. LINK CURRENT TRANSIENT FOR STEP CHANGE IN SPEED REFERENCE FROM 1.0 p.u. TO 0.2 p.u. ( $K_{sp}=10$ ,  $K_c=0.3$ ,  $T=0.05$ )

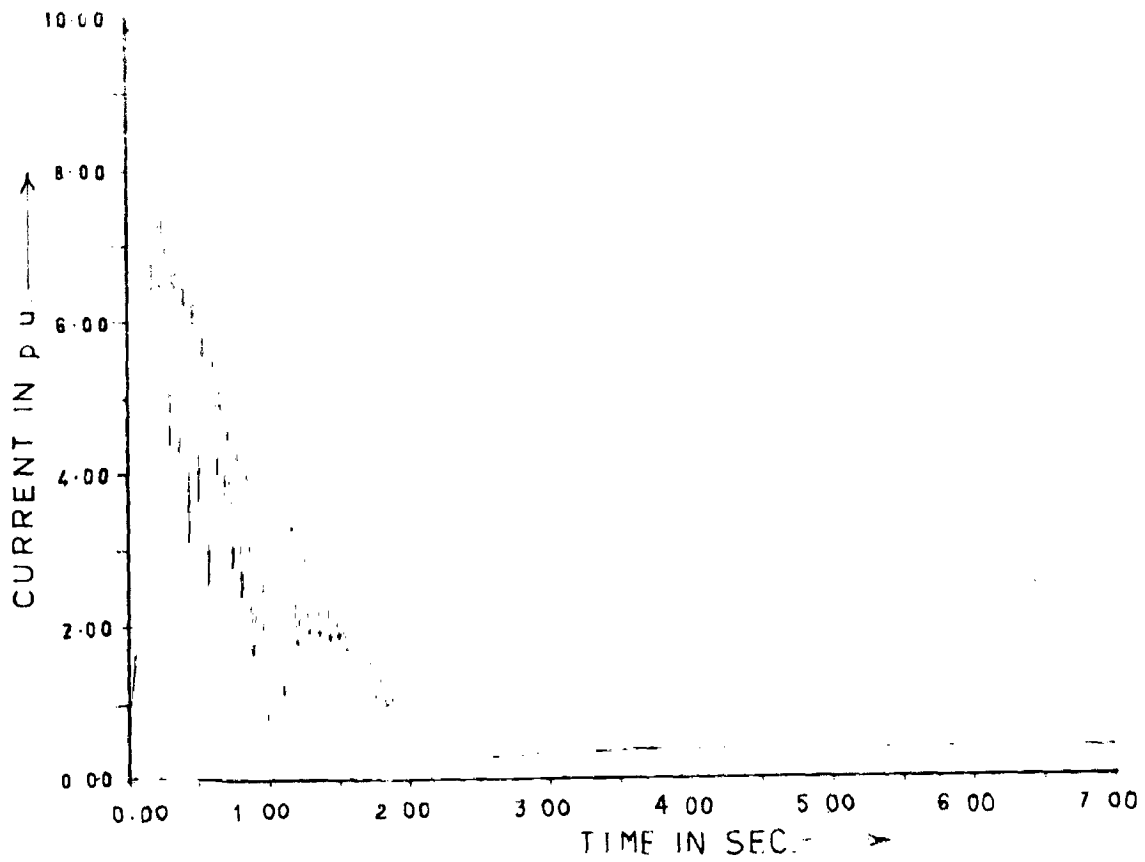


FIG. 6.17. D.C. LINK CURRENT TRANSIENT FOR STEP CHANGE IN SPEED REFERENCE FROM 1.0 p.u. to 0.2 p.u. ( $K_{sp} = 20$ ,  $K_c = 0.2$ ,  $T = 0.05$ )

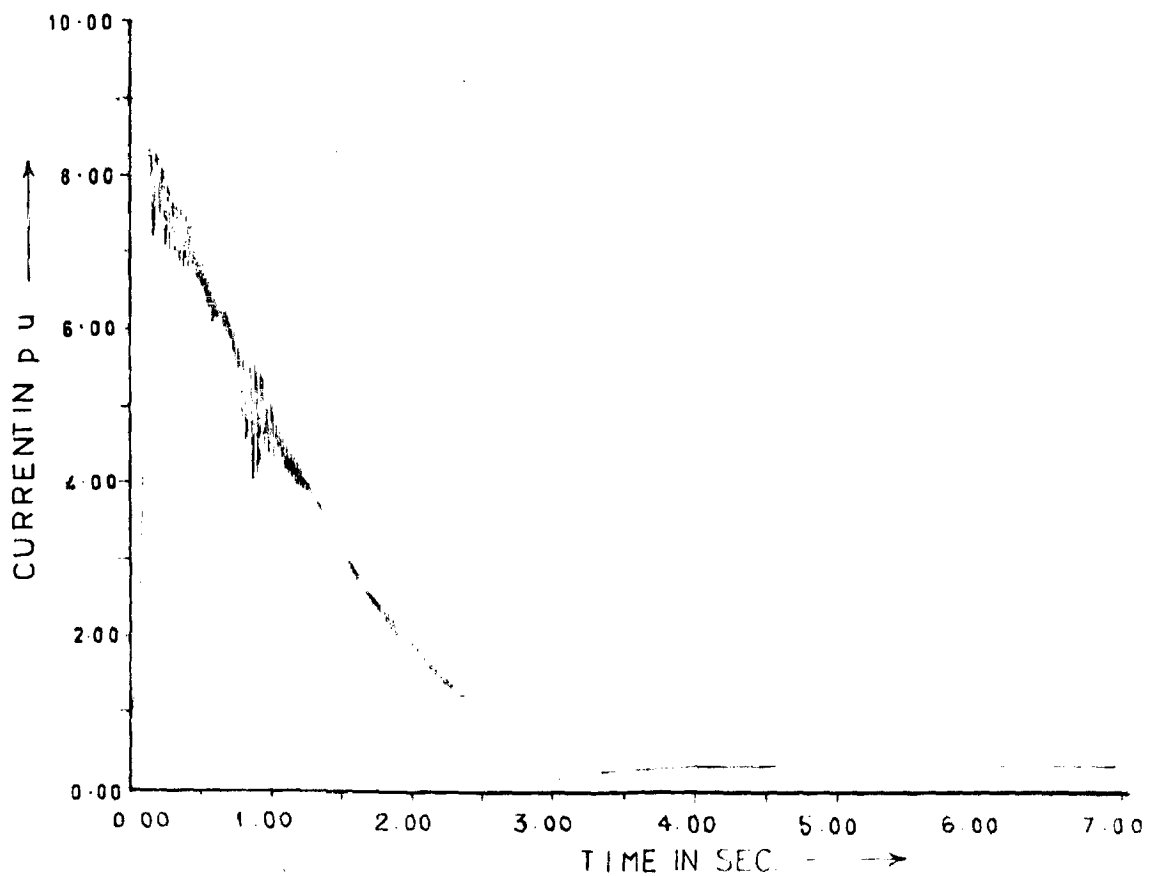


FIG. 6.18. D.C. LINK CURRENT TRANSIENT FOR STEP CHANGE IN SPEED REFERENCE FROM 1.0 p.u. TO 0.2 p.u. ( $K_{sp} = 50$ ,  $K_c = 0.19$ ,  $T = 0.10$ )



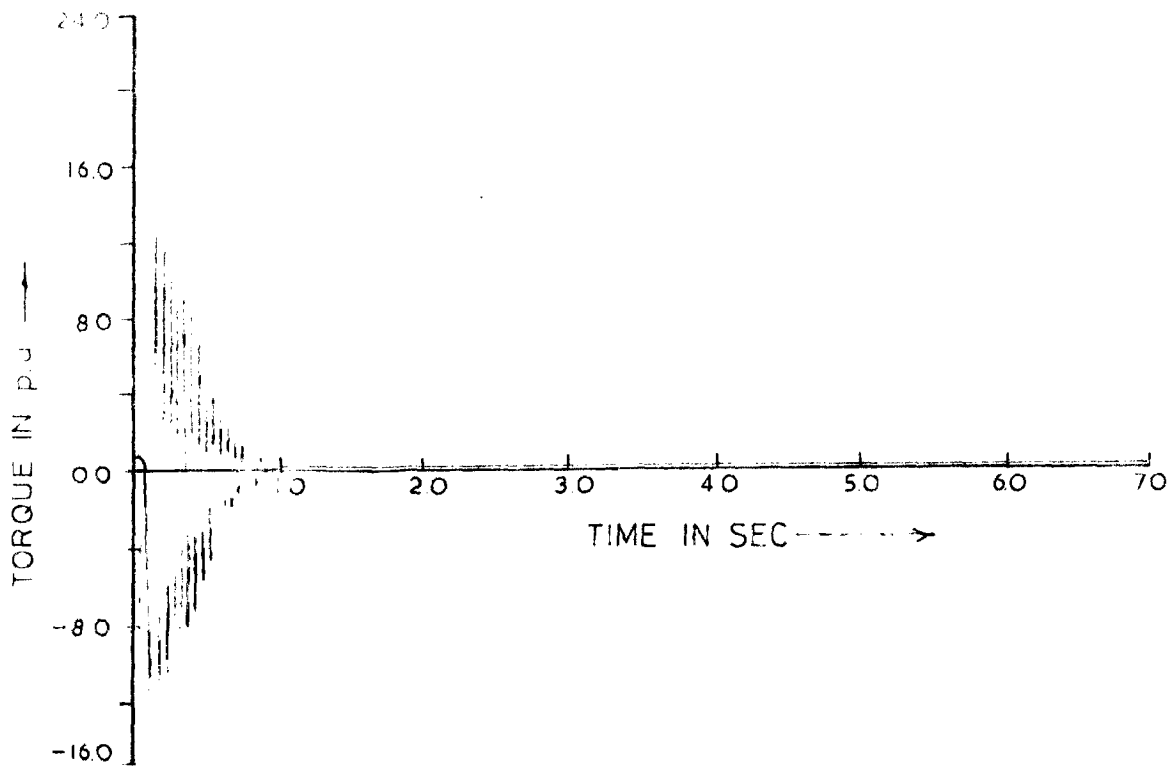


FIG.6.19. TORQUE TRANSIENT FOR STEP CHANGE IN SPEED REFERENCE FROM 1.0 p.u. TO 0.2 p.u. ( $K_{sp}=10$ ,  $K_c=0.3$ ,  $T=0.05$ )

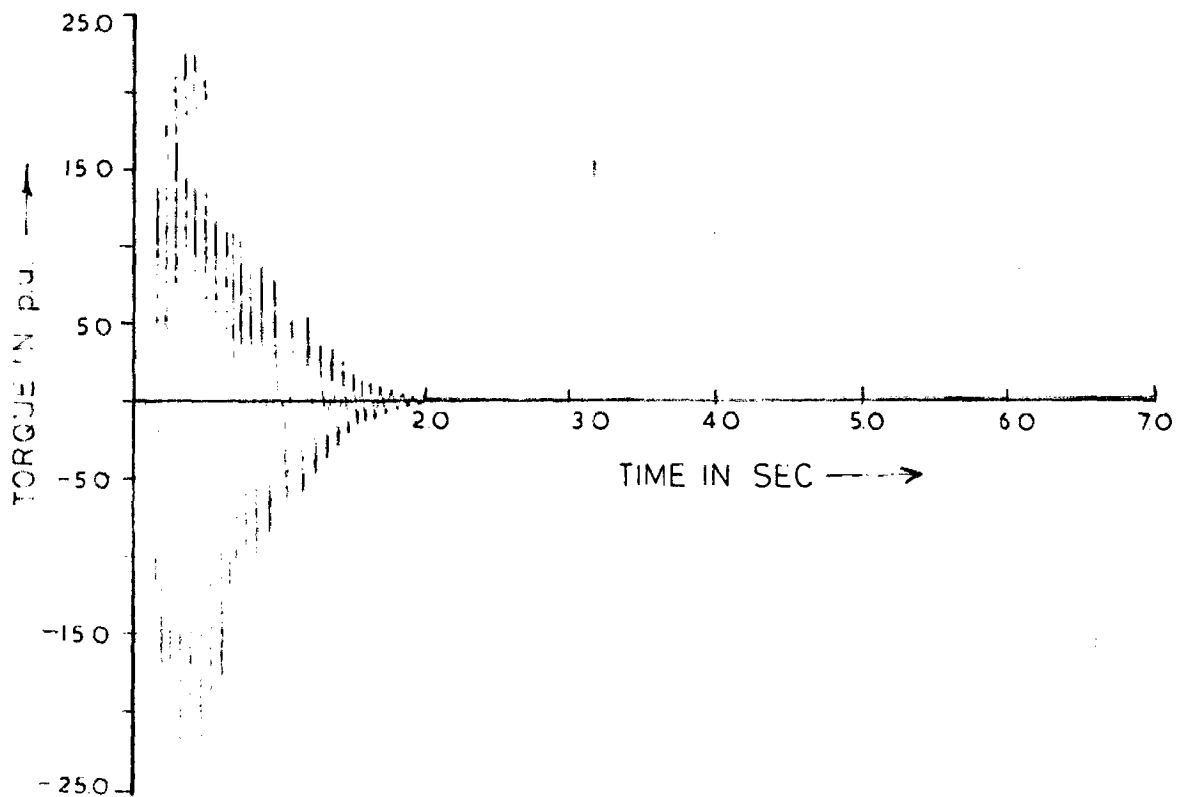


FIG.6.20. TORQUE TRANSIENT FOR STEP CHANGE IN SPEED REFERENCE FROM 1.0 p.u. TO 0.2 p.u. ( $K_{sp}=20$ ,  $K_c=0.2$ ,  $T=0.05$ )

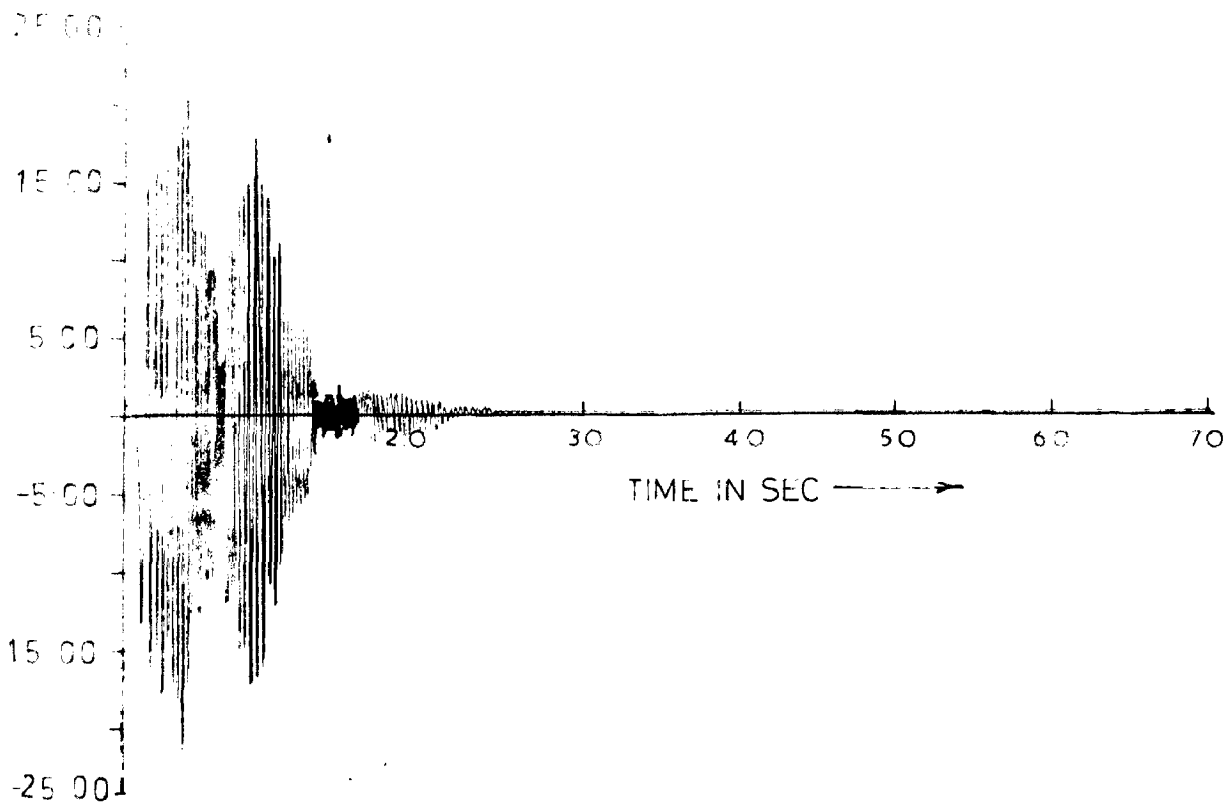


FIG. 6.21. TORQUE TRANSIENT FOR STEP CHANGE IN SPEED REFERENCE FROM 1.0 pu TO 0.2 pu ( $K_{sp}=50, K_c=0.1, T=0.1$ )

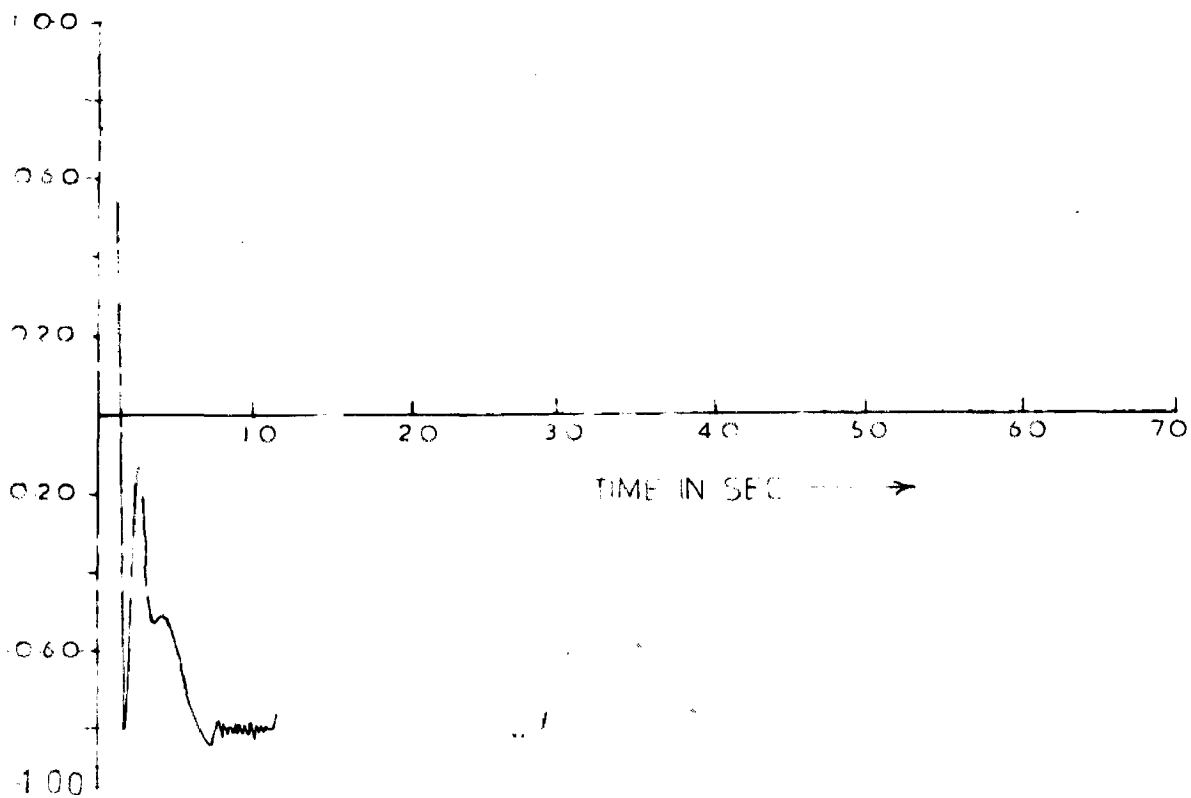


FIG. 6.22 ROTOR SPEED TRANSIENT FOR REVERSAL IN DIRECTION OF ROTATION FROM 0.8 TO -0.8 pu REFERENCE SPEED ( $K_{sp}=10, K_c=0.3, T=0.05$ )

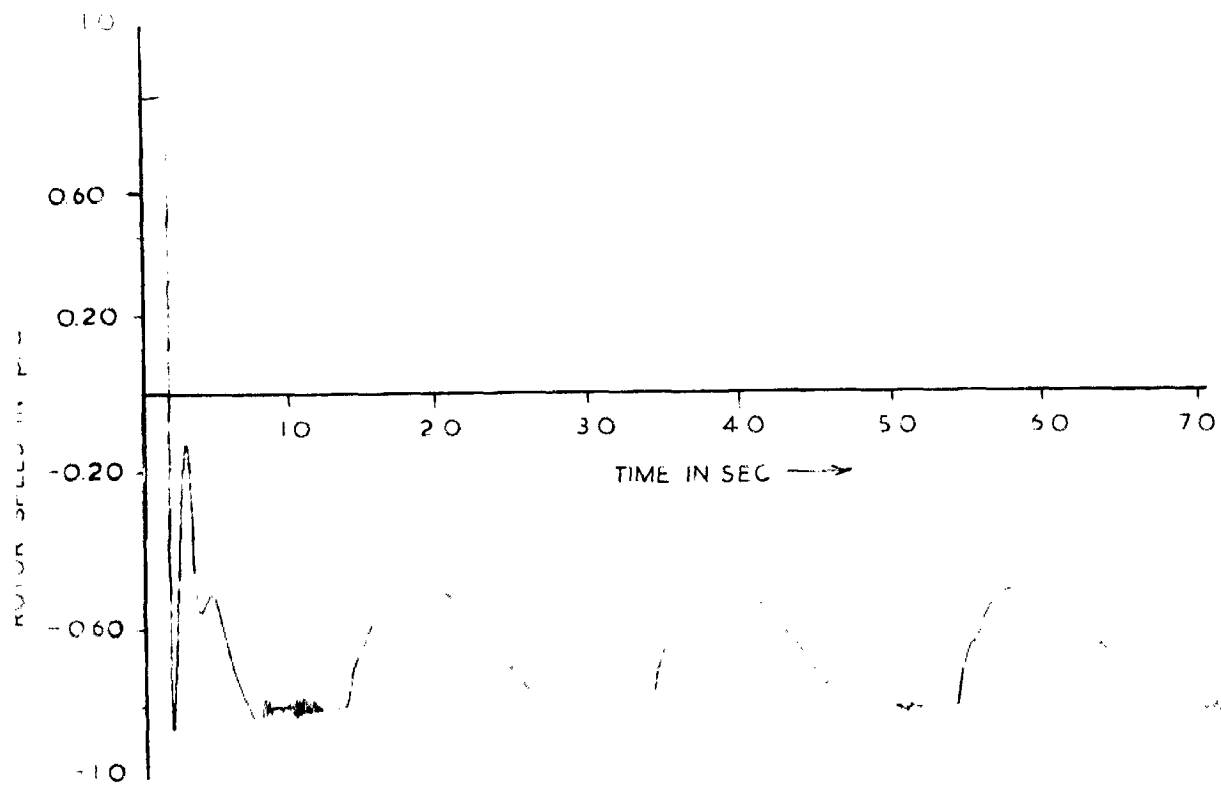


FIG 6.23. ROTOR SPEED TRANSIENT FOR REVERSAL IN DIRECTION OF ROTATION FROM 0.8 TO -0.8 p.u. REFERENCE SPEED ( $K_{sp}=20$ ,  $K_c=0.20$ ,  $T=0.05$ )

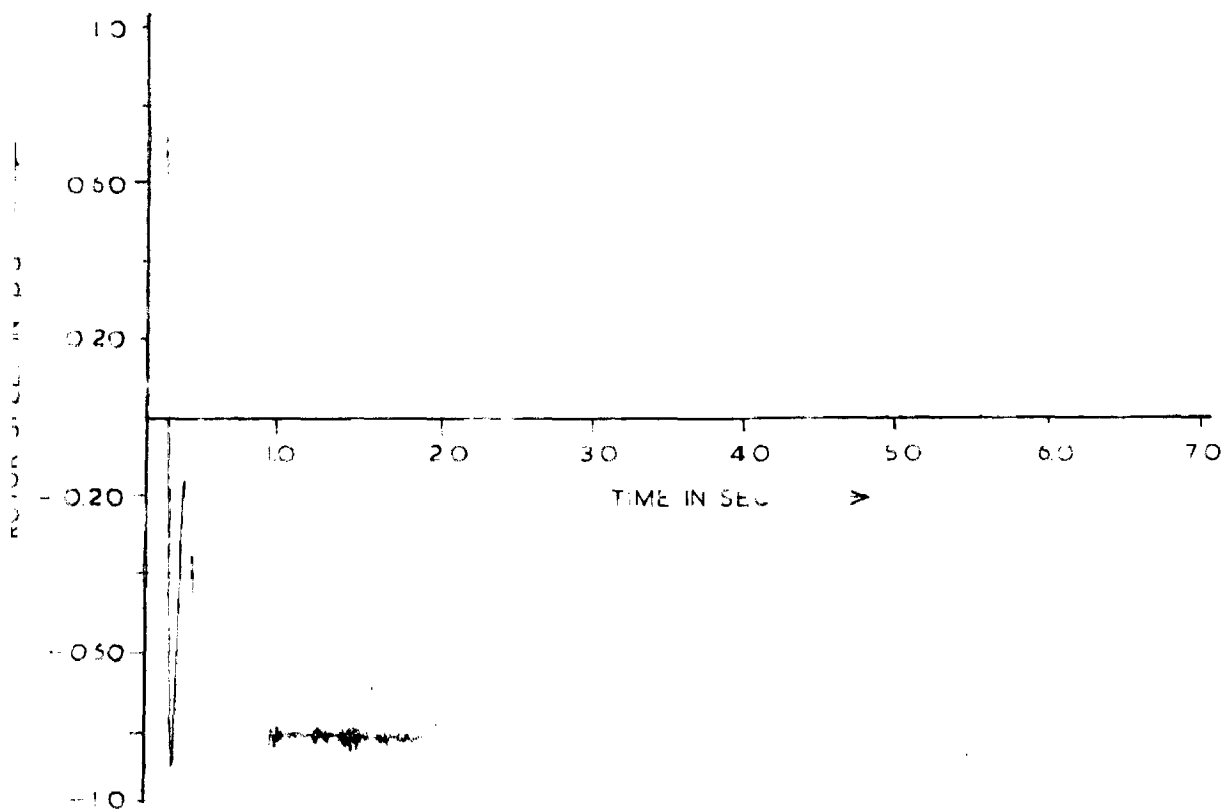


FIG. 6.24. ROTOR SPEED TRANSIENT FOR REVERSAL IN DIRECTION OF ROTATION FROM 0.8 TO -0.8 p.u. REFERENCE SPEED ( $K_{sp}=50$ ,  $K_c=0.10$ ,  $T=0.10$ )

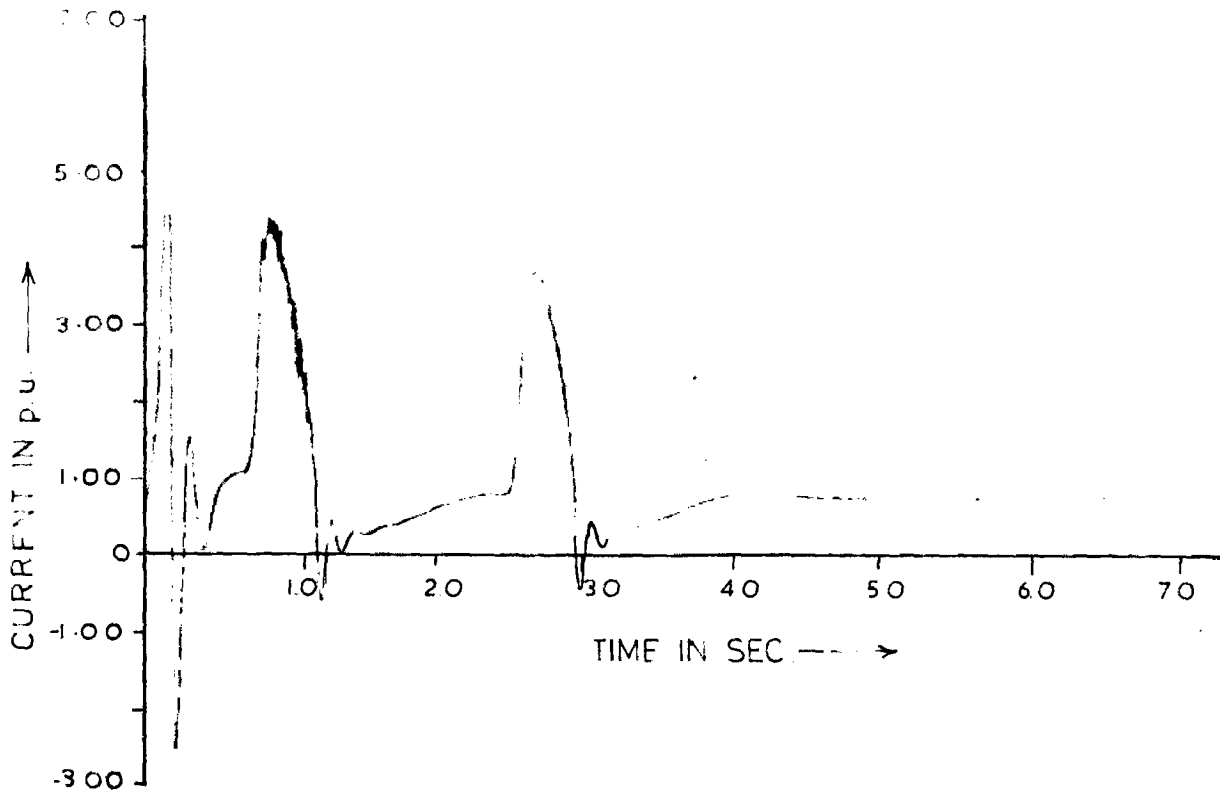


FIG.6.25. D.C. LINK CURRENT TRANSIENT FOR REVERSAL IN DIRECTION OF ROTATION FROM 0.8 TO -0.8 p.u. REFERENCE SPEED ( $K_{sp} = 10, K_c = 0.3, T = 0.05$ )

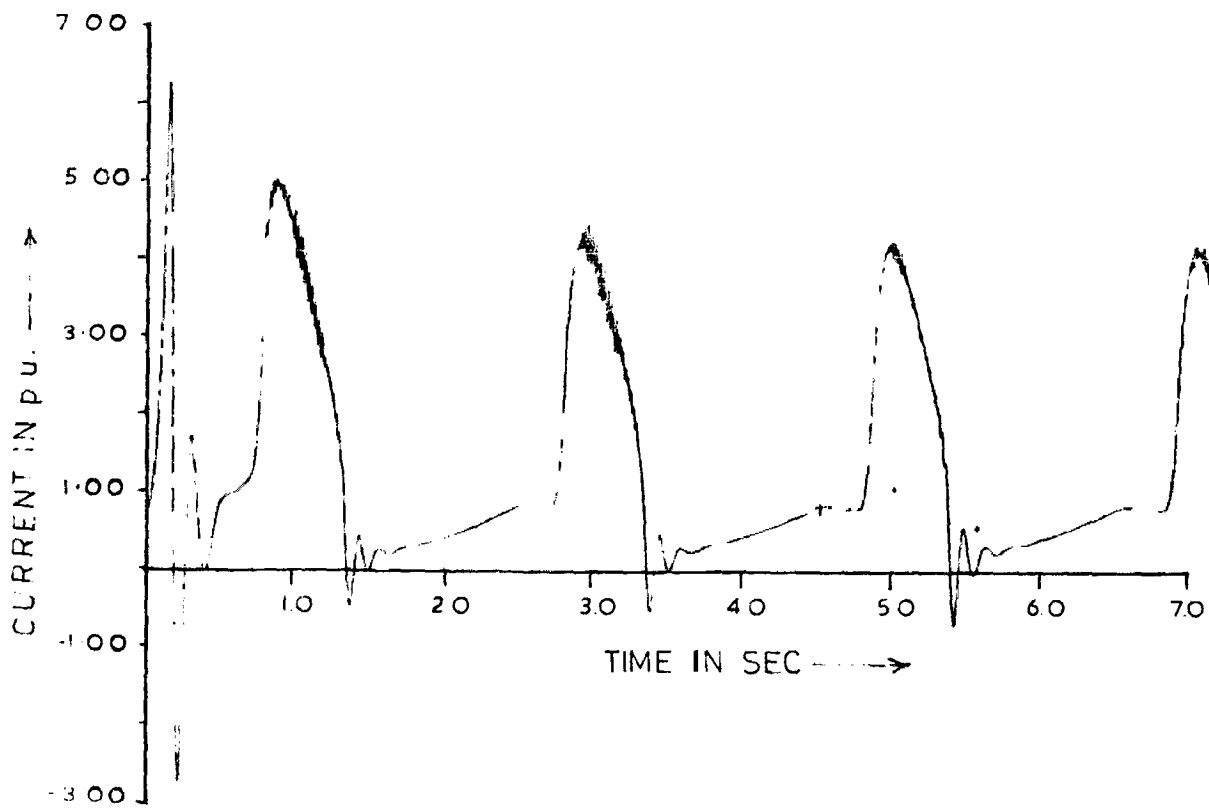


FIG.6.26. D.C. LINK CURRENT TRANSIENT FOR REVERSAL IN DIRECTION OF ROTATION FROM 0.8 TO -0.8 p.u. REFERENCE SPEED ( $K_{sp} = 20, K_c = 0.20, T = 0.05$ )

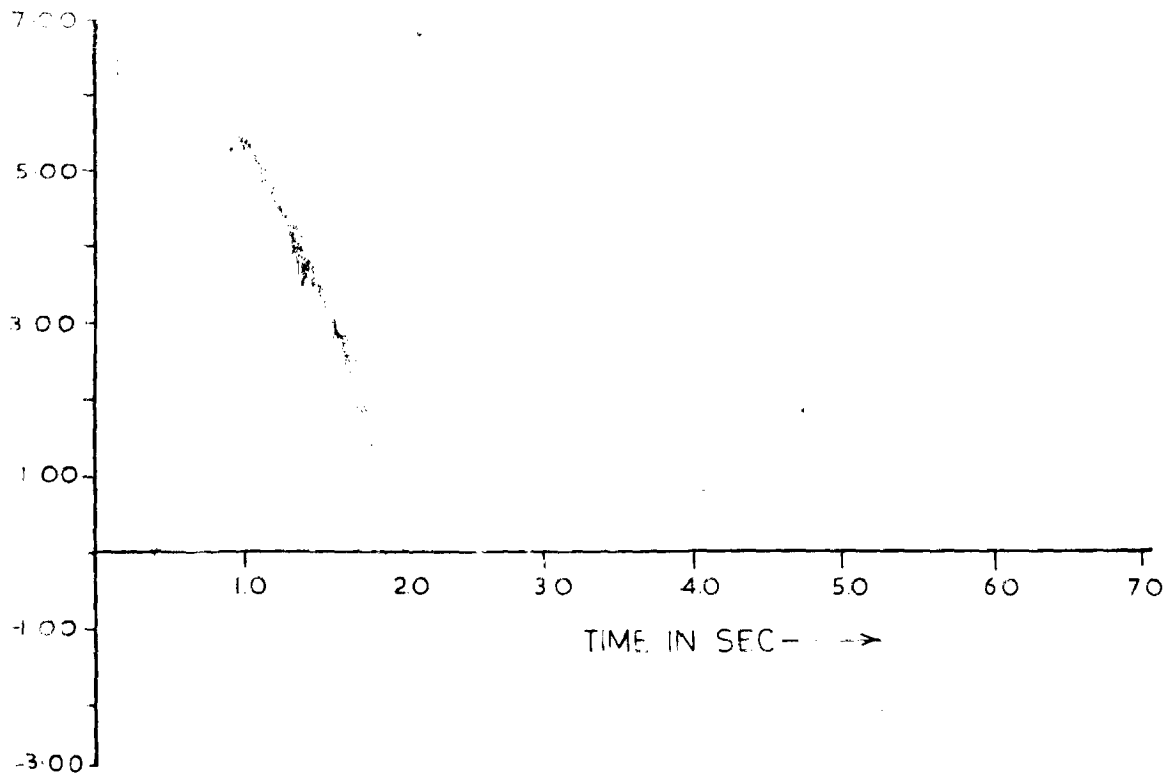


FIG. 6.27. D.C. LINK CURRENT TRANSIENT FOR REVERSAL IN DIRECTION OF ROTATION FROM 0.8 TO -0.8 p.u. REFERENCE SPEED ( $K_{sp}=50$ ,  $K_c=0.10$ ,  $T=0.10$ )

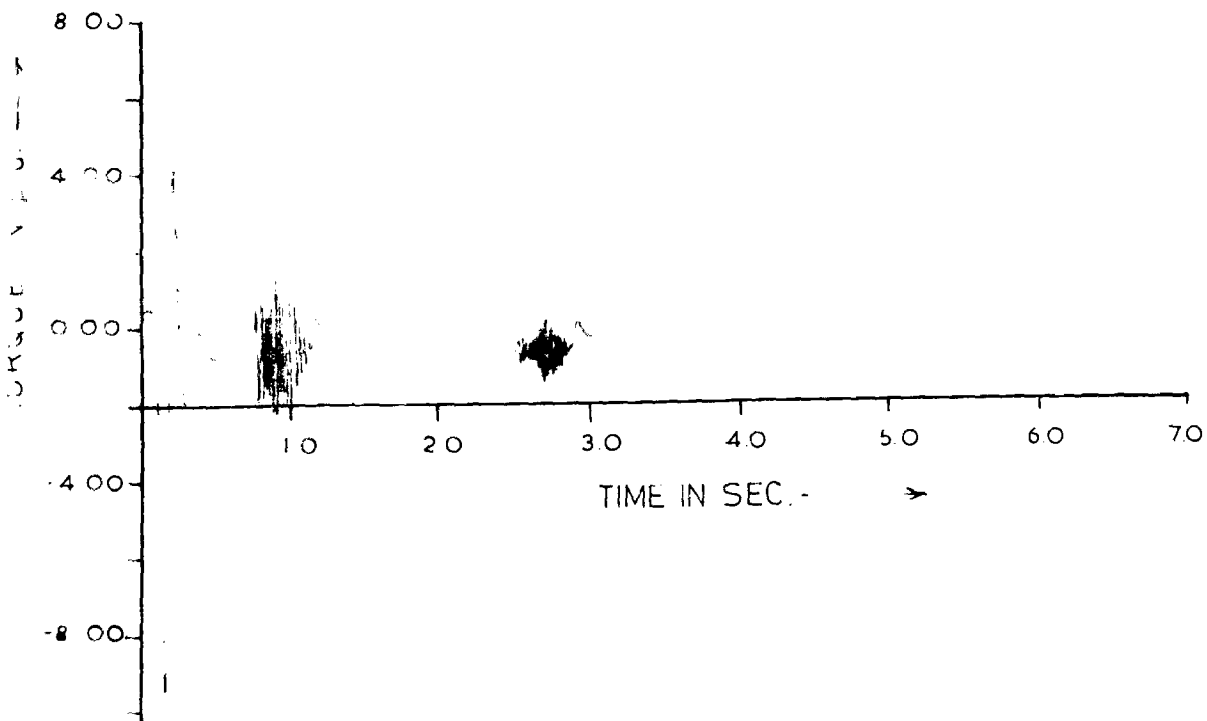


FIG. 6.28 TORQUE TRANSIENT FOR REVERSAL IN DIRECTION OF ROTATION FROM 0.8 TO -0.8 p.u. REFERENCE SPEED ( $K_{sp}=10$ ,  $K_c=0.3$ ,  $T=0.03$ )

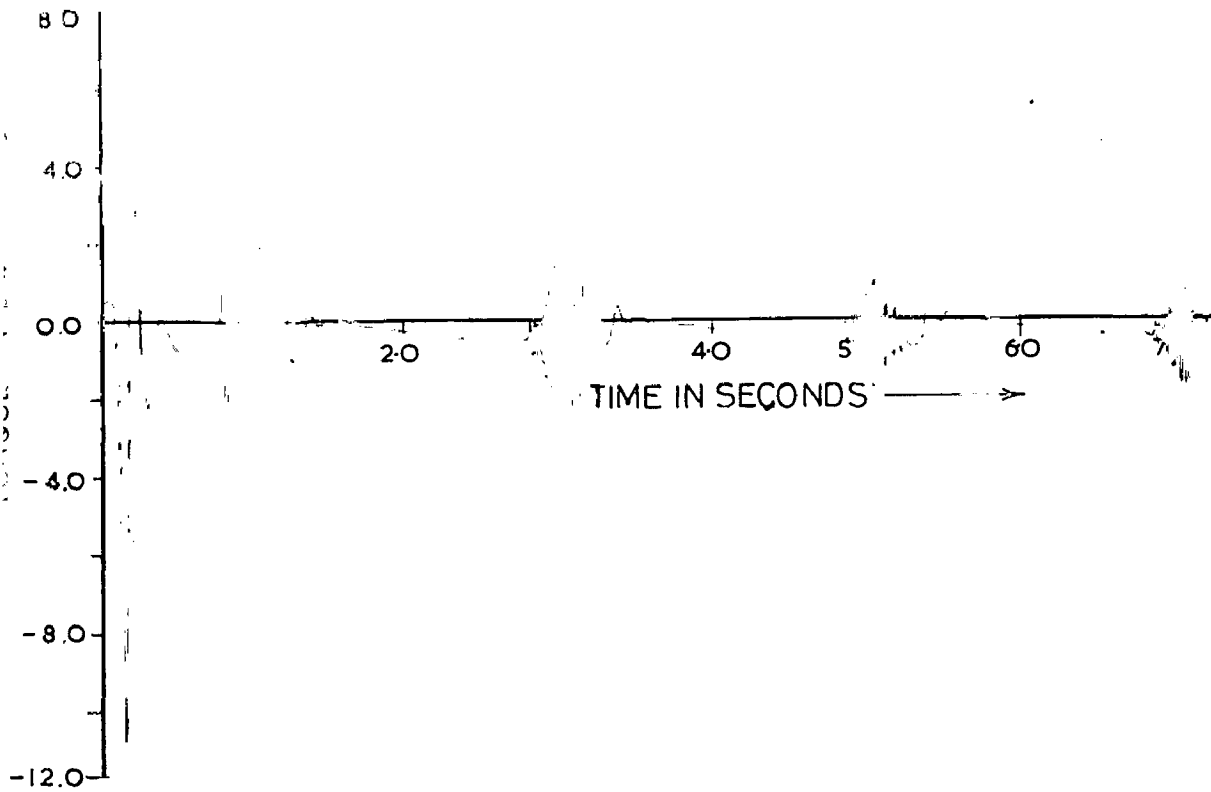


FIG. 6.29. TORQUE TRANSIENT FOR REVERSAL IN DIRECTION OF ROTATION FROM 0.8 TO -0.8 p.u REFERENCE SPEED (Ksp= 20, Kc= 0.2 ,T= 0.05 )

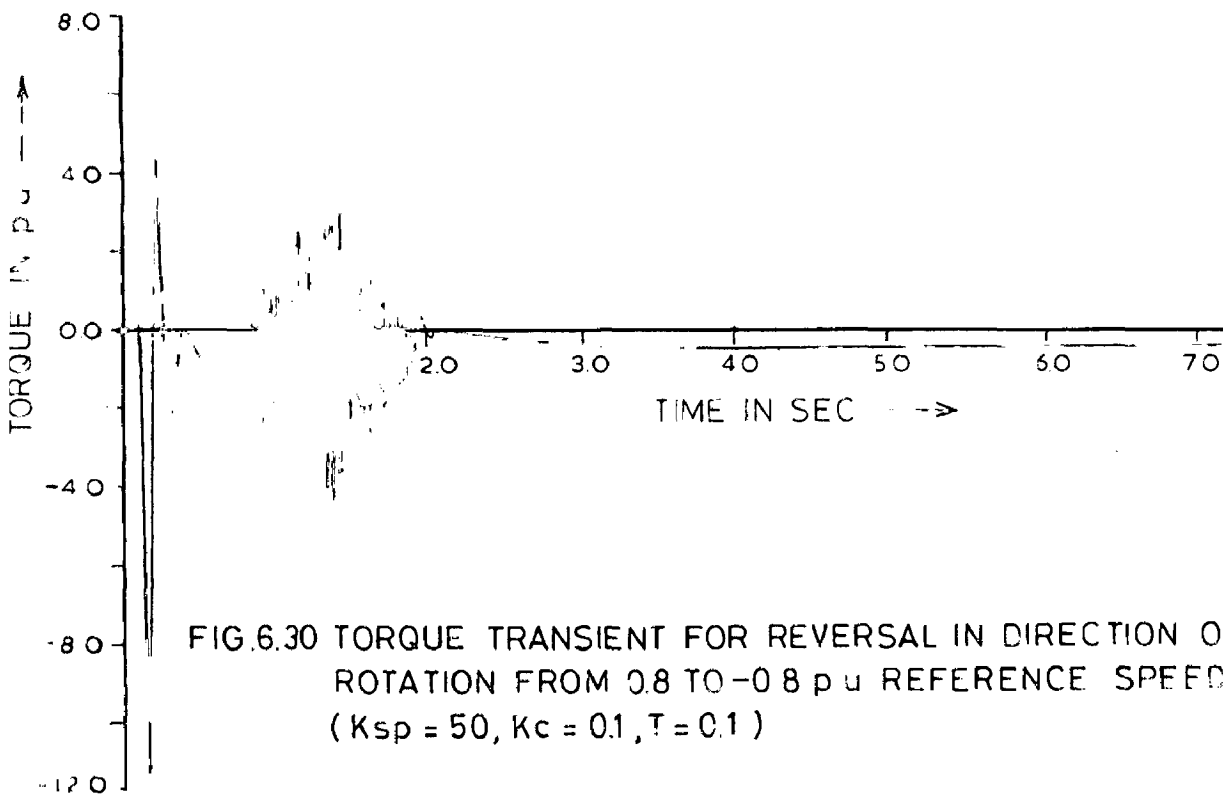


FIG.6.30 TORQUE TRANSIENT FOR REVERSAL IN DIRECTION OF ROTATION FROM 0.8 TO -0.8 p.u REFERENCE SPEED (Ksp = 50, Kc = 0.1 ,T = 0.1 )

## CHAPTER - 7

## CONCLUSION

This dissertation concerns variable speed operation of a induction-motor drive through a rectifier controlled-current inverter source. It is well known that such a drive is unstable in the open-loop mode of operation. To overcome this problem the drive is converted to close-loop from open-loop with the help of three regulators, namely a proportional speed regulator, a p-i current regulator and a slip regulator. The proportional speed regulator works on speed error and sets reference d.c. link current. The p-i current regulator works on d.c. link current error and controls the actual d.c. link current. The slip regulator sets slip speed proportional to d.c. link current so that rated air-gap flux is maintained in induction motor.

CENTRAL LIBRARY UNIVERSITY OF TORONTO  
R00661

An analytical method of determining steady-state performance of the rectifier controlled-current inverter induction motor drive has been discussed in this dissertation. The steady-state performance reveals that in the open-loop unstable region of the torque-slip characteristic the induction motor stator voltages are small, power factor is good in comparison to open-loop stable (i.e. low slip) zone of the torque-slip characteristic. Drive efficiency is poor in unstable zone comparison to stable zone due to neglect of iron-losses in analysis. The drive operation in the open-loop stable

region of the torque-slip characteristic is impossible due to high degree of saturation in the induction motor associated high iron losses and magnetising current. As p.u. operating frequency is decreased stator voltage reduces, power factor improves and efficiency and power output reduces when the drive is operated at a fixed d.c. link current.

Stability studies are carried out to coordinate controller parameters so that system is not only stable but possesses a certain minimum degree of stability. Compact expression for the system characteristic equation is derived from small displacement theory and then, by applying D-partitioning technique, the stability boundaries are determined in the plane of two adjustable parameters of the  $p - i$  regulator. D-partitioning boundaries are determined for three different values of proportional speed regulator constant ( $K_{sp}$ ) namely 10, 20 and 50 and for each  $K_{sp}$ , with four different p.u. operational frequencies namely 0.2, 0.5, 0.8 and 1.0. For each case the maximum degree of stability,  $\sigma$ , has also been determined. Following sets of regulator parameters ensure a minimum of  $2.7 \text{ sec}^{-1}$  degree of relative stability of the drive over 0.2 to 1.0 p.u. frequency range of operation under full-load torque conditions -

$K_{sp} = 10$	$K_c = 0.3$	$T = 0.05$
$K_{sp} = 20$	$K_c = 0.2$	$T = 0.05$
$K_{sp} = 50$	$K_c = 0.1$	$T = 0.1$



Analytical method of determining 6th-harmonic torque, speed and induction motor stator voltage pulsation of rectifier inverter induction motor have been discussed. Sixth-harmonic rotor speed torque and voltage are considerably more in the open-loop stable zone of torque-slip characteristic in compare to in the open-loop unstable zone of torque slip characteristic. As p.u. operating frequency is decreased the 6th-harmonic rotor speed oscillation increases in both zones of operation while the 6th-harmonic voltage oscillation decreases. There is hardly any effect on 6th harmonic torque oscillations due to variation in p.u. operating frequency. Thus, the drive exhibits superior harmonic oscillation performance when operated in the open-loop unstable zone of the torque-slip characteristic, however, the use of regulators will now be absolutely essential.

The transient performance of drive is next carried out, a nonlinear 5th-order state-space model of the system is developed. The various aspects under this study are starting, sudden speed change in both up and down directions and reversal in the direction of rotation of the motor. The transient responses of the drive have been determined each time for the 3 sets of regulator parameters recommended earlier in the linear-model stability analysis of the drive. From the point of view of settling time in the speed transients the following set of regulator parameters are found to be best-

$$K_{sp} = 10, \quad K_c = 0.3 \quad T = 0.05$$

For any reference speed setting the drive is noted to have larger steady-state error in speed for set of controller parameter with smallest  $K_{sp}$  (i.e. 10). However, since, for a fixed set of controller parameters the reference speed selector can be suitably calibrated in terms of the actual drive speed thus much importance need not be given to the steady state error.

#### SCOPE OF FURTHER WORK

Further work can be done on this topic under following aspects -

- (i) The steady state performance, 6th harmonic analysis, stability analysis and transient analysis have been determined theoretically in this dissertation. These must be checked experimentally.
- (ii) A rectifier inverter source has been considered here to feed variable current and frequency supply to the induction motor. An alternate form of the supply source like the inverter operating in the pulse width modulation mode, may be considered.
- (iii) The present work considers only the effect of the 6th harmonic pulsation of the drive whereas 12th and other higher harmonics are neglected. The effect of higher order torque pulsation may also be considered if the drive is to be operated at extremely low speeds.

- (iv) The performance of the variable speed induction motor drive can be studied using different types of controllers like p-i-d controllers.
- (v) In this dissertation drive operation in subsynchronous speed range only has been studied. Drive operation in supersynchronous speed range can also be studied.
- (vi) Effect of variation in the induction-motor parameters, namely inertia constant, may be studied.
- (vii) The present work ignores commutation time of the inverter. Inverter with finite commutation time may be considered and its effect on drive performance may also be studied.

## R E F E R E N C E S

1. Murphy, J.M.D., 'Thyristor Control of A.C.Motors', Pergamon Press Ltd., Oxford, 1973.
2. Paice, D.A., 'Induction Motor Speed Control by Stator Voltage Control', IEEE Trans.(PAS), Vol.87, pp 585, Feb. 1968.
3. Basu, P.R., 'Variable Speed Induction Motor Using Thyristor in the Secondary Circuit', IEEE Trans.(PAS), Vol.90, pp 509, Mar./April 1971.
4. Shepherd, W., and Stanway, J., 'Slip Power Recovery in an Induction Motor by the use of a Thyristor Inverter', IEEE Trans.(IGA), Vol.5, pp 74, Jan./Feb. 1969.
5. Heck, R. and Meyer, M., 'A Static Frequency-Changer-Fed Squirrel-Cage Motor drive for variable speed and reversing', Siemens Rev. 30, pp 401, Nov.1963.
6. Lipo, T.A., and Krause, P.C., 'Stability analysis of rectifier - inverter induction motor drive', IEEE Trans.(PAS), Vol.88, pp 55, Jan. 1969.
7. Fallside, F. and Wortley, A.T., 'Steady-state oscillation and stabilisation of variable frequency inverter fed induction motor drive', IEE Proc., Vol.116, pp 991, June 1969.
8. Klingshim, E.A., and Jordan, H.E., 'Polyphase induction motor performance and losses on non-sinusoidal voltage source', IEEE Trans.(PAS), Vol.87, pp 624, Mar.1968.

9. Jain, G.C., 'The effect of voltage shape on the performance of a 3-phase induction motor', IEEE Trans. (PAS), Vol.83, pp 561, June 1964.
10. Ward, E.E., Kazi, A. and Farakas, R., 'Time domain analysis of inverter fed induction motor', IEE Proc., Vol.114, pp 361, March 1967.
11. Sabbagh, E.M. and Shewan, W., 'Characteristic of an adjustable speed polyphase induction motor', IEEE Trans. (PAS), Vol.87, pp 613, Mar. 1968.
12. Lipo, T.A., Krause, P.C. and Jordan, H.E., 'Harmonic torque and speed pulsations in rectifier-inverter induction motor drive', IEEE Trans.(PAS), Vol.68, pp 579, May 1969.
13. Phillips, K.P., 'Current source converter for AC motor Drives', Trans.(IA), Vol.8, pp 679, Nov./Dec.1972.
14. Nelson, R.H. and Radomski, T.A., 'Design method for current source inverter, induction motor drive system', IEEE Trans.(IECI), Vol.21-22, pp 141, May, 1975.
15. Revankar, G.N. and Bashir, A., 'Effect of circuit and induction motor parameters on current source inverter operation', IEEE Trans.(IECI), Vol.24, pp 126, Feb.1977.
16. Lipo, T.A. and Comell, E.P., 'State-variable steady-state analysis of a controlled current induction motor drive', IEEE Trans.(IA), Vol.11, pp704, Nov./Dec.1975.
17. Comell, E.P. and Lipo, T.A., 'Modelling and design of controlled current induction motor drive system', IEEE Trans.(IA), Vol.13, pp 321, July/Aug.1977.
18. Macdonald, M.L. and Sen P.C., 'Control loop study of induction motor drives using DQ model', IEEE Trans.(IECI), Vol.26, pp 237, Nov.1979.

19. Sawaki, N., 'Steady-state and stability analysis of induction motor drive by current source inverter', IEEE Trans.(IA), Vol.13, pp 244 May/June 1979,
20. Novotny, D.W., 'Steady-State performance of inverter fed induction machines by means of time domain complex variables', IEEE Trans.(PAS), Vol.95, pp 927, May/June 1976.
21. Rao, K.P. and Sastry, V.V., 'Current-fed induction motor analysis using boundary-value approach', IEEE Trans(IECI) Vol.24, pp 178, May 1977.
22. Defornel, B. and Noyes, D., 'Transient characteristic of an Asynchronous machine current fed from a static converter', Proc.IEEE, Vol.124, pp 884, Oct.1977.
23. Samir, S., Hamid, ABD-EL, 'Analysis and Simplified representation of a current source inverter induction motor drive', IEEE Trans.(IECI), Vol.27, Nov.1980.
24. Adkins, 'The General Theory of Alternating Current Machines'
25. Concordia, Synchronous Machine Theory and Performance.
26. Meerov, Automatic Regulating of Electrical Machines.
27. Aizeman, Theory of a Automatic Control.
28. Lawrenson, P.J. and Bowes, S.R., 'Stability of reluctance machine', Proc. IEE Vol.118, pp 356, Feb.1971.

## APPENDIX - I

## THE SLIP REGULATOR - CONTROL STRATEGY

The drive under study makes use of a slip-regulator to maintain the air-gap flux of the induction motor near its rated value under below-rated speed operation of the drive. Such an aim can be met by varying the set value of  $\omega_{s\%}$  nearly proportional to the d.c. link current. This control strategy can be proved as follows.

The equivalent circuit of an induction motor is shown in Fig.(I.1) and its approximate equivalent circuit is shown in Fig.(I.2).

From approximate equivalent circuit rotor current can be written as

$$I_R \approx \frac{V}{\sqrt{\left(r_s + r_r \frac{\omega_e}{\omega_{s\%}}\right)^2 + \left(\omega_e x_{\%1} + \omega_e x_{\%2}\right)^2}} \quad \dots (I.1)$$

where

- $x_{\%1}$  and  $x_{\%2}$  p.u. reactances at base frequency
- $\omega_e$  p.u. frequency of operation
- $\omega_{s\%}$  p.u. slip speed

Rewriting above equation

$$I_R = \frac{V/\omega_e}{\sqrt{\left(\frac{r_s}{\omega_e} + \frac{r_r}{\omega_{s\%}}\right)^2 + \left(x_{\%1} + x_{\%2}\right)^2}} \quad \dots (I.2)$$

For constant air-gap flux voltage/frequency ratio must be kept constant and ignoring the stator resistance term since  $\omega_e \gg \omega_{s\ell}$  the above equation can be simplified to

$$i_R = \frac{\text{Constant}}{\sqrt{\left(\frac{r_r}{\omega_{s\ell}}\right)^2 + (x_{\ell 1} + x_{\ell 2})^2}} \quad \dots(I.3)$$

since,  $\omega_{s\ell}$  is very small in actual cases resulting in  $\frac{r_r}{\omega_{s\ell}} \gg (x_{\ell 1} + x_{\ell 2})$ , hence above equation can be written as

$$i_R = \frac{\text{Constant} \cdot \omega_{s\ell}}{r_r} \\ = \text{Constant} \cdot \omega_{s\ell} \quad \dots (I.4)$$

Thus, Rotor current is directly proportional to  $\omega_{s\ell}$  and is not dependent upon the p.u. speed of operation.



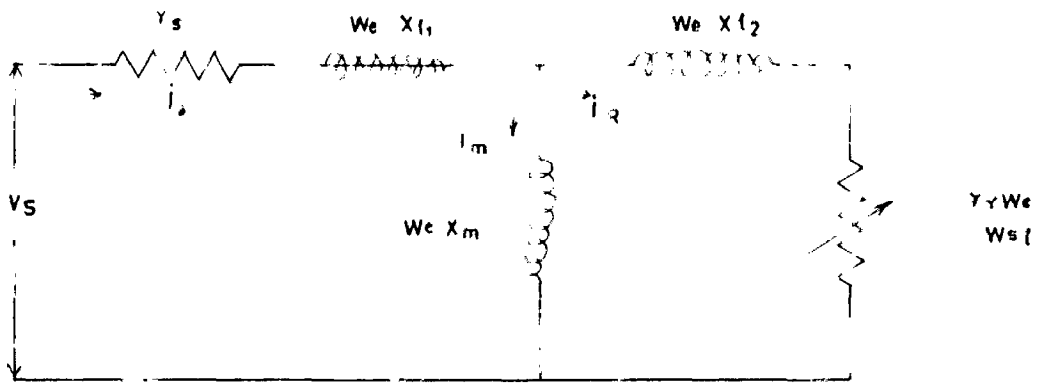


Fig I 1 EQUIVALENT CIRCUIT OF INDUCTION MOTOR

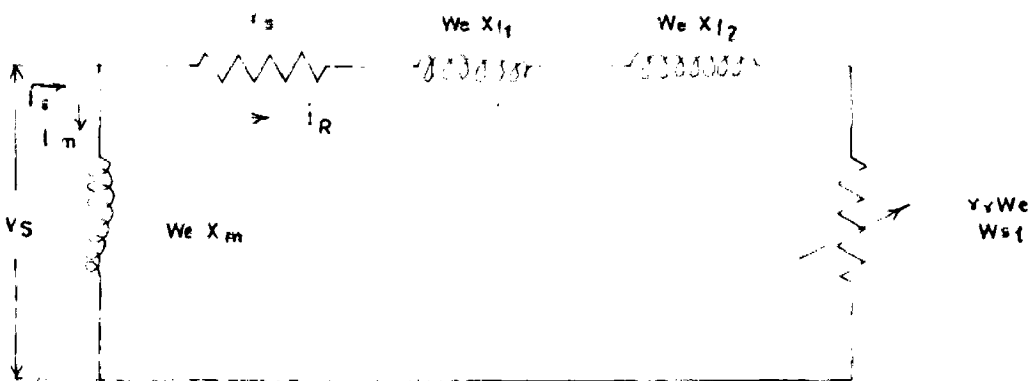


Fig I 2 APPROXIMATE EQUIVALENT CIRCUIT OF INDUCTION MOTOR

## APPENDIX - 11

PROGRAM FOR STEADY STATE ANALYSIS

DIMENSION WE(4),FIGS(8),WSL(100),U(100)

OPEN(UNIT=1,FILE='TS.DAT',DEVICE='DSK')

OPEN(UNIT=3,FILE='TS1.DAT',DEVICE='DSK')

OPEN(UNIT=4,FILE='TS2.DAT',DEVICE='DSK')

OPEN(UNIT=5,FILE='TS3.DAT',DEVICE='DSK')

OPEN(UNIT=6,FILE='TS4.DAT',DEVICE='DSK')

OPEN(UNIT=7,FILE='TS5.DAT',DEVICE='DSK')

OPEN(UNIT=8,FILE='TS6.DAT',DEVICE='DSK')

READ(1,\*),J,M,N

READ(1,\*),(WE(I),I=1,J)

READ(1,\*),(FIGS(L),L=1,M)

READ(1,\*),(U(K),K=1,N)

READ(1\*),RS,RR,XS,XR,XM,RF,XCO,WB

PRINT\*,J,M,N

PRINT\*,(WE(I),I=1,J)

PRINT\*,(FIGS(L),L=1,M)

PRINT\*,(U(K),K=1,N)

PRINT\*,RS,RR,XS,XR,XM,RF,XCO,WB

A=XR\*XR

B=RR\*RR

C=XM\*XM

DO 2 K=1,N

WSL(K)=U(K)/WB

DO 5 I=1,J

DO 5 L=1,M

```

10  FORMAT(30X,'P U OPERATING FREQUENCY =',F8.3,5X,F12.8)

    DO 5 K=1,N

      D=WSL(K)*WSL(K)

      E=D*A+B

      FIDR=WSL(K)*XM*RR*FIQS(L)/E

      FIQR=-WSL(K)*XR*FIDR/RR

      T=XM*FIQS(L)*FIDR

      TL=FIQS(L)*FIQS(L)*(RS+RF+D*C*RR/E)

      PO=T*(WE(I)-WSL(K))

      EFF=PO/(PO+TL)

      SLIP=WSL(K)/WE(I)

      WRITE(3,*) ,T,EFF

      WRITE(4,*) ,T,PO

      WRITE(5,*) ,T,SLIP

      WRITE(8,*) ,T,TL

5   PRINT* ,T,SLIP,FIDR,FIQR,TL,PO,EFF

      CLOSE(UNIT=3)

      CLOSE(UNIT=4)

      CLOSE(UNIT=5)

      CLOSE(UNIT=8)

      DO 6I=1,J

        DO 6L=1,M

          PRINT 10,WE(I),FIQS(L)

          DO 6K=1,N

            D=WSL(K)*WSL(K)

            E=D*A+B

            FIDR=WSL(K)*XM*RR*FIQS(L)/E

            T=XM*FIQS(L)*FIDR

            VQS=(RS+WE(I)*WSL(K)*C*RR/E)*FIQS(L)

```

```

VDS=WE(I)*FIQS(L)*(-XS+C*D*XR/E)
PFA=ATAN(-VDS/VQS)
PF=COS(PFA)
V=SQRT(VQS*VQS+VDS*VDS)
VR=(VQS+(RF+XCO)*FIQS(L))
PO=WSL(K)*FIQS(L)*FIQS(L)*C*RR/E*(WE(I)-WSL(K))
SLIP=WSL(K)/WE(I)
PRINT *,WSL(K),VQS,VDS,PF,V,VR,PO,SLIP
WRITE(6,*)T,V
WRITE(7,*)T,PF
6 CONTINUE
CLOSE(UNIT=1)
CLOSE(UNIT=6)
CLOSE(UNIT=7)
STOP
END
    
```

GRAMS CALLED

ATAN,

; AND ARRAYS [ "\*" NO EXPLICIT DEFINITION - "%" NOT REFERENCED ]

1 \*WB 2 \*RF 3 \*EFF 4 \*T 5

13	WSL	14	*TL	160	*V	161	*M	162
163	FIGS	164	WE	174	.S0007	200	*VR	201
06 202	*D	203	.S0005	204	.S0004	205	*A	206
03 207	.S0002	210	*XCO	211	.S0001	212	.S0000	213
214	*XS	215	*PF	216	*RS	217	*XM	220
221	.S0014	365	*SLIP	366	.S0013	367	.S0012	370
11 371	.S0010	372	*L	373	*I	374	*XR	375
376	*PFA	377	*RR	400	*VQS	401		

RARIES

00 414

[ NO ERRORS DETECTED ]

IMPLICIT COMPLEX(Y,Z)

COMPLEX P

```
C PROGRAM FOR STABILITY ANALYSIS

DIMENSION FR(4),U(90),V(10)

OPEN(UNIT=1,DEVICE='DSK',FILE='SA1.DAT')

READ(1,*) ,N,M

READ(1,*) ,RS,RR,XS,XR,XM,RF,XCO,XF

READ(1,*) ,WB,FKSL,KSP

READ(1,*) ,(U(K),K=1,N)

READ(1,*) ,(FR(I),I=1,M)

READ(1,*) ,FS,FIQS

READ(1,*) ,(V(J),J=1,3)

PRINT* ,N,M

PRINT* ,RS,RR,XS,XR,XM,RF,XCO,XF

PRINT* ,WB,FKSL,KSP

PRINT* ,(U(K),K=1,N)

PRINT* ,(FR(I),I=1,M)

PRINT* ,FS,FIQS

PRINT* ,(V(J),J=1,3)

G=FS*FS*XR*XR+RR*RR

FIDR=FS*XM*RR*FIQS/G

R=RS+RF+XCO

X=XS+XF-XM*XM/XR

RA=XM*RR/XR

RB=RR*RR/XR

RC=2.*RR
```

```

A=-RA*FS+2.*XR*FS*FKSL*FJDR-RA*FKSL*FIQS
D=FS*(1.-KSP*FKSL)
PRINT*,G,FIDR,R,X,RA,RB,RC,F,A,D
DO 5 I=1,M
VR=(R+FR(I)*FS*XM*XM*RR/G)*FIQS
B=FS*R+R*FKSL*FIQS+XM*FR(I)*FKSL*FIDR-VR*FKSL
PRINT *,VR,B
DO 5 J=1,3
Q=V(J)
PRINT*,Q
DO 5 K=1,N
W=U(K)
P=CMPLX(-Q,W)
Z1=.2960462*P
Z2=FS*FR(I)*XM+P*RA/WB+P*P*XM/F
Z3=FS*FS*XR+RB+P*RC/WB+P*P*XR/F
Z4=FS*X*P/WB+B
Z5=XM*FIDR+FKSL*Z1
Z6=A*XM*FIQS-Z3*Z5
Y2=-D*Z1*Z3+KSP*FS*Z6
IF(W.EQ.0.) GO TO 10
Y1=Y2/P
Y3=Z1*(Z2*A-Z3*Z4)+FS*XM*FIDR*Z6
DENO=REAL(Y1)*AIMAG(Y2)-REAL(Y2)*AIMAG(Y1)
FNEN1=REAL(Y2)*AIMAG(Y3)-REAL(Y3)*AIMAG(Y2)
FNEN2=REAL(Y3)*AIMAG(Y1)-REAL(Y1)*AIMAG(Y3)
IF(DENO.EQ.0.0) GO TO 4
FKC=FNEN1/DENO
FKCT=FNEN2/DENO

```

T=FNEN2/FNEN1

4 PRINT \*,FR(I),W,FKC,FKCT,Y1,Y2,Y3

GO TO 5

10 Y3=Z1\*(Z2\*A-Z3\*Z4)+FS\*XM\*FIDR\*Z6

Y1=Y2/P

FKC=-REAL(Y3)/REAL(Y1)

FKCT=-REAL(Y3)/REAL(Y2)

PRINT \*,FR(I),W,Z1,Z2,Z3,Z4,Z5,Z6,Y1,Y2,Y3,FKC,FKCT

5 CONTINUE

CLOSE(UNIT=1)

STOP

END

RAMS CALLED

AIMAG.

AND ARRAYS [ "\*" NO EXPLICIT DEFINITION - "%" NOT REFERENCED ]

1	*Y3	2	FR	4	*Z1	10	*FIDR	12
13	*RF	14	*W	15	*T	16	*FKCT	17
20	*Z6	21	*W	23	*K	24	*Y2	25
27	*Z5	30	*Y1	32	V	34	P	46
50	*Z4	51	*KSP	53	*J	54	*FIQS	55



63	*RC	64	.S0004	65	*A	66	.S0003	67
70	.S0001	71	*XCO	72	*FNEN2	73	.S0000	74
75	*Z3	76	*XS	100	*X	101	*RS	102
103	*XM	104	U	105	*R	237	*FKSL	240
241	.S0010	242	*FS	243	*Z2	244	*I	246
247	*F	250	*RR	251	*RA	252	*XF	253

RIES

[ NO ERRORS DETECTED ]

## APPENDIX IV

```

IMPLICIT COMPLEX(Z,C)

      DIMENSION SL(100), F(4), U(100)

      OPEN(UNIT=1, FILE='H.DAT', DEVICE='DSK')
      OPEN(UNIT=2, FILE='H2.DAT', DEVICE='DSK')
      OPEN(UNIT=3, FILE='H3.DAT', DEVICE='DSK')
      OPEN(UNIT=4, FILE='H4.DAT', DEVICE='DSK')
      OPEN(UNIT=5, FILE='H5.DAT', DEVICE='DSK')
      OPEN(UNIT=6, FILE='H6.DAT', DEVICE='DSK')
      OPEN(UNIT=7, FILE='H7.DAT', DEVICE='DSK')
      OPEN(UNIT=8, FILE='H8.DAT', DEVICE='DSK')

      READ(1,*) , N, M

      READ(1,*) , (OE(J), J=1, N)

      READ(1,*) , FIOS, FIDS

      READ(1,*) , (U(K), K=1, M)

      READ(1,*) , RS, RR, XS, XR, XH, RF, XCO, WB, XF

      READ(1,*) , TO, FKC, T, KSP, FKSL

      PRINT*, N, M

      PRINT*, (OE(J), J=1, N)

      PRINT*, FIOS, FIDS

      PRINT*, (U(K), K=1, M)

      PRINT*, RS, RR, XS, XR, XH, RF, XCO, WB, XF

      PRINT*, TO, FKC, T, KSP, FKSL

      AA=XR*XR

      H=RR*RR

      AC=XH*X

      PRINT*, AA, H, AC

```

```

DO 2 K=1, 4
2 WSL(K)=H(K)/WB

DO 5J=1, 4
DO 5 I=1, 4

D=WSL(I)*WSL(I)

E=D*AA+B

FIDR=WSL(I)*XR*RR*FIQS/E

FIQR=-WSL(I)*XR*FIDR/RR

VQS=(RS+WE(J)*WSL(I)*AC*RR/E)*FIQS

VDS=WE(J)*FIQS*(-XS+AC*D*XR/E)

V=SQRT(VQS*VQS+VDS*VDS)

TE=XR*FIQS*FIDR

FKT=XM/(6.*TQ*WE(J))

PRINT*, WE(J), WSL(I), FIDR, FIQR, VQS, VDS, V, TE

ZA=FKSL-ZJ*FKT*FIDR

ZB=-ZJ*FKC/(6.*WB*WE(J))+FKC*T

Z=ZJ*6.*WE(J)

YQR=XM*FIQS+XR*FIQR

YDR=XM*FIDS+XR*FIDR

YQS=XS*FIQS+XM*FIQR

YDS=XS*FIDS+XM*FIDR

Z11=RS+RF+XCO+Z*(XF+XS)+YDS*ZA+ZB-ZJ*KSP*FKT*FIDR*ZB

Z12=WE(J)*XS+ZJ*FKT*FIQR*YDS+ZJ*KSP*FKT*FIQR*ZB

Z13=Z*XM

Z14=WE(J)*XM-ZJ*FKT*YDS*FIQS-ZJ*KSP*FKT*FIQS*ZB

Z21=-WE(J)*XS-YQS*ZA

Z22=RS+Z*XS-ZJ*FKT*FIQR*YQS

Z23=-WE(J)*XM

Z24=Z*XM+ZJ*FKT*YQS*FIQS

```

Z31=Z\*X+YDR\*FKSL

Z32=WSL(I)\*XF

Z33=RR+Z\*XR

Z34=WSL(I)\*XR

Z41=-WSL(I)\*XF-YQR\*FKSL

Z42=Z\*λ

Z43=-WSL(I)\*XR

Z44=RR+Z\*XR

A=2./35.\*FIQS\*FKSL

Z1=-(Z5+Z\*XF+RF+XCO)\*2./35.\*FIQS-A\*YDS-ZJ\*12./35.\*Z12\*FIQS+2./35.

1 \*(VQS-ZJ\*6.\*VDS)

Z2=YQS\*A-ZJ\*Z22\*12./35.\*FIQS

Z3=-YDR\*A-ZJ\*Z32\*12./35.\*FIQS

Z4=-YQR\*A-ZJ\*Z42\*12./35.\*FIQS

Z5=Z3-Z34\*Z4/Z44

Z51=Z31-Z34\*Z41/Z44

Z52=Z33-Z34\*Z43/Z44

Z6=Z1-Z13\*Z5/Z52-Z14/Z44\*(Z4-Z43\*Z5/Z52)

Z53=Z11-Z13\*Z51/Z52+(Z43\*Z51/Z52-Z41)\*Z14/Z44

CIQS=Z6/Z53

FIQS6=SQRT((REAL(CIQS))\*(REAL(CIQS))+(AIMAG(CIQS))\*AIMAG(CIQS))

CIQS=ZJ\*12./35.\*FIQS

FIQS6=SQRT((REAL(CIQS))\*(REAL(CIQS))+(AIMAG(CIQS))\*AIMAG(CIQS))

CIQR=(Z5-Z51\*CIQS)/Z52

FIQR6=SQRT((REAL(CIQR))\*(REAL(CIQR))+(AIMAG(CIQR))\*AIMAG(CIQR))

CIQR=(Z1-Z41\*CIQS-Z43\*CIQR)/Z44

```

FJ56=SQRT(FIDS6*FIDS6+FIQS6*FIQS6)
FIK6=SQRT(FIDR6*FIQR6+FIDR6*FIQR6)
CVDS=Z21*CIQS+Z23*CIQR+Z24*CIDR-Z2
VDS6=SQRT((REAL(CVDS))*(REAL(CVDS))+(AIMAG(CVDS))*AIMAG(CVDS))
CWR=-ZJ*FKT*(FIQS*(CIDR-ZJ*12./35.*FIQR)+FIDR*CIQS)
WR6=SQRT((REAL(CWR))*(REAL(CWR))+(AIMAG(CWR))*AIMAG(CWR))
CIR=CIQS+2./35.*FIQS
FIR6=SQRT((REAL(CIR))*(REAL(CIR))+(AIMAG(CIR))*AIMAG(CIR))
CSIR=-KSP*CWR
FSIR6=SQRT((REAL(CSIR))*(REAL(CSIR))+(AIMAG(CSIR))*AIMAG(CSIR))
CVR=ZL*(-KSP*CFR-CTR)
VR6=SQRT((REAL(CVR))*(REAL(CVR))+(AIMAG(CVR))*AIMAG(CVR))
CVI=CVR-(Z*XF+RF+XCO)*CTR
VI6=SQRT((REAL(CVI))*(REAL(CVI))+(AIMAG(CVI))*AIMAG(CVI))
CVQS=CVI+2./35.*VDS-ZJ*12./35.*VDS
VQS6=SQRT((REAL(CVQS))*(REAL(CVQS))+(AIMAG(CVQS))*AIMAG(CVQS))
CTE=XJ*(FIQS*(CIDR-ZJ*12./35.*FIQR)+FIDR*CIQS)
TF6=SQRT((REAL(CTE))*(REAL(CTE))+(AIMAG(CTE))*AIMAG(CTE))
CSSL=FKSL*CIR
FSSL6=SQRT((REAL(CSSL))*(REAL(CSSL))+(AIMAG(CSSL))*AIMAG(CSSL))
CWE=CWR+CSSL
WE6=SQRT((REAL(CWE))*(REAL(CWE))+(AIMAG(CWE))*AIMAG(CWE))
V6=SQRT(VQS6*VQS6+VDS6*VDS6)
PRINT*,FJ56,FIQS6,FIQS6,FJ56,FIQR6,FIDR6,FIRR6,FIR6,FSIR6
PRINT*,VDS6,VQS6,VR6,VI6,V6
PRINT*,R6,E6,CSSL,TF6
WRITE(2,*),TF,TF6
WRITE(3,*),TF,R6
WRITE(4,*),TF,V6

```

WRITE(5,\*) ,TE,FIS6

WRITE(6,\*) ,TE,FIR6

WRITE(7,\*) ,TE,WSI,6

WRITE(8,\*) ,TE,WE6

5 CONTINUE

CLOSE(UNIT=1)

CLOSE(UNIT=2)

CLOSE(UNIT=3)

CLOSE(UNIT=4)

CLOSE(UNIT=5)

CLOSE(UNIT=6)

CLOSE(UNIT=7)

CLOSE(UNIT=8)

STOP

END

PROGRAMS CALLED

CMPLX. AIFAG.

VARIABLES AND ARRAYS [ "\*" NO EXPLICIT DEFINITION - "%" NOT REFERENCED ]

1	*ZB	2	*Z1	4	*Z12	6	*Z	10
12	*B	13	*RF	14	*Z51	15	*C1OR	17

32	*R	33	*PTR6	34	*ZA	35	*YDS	37
40	*CVDS	41	*Z41	43	*VDS	45	*Z34	46
50	*CVW	51	*VI6	53	*SL	54	*Z5	220
222	*R6	224	*FIQS6	225	*Z52	226	*AC	230
231	*V	233	*TO	234	*Z24	235	*CWF	237
241	*FSTR6	242	*FIOR6	243	*M	244	*Z4	245
247	*V6	250	*Z42	251	*FIQS	253	*J	254
255	*CIQS	261	*TE	263	.S0006	264	*CIR	265
267	.S0005	270	.S0004	271	*VQS6	272	*A	273
274	.S0003	276	*Z14	277	*ZJ	301	.S0002	303
304	*Z53	306	*XC0	310	.S0001	311	*YQR	312
00 313	*E6	314	*TE6	315	*FIOR	316	*CISL	317
321	*Z3	322	*CSIR	324	*CIQR	326	*Z32	330
332	*FIDS6	333	*FKT	334	*AA	335	*RS	336
337	*XM	341	U	342	*FIRR6	506	*Z11	507
511	*Z43	512	*Z2	514	*I	516	*FIOR6	517
520	*XR	522	*VDS6	523	*FIDS	524	*YQS	525
526	*RR	530	*YDR	531	*VQS	532	*WSL6	533
534	*CTE	536	*XF	540				

ARIES

0 541

[ NO ERRORS DETECTED ]

## APPENDIX - IV

```
C      PROGRAM FOR TRANSIENT ANALYSIS

      OPEN(UNIT=1,DEVICE='DSK',FILE='AT1.DAT')
C      OPEN(UNIT=2,DEVICE='DSK',FILE='AT2.DAT')
C      OPEN(UNIT=3,DEVICE='DSK',FILE='AT3.DAT')
C      OPEN(UNIT=4,DEVICE='DSK',FILE='AT4.DAT')

      READ(1,*) ,RS,RR,XS,XR,XM,RF,XCO,XF

      READ(1,*) ,KSP,FKSL,TQ,TLO,WB

      READ(1,*) ,FIQSO,WSL,WE,WRO

      READ(1,*) ,SWR,SFIRO,FIMAX,TI

      READ(1,*) ,FKC,T,G

      PRINT *,RS,RR,XS,XR,XM,RF,XCO,XF

      PRINT *,KSP,FKSL,TQ,TLO,WB

      PRINT *,FIQSO,WSL,WE,WRO

      PRINT *,SWR,SFIRO,FIMAX,TI

      PRINT*,FKC,T,G

      R=RS+RF+XCO

      X=XS+XF

      D=WSL*WSL*XR*XR+RR*RR

      FIQRO=-WSL*WSL*XM*XR*FIQSO/D

      FIDRO=WSL*XM*RR*FIQSO/D

      VQSO=(RS+WSL*WE*XM*XM*RR/D)*FIQSO

      VRO=VQSO+(RF+XCO)*FIQSO

      TE=XM*FIDRO*FIQSO

      PRINT*,FIQSO,FIQRO,FIDRO,WRO,VRO,WSL,WE,TE

      K=1

      TIME=0.0
```



```

Q20=0.0

Q30=0.0

Q40=0.0

Q50=0.0

KK=0

C   STEP=1

10  A=1./(X*XR-XM*XM)

C   WRITE(3,*) ,TIME,FIGS0

C   WRITE(2,*) ,TIME,WRO

C   WRITE(4,*) ,TIME,TE

IF(SWR.GE.WRO) GO TO 11

WSL=-FIGS0*FKSL

GO TO 12

11  WSL=+FIGS0*FKSL

12  WE=WRO+WSL

TL=TL0+G*WRO*WRO

IF(WRO.LT.0.0) TL=-TL

F1=A*(-R*XR*FIGS0+XM*RR*FIGR0+XR*VRO-XM*XR*(WE-WSL)*FIDR0)

F2=A*(R*XM*FIGS0-X*RR*FIGR0-XM*VRO+(WE*XM*XM-WSL*XR*X)*FIDR0)

F3=1./XR*(WSL*XM*FIGS0+WSL*XR*FIGR0-RR*FIDR0)

F4=1./TQ*(XM*FIGS0*FIDR0-(TL))

FK10=TI*F1

R11=.5*FK10-Q10

FIGS1=FIGS0+R11

Q11=Q10+3.*R11-.5*FK10

FK20=TI*F2

R21=.5*FK20-Q20

FIGR1=FIGR0+R21

Q21=Q20+3.*R21-.5*FK20

```

```

05700      FK30=TI*F3
05800      R31=.5*FK30-Q30
05900      FIDR1=FIDR0+R31
06000      Q31=Q30+3.*R31-.5*FK30
06100      FK40=TI*F4
06200      R41=.5*FK40-Q40
06300      WR1=WR0+R41
06400      Q41=Q40+3.*R41-.5*FK40
06500      SIR=SFIR0+KSP*ABS(SWR-WR0)
06600      DSIR=-KSP*F4
06700      IF(SIR-FIMAX)2,3,3
06800      3      SIR=FIMAX
06900      DSIR=0.0
07000      2      DVR=FKC/WB*(SIR-FIQS0)+FKC*T*(DSIR-F1)
07100      FK50=TI*DVR
07200      R51=.5*FK50-Q50
07300      VR1=VR0+R51
07400      Q51=Q50+3.*R51-.5*FK50
07500      C      STEP-2
07600      B=(1.-1./SQRT(2.))
07700      IF(SWR.GE.WR1) GO TO 13
07800      WSL=-FIQS1*FKSL
07900      GO TO 14
08000      13      WSL=+FIQS1*FKSL
08100      14      WE=VR1+WSL
08200      TI=TI,0+G*WR1*WR1

```

```

08400      F1=A*(-R*XR*FIQS1+XM*RR*FIQR1+XR*VR1-XM*XR*(WE-WSL)*FIDR1)
08500      F2=A*(R*XM*FIQS1-X*RR*FIQR1-XM*VR1+(WE*XM*XM-WSL*XR*X)*FIDR1)
08600      F3=1./XR*(WSL*XM*FIQS1+WSL*XR*FIQR1-RR*FIDR1)
08700      F4=1./TJ*(XM*FIQS1*FIDR1-(TL))
08800      FK11=TI*F1
08900      R12=(FK11-Q11)*B
09000      FIQS2=FIQS1+R12
09100      Q12=Q11+3.*R12-B*FK11
09200      FK21=TI*F2
09300      R22=(FK21-Q21)*B
09400      FIQR2=FIQR1+R22
09500      Q22=Q21+3.*R22-B*FK21
09600      FK31=TI*F3
09700      R32=(FK31-Q31)*B
09800      FIDR2=FIDR1+R32
09900      Q32=Q31+3.*R32-B*FK31
10000      FK41=TI*F4
10100      R42=(FK41-Q41)*B
10200      WR2=WR1+R42
10300      Q42=Q41+3.*R42-B*FK41
10400      SIR=SFIR0+KSP*ABS(SWR-WR1)
10500      DSIR=-KSP*F4
10600      IF(SIR-FIMAX)4,5,5
10700      5      SIR=FIMAX
10800      DSIR=0.0
10900      4      DVR=FKC/WR*(SIR-FIQS1)+FKC*T*(DSIR-F1)
11000      FK51=TI*DVR
11100      R52=(FK51-Q51)*B
11200      VR2=VR1+R52

```

```

11300      Q52=Q51+3.*R52-B*FK51
11400  C      STEP-3
11500      C=1.+1./SQRT(2.)
11600      IF(SWR.GE.WR2) GO TO 15
11700      WSL=-FIQS2*FKSL
11800      GO TO 16
11900  15     WSL=+FIQS2*FKSL
12000  16     WE=WR2+WSL
12100      TI=TL0+G*WR2*WR2
12200      IF(WR2.LT.0.0) TL=-TL
12300      F1=A*(-R*XR*FIQS2+XM*RR*FIQR2+XR*VR2-XM*XR*(WE-WSL)*FIDR2)
12400      F2=A*(R*XM*FIQS2-X*RR*FIQR2-XM*VR2+(WE*XM*XM-WSL*XR*X)*FIDR2)
12500      F3=1./XR*(WSL*XM*FIQS2+WSL*XR*FIQR2-RR*FIDR2)
12600      F4=1./TQ*(XM*FIQS2*FIDR2-(TL))
12700      FK12=TI*F1
12800      R13=C*(FK12-Q12)
12900      FIQS3=FIQS2+R13
13000      Q13=Q12+3.*R13-C*FK12
13100      FK22=TI*F2
13200      R23=C*(FK22-Q22)
13300      FIQR3=FIQR2+R23
13400      Q23=Q22+3.*R23-C*FK22
13500      FK32=TI*F3
13600      R33=C*(FK32-Q32)
13700      FIDR3=FIDR2+R33
13800      Q33=Q32+3.*R33-C*FK32
13900

```

```

14000      R43=C*(FK42-Q42)
14100      WR3=WR2+R43
14200      Q43=Q42+3.*R43-C*FK42
14300      SIR=SFIR0+KSP*ABS(SWR-WR2)
14400      DSIR=-KSP*F4
14500      IF(SIR-FIMAX)6,7,7
14600  7    SIR=FIMAX
14700      DSIR=0.0
14800  6    DVR=FKC/WB*(SIR-FIQS2)+FKC*T*(DSIR-F1)
14900      FK52=TI*DVR
15000      R53=C*(FK52-Q52)
15100      VR3=VR2+R53
15200      Q53=Q52+3.*R53-C*FK52
15300  C    STEP-4
15400      IF(SWR.GE.WR3) GO TO 19
15500      WSL=-FIQS3*FKSL
15600      GO TO 20
15700  19   WSL=+FIQS3*FKSL
15800  20   WE=WR3+WSL
15900      TL=TL0+G*WR3*WR3
16000      IF(WR3.LT.0.0) TL=-TL
16100      F1=A*(-R*XR*FIQS3+XM*RR*FIQR3+XR*VR3-XM*XR*(WE-WSL)*FIDR3)
16200      F2=A*(R*XM*FIQS3-X*RR*FIQR3-XM*VR3+(WE*XM*XM-WSL*XR*X)*FIDR3)
16300      F3=1./XR*(WSL*XM*FIQS3+WSL*XR*FIQR3-RR*FIDR3)
16400      F4=1./TQ*(XM*FIQS3*FIDR3-(TL))
16500      FK13=TI*F1
16600      R14=.16667*(FK13-2.*Q13)
16700      FIQS4=FIQS3+R14
16800      Q14=Q13+3.*R14-.5*FK13

```

```

16900      FK23=TI*F2
17000      R24=.16667*(FK23-2.*Q23)
17100      FIQR4=FIQR3+R24
17200      Q24=Q23+3.*R24-.5*FK23
17300      FK33=TI*F3
17400      R34=.16667*(FK33-2.*Q33)
17500      FIDR4=FIDR3+R34
17600      Q34=Q33+3.*R34-.5*FK33
17700      FK43=TI*F4
17800      R44=.16667*(FK43-2.*Q43)
17900      WR4=WR3+R44
18000      Q44=Q43+3.*R44-.5*FK43
18100      SIR=SFIR0+KSP*ABS(SWR-WR3)
18200      DSIR=-KSP*F4
18300      IF(SIR-FINAX)8,9,9
18400  9      SIR=FINAX
18500      DSIR=0.0
18600  8      DVR=FKC/4B*(SIR-FIQS3)+FKC*T*(DSIR-F1)
18700      FK53=TI*DVR
18800      R54=.16667*(FK53-2.*Q53)
18900      VR4=VR3+R54
19000      Q54=Q53+3.*R54-.5*FK53
19100      TE=XH*FIQS4*FIDR4
19200      TIME=K*TI/314.
19300      IF(KK.LT.10) GO TO 50
19400      PRINT*,FIQS4,FIQR4,FIDR4,WR4,VR4,WSL,WE,TE,SIR,DSIR,TIME

```

19600 GO TO 60  
19700 50 KK=KK+1  
19800 60 FIO50=FIQS4  
19900 FIOR0=FIOR4  
20000 FIDR0=FIDR4  
20100 WR0=WR4  
20200 VR0=VR4  
20300 Q10=Q14  
20400 Q20=Q24  
20500 Q30=Q34  
20600 Q40=Q44  
20700 Q50=Q54  
20800 K=K+1  
20900 IF(K.LE.2200) GO TO 10  
21000 CLOSE(UNIT=1)  
21100 CLOSE(UNIT=2)  
21200 CLOSE(UNIT=3)  
21220 CLOSE(UNIT=4)  
21300 STOP  
21400 END

SUBPROGRAMS CALLED

SQRT.

ABS.

SCALARS AND ARRAYS ( "\*" NO EXPLICIT DEFINITION - "%" NOT REFERENCED )

*VR0	1	*FIDR0	2	*FKC	3	*Q40	4	*Q33	5
*WB	6	*RF	7	*FIQR3	10	*R13	11	*R52	12
*FK42	13	*FIQS2	14	*SIR	15	*T	16	*FK13	17
*VR4	20	*Q12	21	*FK30	22	*Q51	23	*Q44	24
*R31	25	*R24	26	*K	27	*Q30	30	*FK53	31
*Q23	32	*R2	33	*FIDR4	34	*R42	35	*FK41	36
*FIQR2	37	*R	40	*FK12	41	*VR1	42	*FIQS1	43
*WSL	44	*TL	45	*Q41	46	*Q34	47	*R21	50
*R14	51	*F4	52	*R53	53	*DSIR	54	*FK52	55
*FKZ3	56	*Q20	57	*Q13	60	*FK40	61	*Q52	62
*FK11	63	*TQ	64	*R32	65	*FIDR3	66	*FIQR1	67
*FIQS0	70	*Q31	71	*SFIR0	72	*Q24	73	*WR3	74
*R11	75	*VQS0	76	*FLMAX	77	*KSP	100	*F3	101
*WF	102	*R43	103	*FK51	104	*FK22	105	*TE	106
*G	107	*KK	110	*VR2	111	*FK10	112	*Q10	113
*D	114	*Q42	115	*A	116	*R22	117	*SWR	120
*XCO	121	*R54	122	*FIDR2	123	*FIQR0	124	*FK33	125
*Q21	126	*WR0	127	*Q14	130	*FK50	131	*Q53	132
*FK21	133	*F2	134	*XS	135	*R33	136	*FIQS4	137
*X	140	*TIME	141	*RS	142	*TLO	143	*XA	144
*Q32	145	*R4	146	*R12	147	*R	150	*FKSL	151
*R51	152	*R44	153	*FK32	154	*FIDR1	155	*TI	156
*VR3	157	*FK20	160	*Q11	161	*Q50	162	*FIQR4	163
*Q42	164	*R4	165	*R4	166	*R4	167	*R4	168



	171	*DVR	172	*RR	173	*FK43	174	*Q22	175
R1	176	*Q54	177	*FK31	200	*R41	201	*R34	202
F	203								

TEMPORARIES

IN. [ NO ERRORS DETECTED ]